Nonlinear & Linear MIMO Control Of An Industrial Mixing Process

By

Suet Yan Deng

Department of Electrical & Computer Engineering

McGill University, Montreal

Dec 2002

A Thesis submitted to McGill University in partial fulfillment of the requirements of the degree of Master in Engineering

Abstract

In this study, we investigate the feasibility of applying advanced control design strategies to the mixing tank process of the plant of Falconbridge Ltd. in Sudbury, Ontario. The mixing tank receives Strathcona slurry, Strathcona filter cakes, dry Raglan powder and water as its inputs. Our objective is to control the Raglan to Strathcona ratio, the mixing tank level and the pulp density of the output mixed slurry to their respective set points so that the effects of all model uncertainties could be reduced. Static optimization is first carried out to investigate the solution set of the existing process. Then linearization and analysis of the existing system at its equilibrium point are performed. Hereinafter, besides the existing Repulper tank process, a new Three-Phase alternative process is suggested so that all uncertainties can be handled properly. Different controllers are then designed to determine if they are able to perform satisfactorily while undertaking all the uncertainties. Nonlinear controllers of "Input–Output linearization" and switching control, which is a variant of sliding control, are used. Robust switching control is found to have the robust capability with guaranteed robust performance and stability for system that has linear parametric bounded uncertainties and has a diagonal or triangular g matrix, the matrix that maps from the inputs to the state differentials. Linear MIMO controllers of state feedback pole placement and H_2 optimal control are used. Comparison of performance and robustness is made among different nonlinear and linear controllers.

Résumé

Dans cette thèse, nous nous penchons sur l'applicabilité de certaines techniques de conception de lois de commande évoluées à un procédé de mélange de concentrés de minerai de la fonderie Falconbridge Ltd. de Sudbury en Ontario. Le réservoir de mélange de ce procédé reçoit la pulpe de concentré Stratchcona, les gâteaux de Strathcona provenant des filtres, le concentré Raglan sous forme de poudre, et l'eau. Notre objectif est de réguler le ratio de masses sèches de Strathcona et Raglan, le niveau du réservoir de mélange, et la densité de pulpe de sortie à leurs valeurs désirées de telle sorte que l'effet des incertitudes du modèle soit réduite. Une optimisation statique est effectuée pour trouver l'ensemble des solutions d'équilibre du procédé.

Ensuite, en plus du procédé de mélange existant, un procédé en trois phases avec trois réservoirs est suggéré pour faciliter la réduction de la sensibilité aux incertitudes. Différents algorithmes de commande sont conçus pour déterminer leur niveau de performance tout en réduisant l'effet des incertitudes. Des compensateurs non-linéaires des types linéarisation entrée-sortie et commande par commutation, qui est une variante de la commande glissante, sont utilisés. La commande par commutation s'avère être la plus robuste, tout en offrant une performance garantie et la stabilité pour les systèmes qui ont des incertitudes linéaires paramétriques et une matrice g triangulaire. Des compensateurs multivariables linéaires à retour d'état et optimaux $\mathcal{H}_2$ sont aussi conçus. Finalement, nous comparons la performance et la robustesse des compensateurs linéaires et non-linéaires.

Acknowledgements

I would like to thank my supervisor Professor Benoit Boulet for his patience and guidance for the last three years. Without his insightful comments and guidance, it would not be possible for me, a civil engineering student to study the difficult subject of control. Also, I would like to thank him for his financial support for my study. I have learned a lot both in terms of knowledge and the methodologies of research during the course of the study. In addition, I would like to thank all the control professors in the electrical engineering department: Prof. Hannah Michalska, Professor Pierre Bélanger, Prof. Peter Caines and Prof. Vincent Hayward. They have enriched my knowledge in control systems greatly and have given me valuable insights for my research. Moreover, I would like to thank Cynthia, the secretary of CIM. She is always smiling and helpful. Furthermore, I would like to thank Jan and Danny for their generous help in providing the best computing environment.

Last but not least, I would like to especially thank my parents for their continual support and encouragement. Most importantly, I would like to thank Him for His grace and peace, to confirm me to finish this research and study.

Contents

Abstract ..…..……ii
Résumé ..…..……iii
Acknowledgments ……..……iv
Contents …...……v
List of Figures ……..x
List of Tables ……..……..xiv

1 Introduction ……1

2 System Analysis and Dynamics of Repulper Tank Mixing Process ….. 6

2.1 Importance of Mixing Process ……..6
2.2 Systems Analysis ……..……7
2.2.1 Inputs to the Repulper Tank…….…. 7
2.2.2 Repulper Tank Mixing Process……. 7
2.2.3 Outputs of the Repulper Tank……..…. 8

2.3 Notation and Nominal Operating Point …… 9
2.4 Dynamic Analysis ……10

2.4.1 Repulper Tank ……...10

2.4.2 Transfer Pump ……. 12
2.4.3 Solutions of the Nonlinear Equations to Respective Set Points ..…. 12

3 Static Optimization with Inequality Constraints ……13

3.1 Existence and Uniqueness of the Solutions …….. 14
3.2 Objective Function Formulation ……14
3.3 Local Minimum or Saddle Point ……...17
3.4 Finding the Solution Sets ……..20
3.5 Feedforward Scheme with Zero Input from Filter Cake …….. 27

4 Linearization of Existing Repulper Tank Process …….. 31

4.1 Introduction …….. 31
4.2 Theoretical Basics of Linearization …….. 34
4.3 Linearizing System *P* ……... 37
4.4 Properties of *Z*……43

5 Nonlinear Control Theory and System Analysis ……. 48

5.1 Nonlinear Control Theory Overview ……48

5.1.1 Theory of Input-Output Linearization …….. 50

5.1.1.1 Introductory Theory of Input-Output Linearization …... 50
5.1.1.2 SISO Case ……. 51
5.1.1.3 MIMO Case …… 56

5.1.2 Switching Control ……...….. 63

5.1.2.1 Switching Control …….….. 63
5.1.2.2 Robust Switching Control ……...67

5.1.2.3 Robust Switching Control for Linear ……. 72
Parametric Bounded Uncertainty

5.2 System Uncertainties and Dynamics …… 73

5.2.1 Model Uncertainties ……. 73

5.2.2 Alternative Control Design: 3 phases Design ……..….74

6 Nonlinear Design, Simulation and Analysis of Existing Process ……85

6.1 System Analysis: Repulper Tank ("Rep") …… 85

6.2 Input-Output Linearization ……... 92

6.2.1 Input-Output Linearization Formulation …….. 92

6.2.2 Input-Output Linearization Simulation ……98

6.2.3 Input-Output Linearization Conclusion …….……... 107

6.3 Switching Control ……. 107

6.3.1 Switching Control Formulation …… 107

6.3.2 Switching Control Simulation …….. 108

6.4 Conclusion on Control of Existing Process……. ……. 110

7 Nonlinear Analysis, Design & Simulation of Alternative Process ……..113

7.1 Phase I. Filter Cake's Normalizing Tank ("fil") …….. 113

7.1.1 System Analysis …….……... 113

7.1.2 Input-Output Linearization …….…….. 120

7.1.2.1 Input-Output Linearization Formulation …..……...120

7.1.2.2 Simulation of Input-Output-Linearization ……..128

7.1.2.3 Conclusion of Input-Output Linearization ……..130
of Phase I

7.1.3 Robust Switching Control of Phase I ……..…. 130

7.1.3.1 Robust Switching Control Formulation ……. 130

7.1.3.2 Simulation of Robust Sliding Control of Phase I ……... 131

7.1.3.3 Conclusion of Robust Sliding Control ……..……..138

7.1.4 Conclusion of Phase I Design of Phase I……...138

7.2 Phase II. Strathcona Normalizing Tank (“Str”) …… 139

7.2.1 State Space System Formulation …….. 139

7.2.2 Control Law Formulation and Simulation …… 146

7.2.3 Simulation Results & Discussion …….…… 151

7.2.4 Conclusion of Phase II Design ……..158

7.3 Phase III Repulper Tank (“Rep”) ……...159

7.3.1 Phase III State Space Formulation …… 159

7.3.2 Simulation …….…… 165

7.3.3 Conclusion of Phase III Design …… 171

7.4 Conclusion of Alternative Three-Phase Process ……...171

7.5 Conclusion of Nonlinear Control Design ……. 172

8 Linear MIMO Control ……... 175

8.1 Introduction …….. 175

8.2 State Feedback with Pole Placement …… 177

8.2.1 Pole Placement State Feedback Formulation ……177

8.2.2 Simulation ……178

8.2.3 Pole Placement Conclusion …….. 182

8.3 H_2 Optimal Control ……...184

8.3.1 Theory of H_2 Optimal Control …….…… 185

8.3.2 Control Formulation ……. 192
8.3.3 Simulation Results …… 195
8.3.4 Conclusion of H_2 optimal control ……..198

8.4 Conclusion of Linear MIMO Control ……... 199

9 Conclusion ……... 200

References ……202

List of Figures

Fig. 1.1: Feed Blending System of Falconbridge Ltd……. 5

Fig. 5.2.1: State flow Diagram for the Alternative Process ……..… 83

Fig. 6.2.1: Ratio of Outputs Values to their setpoints, (y/y_d), under … 104
input-output linearization with uncertain parameters for
the existing Repulper process

Fig. 6.2.2: Mass Flow Rate Controls commanded under input-output…105
linearization with uncertain parameters for the existing
Repulper tank process.

Fig. 6.2.3: Pump Speed Controls commanded under input-output …… 106
linearization with uncertain parameters for the existing
Repulper tank process.

Fig. 7.1.1.1: State flow Diagram for the Pump Speed …… 116

Fig. 7.1.1.2: Phase I System Plan …… 119

Fig. 7.1.3.2.1: Input Filter Cakes' Density Variation and Output Solid… 132
Density Variation of Filter Normalizing Tank regulated with Robust Switching Control.

Fig. 7.1.3.2.2: Total Masses of Filter Normalizing Tank with Robust…… 133
Switching Control.

Fig. 7.1.3.2.3: Inputs of Filter Normalizing Tank with Robust Switching . 134
Control

Fig. 7.1.3.2.4: Output Mass Flow Rate of Filter Tank with Robust……..136
Switching Control.

Fig. 7.1.3.2.5: Pump Speed of Filter Tank with Robust Switching Control. 137

Fig. 7.2.1.1: Phase II System Plan …… 145

Fig. 7.2.3.1: Output Solid densities of two initial state conditions..……. 153
for Phase II Strathcona normalizing tank.

Fig. 7.2.3.2: Total Masses of two initial state conditions for Phase II…. 154
Strathcona normalizing tank.

Fig. 7.2.3.3: The output mix flow pump speed of Strathcona …… 155
normalizing tank.

Fig. 7.2.3.4: Input Strathcona Mass flow rate of Strathcona normalizing 156
tank.

Fig. 7.2.3.5: Input Strathcona Mass flow rate of Strathcona normalizing 157
tank.

Fig. 7.3.1.1: Phase III System Plan ……... 164

Fig. 7.3.2.1: Output solid density using switching control for ……..…. 166
Strathcona density for Phase II for the two initial state conditions.

Fig. 7.3.2.2: Output solid density using switching control for……..…. 167
Strathcona density for Phase III for two initial state conditions.

Fig. 7.3.2.3: Pump Speed of Phase III using switching control for the 169
two initial state conditions.

Fig. 7.3.2.4: Output Mass Flow Rate of Phase III using switching…. 170
control for the two initial state conditions.

Fig. 8.2.2.1: Total solid density of existing Repulper tank process …. 179
which controlled with pole placement state feedback.

Fig. 8.2.2.2: Total Mass of existing Repulper tank process which is … 180
controlled with pole placement state feedback.

Fig. 8.2.2.3: Total Mass Output Flow Rate of existing Repulper tank... 181
process which is controlled with pole placement state feedback.

Fig. 8.2.2.4: Pump Speed of existing Repulper tank process which is…. 182
controlled with pole placement state feedback.

Fig. 8.2.2.5: Input Mass Flow Rate of existing Repulper tank process 183
which is controlled with pole placement state feedback.

Fig. 8.2.2.6: Raglan to Strathcona Ratio of existing Repulper tank …. 184
process which is controlled with pole placement state feedback.

Fig. 8.3.1.1: Typical Feedback Control Diagram …… 187

Fig. 8.3.1.2: Typical H_2 optimal Control Design …….. 188

Fig. 8.3.1.3: Standard LFT diagram for H_2 optimal control design……. 188

Fig. 8.3.3.1: Total solids density of existing Repulper tank process which is controlled with H_2 optimal control. 195

Fig. 8.3.3.2: Total mass of conventional Repulper tank system which is controlled with H_2 optimal control. 196

Fig. 8.3.3.3: State Errors of existing Repulper tank process which is……. controlled with H_2 optimal control. 197

Fig. 8.3.3.4: Raglan to Strathcona ratio of existing Repulper tank process which is controlled with H_2 optimal control. ……... 198

List of Tables

Table 7.1.2.1.1 Filter Normalizing Tank Level Changes Variations ….. 123
in SG_S Changes.

Chapter 1

Introduction

Falconbridge Ltd. is a mining and metallurgy company which processes ores to produce various metals, mostly nickel. The company has found a prominent nickel ore, namely, Strathcona which is situated at its founding town, Sudbury of Ontario. Elsewhere, Raglan is another prominent nickel ore located at Nunavik territory of northern Quebec. To reduce the cost of processing, Raglan is brought to Sudbury in powder format for further processing. Meanwhile, Strathcona ore is processed into a slurry format for further processing. It is determined that Strathcona slurry and Raglan powder can be mixed together for further refining of nickel, putting into the oven. Henceforth, there is the plant which produces this mix and this plant is the subject of this study.

The plant contains two processes. Firstly, a feed blending system which mixes dry Raglan concentrate with Strathcona slurry and water in a tank, Repulper tank. Then the

output from the Repulper tank is pumped to the second system, the roaster feed tank for better mixing of the mix before sending it to the roaster. The plant is illustrated in Fig. 1.1. Since the roaster tank only acts as a sink to average out the quality of the output, this study only deals with the system control of the first process, the Repulper tank mixing process.

The Repulper tank process may seem to be rather simple. But in fact it has significant uncertainties which can cause discrepancies in the quality of the output solution and overflow if not being cautious. There are four parameters to be controlled in this process. The solids density of the output of the Repulper tank, the dry weight ratio between Strathcona and Raglan, the Repulper tank level and the output mass flow rate of the Repulper tank. It is the primal priority of the process to control the output of the slurry of the Repulper tank at the density of 70%. Also the dry mass ratio of Strathcona and Raglan in the output solution has to be kept at 0.309 with little error tolerance. Besides, the Repulper tank level is to be controlled at 80% full, 2.4m as well. Lastly, the output slurry flow rate of the Repulper tank is set at 51.43 t/hr by the corresponding operation of the pump.

Due to the disastrous effects of the disturbances to the system, Falconbridge Ltd. had contracted Hatch Engineering Consultant Firm to design appropriate controllers which would stabilize the process and maintains the required density and ratio requirement of the process. Under the leadership of Dr. B. Boulet, the chief engineer of the project, 3 PID controllers were designed for the process: density PI controller, Raglan to Strathcona Ratio PI Controller and Repulper tank Level PI controller. The PI controllers have worked satisfactorily. But as higher performance requirements are sought, new control schemes are investigated in this thesis. First, we study the nonlinear equations of the process and its dynamics. Then we introduce new designs to reach the goals of the plant process without and with the use of feedback control.

Problems

The plant is subject to various disturbances which have caused undesirable results in terms of diluted mix which reduce the efficiency of the oven, and occasionally causing overflow. One of the major disturbances is the non-uniform solids density of the incoming Strathcona. Since Strathcona is brought in by different loads of trucks, *fs,* Strathcona slurry solids density can varies from truckload to truckload. Therefore, filter cakes are used to increase the density of the mix when incoming Strathcona slurry solid density is below 64.067%. However the mechanism of putting filter cakes into the Repulper tank is not well controlled. As seen in Fig. 1.1, filter cakes are being put into the Repulper tank with rotating mechanical arms. The filter cakes are dropped freely from the arm by the pull of gravity when the arm is rotated at the position of above the tank. However, there is no idea of exactly how much filter has been dropped into the Repulper tank. Furthermore, the solid density of the filter cakes could vary considerably. Hence, this freely dropping mechanism makes the Repulper system become virtually impossible to fine tune the solid density of the output solution and the sensitive dry mass ratio of Strathcona and Raglan. Besides, the specific gravities of Strathcona and Raglan vary as well. Since the output, the Repulper tank level depends on the specific gravities of Strathcona and Raglan, it poses more challenge to control the system. In addition, the pump characteristic constant of the pump varies when viscosity of the solution changes.

Prospective Solutions:

The simplest solution could have been to redesign the filter cakes' input mechanism so that it is more accurate. However due to various constraints, this direction is not being pursued. Hence, intrinsically, the plant could not be well controlled due to the input uncertainties. To resolve the problem of input uncertainties, different control schemes are being designed to alleviate the problem.

Since the system itself is highly nonlinear, nonlinear feedback control strategies is used first to try to attain the design objectives. This is because although there are very rich linear control techniques, they all need to sacrifice the intrinsic nonlinear nature of the system. It is difficult to design a linear controller which can track the system in all

circumstances. This is because the linear controller can only function in the neighborhood of a set of operating conditions. But the Repulper tank mixing system has an infinite set of operating conditions due to the significant model uncertainties and variations of parameters. Hence, it is not possible to linearize at all possible operating sets. Henceforth, linear designs are considered at last.

Subsequently, two nonlinear control strategies are used; input-output linearization and sliding control. This is to compare the characteristics and effectiveness of the two current nonlinear control schemes. Nonlinear control has the advantage that it does not need to operate at a defined set of states. Hence, state variations are not a concern to nonlinear control. Furthermore, robust capabilities of the two nonlinear control schemes are being explored. It is most desirable to have a nonlinear control scheme which can handle model uncertainties as well. Since then the system can attain its regulation objectives without worrying the disturbances and instability caused by its model uncertainties.

Fig. 1.1: Feed Blending System of Falconbridge Ltd.

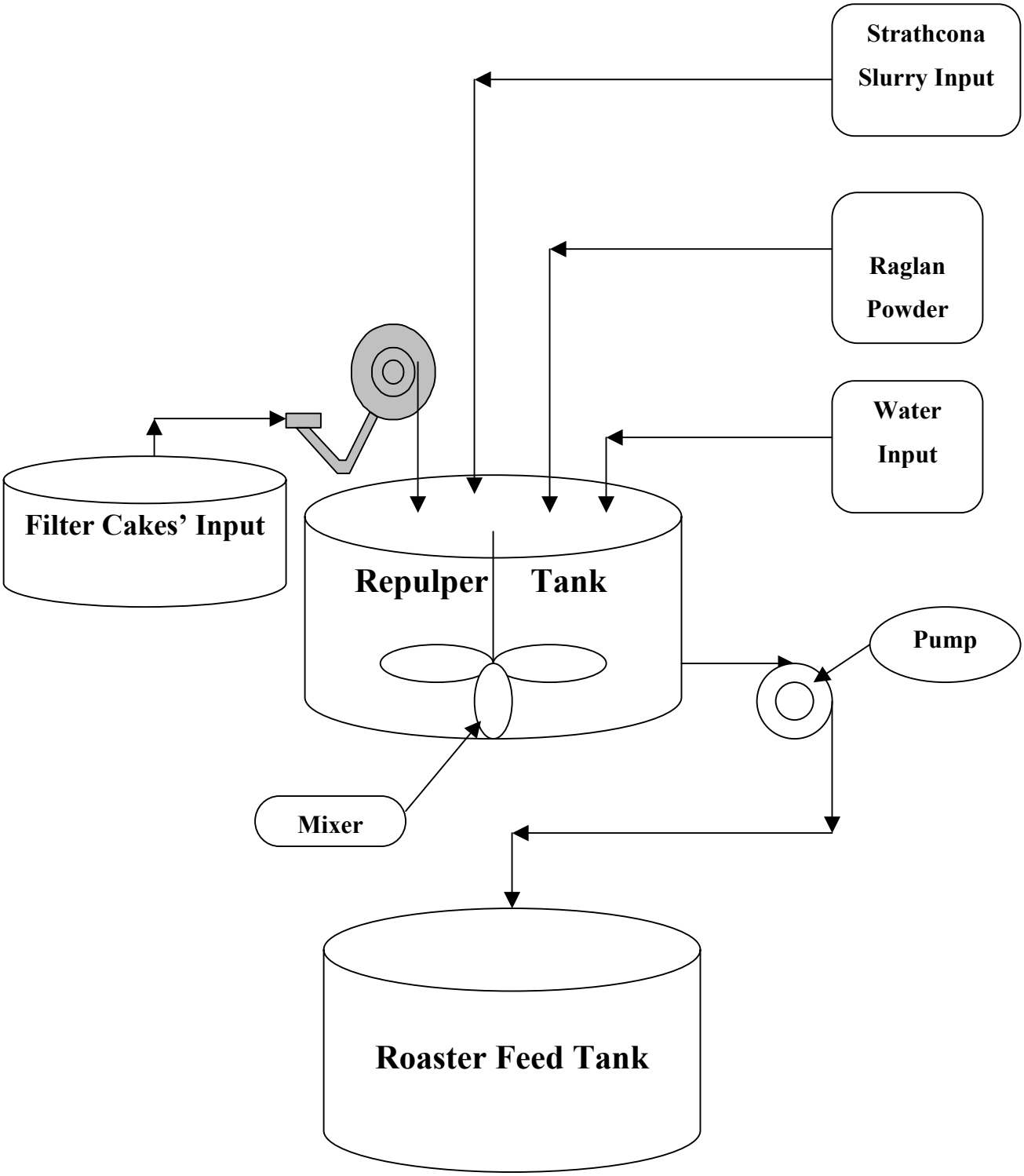

Chapter 2

System Analysis and Dynamics of Repulper Tank Mixing Process

2.1 Importance of Mixing Process

In process industries, it is common to have different substrates, each with the respective concentration, blending together to form a mixed substrate for further processes. This initial feed blending process in most cases is crucial to the quality production of the products. For some processes, even a slight error in the final composition of the substrates could seriously affect the performance of processes downstream.

In this chapter, each component of the Falconbridge's Repulper tank process is analyzed.

2.2 Systems Analysis

2.2.1 Inputs to the Repulper Tank

The system is divided into two parts, the Repulper tank and the roaster tank. The output of the Repulper tank goes into the roaster tank. While the role of the Repulper tank is to make the right composition of the output slurry, the roaster tank is used to give a more homogenous medium by stirring the slurry before going into the roaster. There are four inputs to the Repulper tank, namely, Strathcona slurry, Raglan powder, filter cakes and water. Since the mixing of different components of Repulper tank determines the final composition of the slurry, in this study we only concentrate on the Repulper tank subsystem.

2.2.2 Repulper Tank Mixing Process

The Raglan powder is fed at the dry mass flow rate of 8.5 tonnes/h into the Repulper tank. Water is flowing into the tank at the rate of 0.624 tonnes/hr. Strathcona is in a slurry form The Strathcona slurry mass flow rate is at 27.5 tonnes/hr. While the output density of the slurry has to be kept at 70% in solids, Strathcona has about 65% in solids. Even though the input and output flow rates are set to obtain the required density and composition, there are disturbances which could alter the final density and the ratio of the slurry. These disturbances could come from variations of the Strathcona slurry flow rate or inconsistencies in the Strathcona slurry solid density %. Therefore we need to have two counter acting inputs, one is to make the Repulper tank slurry denser and the other one is to dilute the slurry in the Repulper tank. These two forces should act accordingly to ensure that the final mix has the desired solids density. It would be easy to increase the dilution by simply increasing the flow rate of water. However, to make the slurry in the Repulper tank denser, we need to have a substance which has a higher solid density than the Strathcona slurry coming from the valve. This is done by having the filter cakes

coming into the Repulper tank when necessary. Since the function of the filter is only for regulation of the disturbances, the filter mass flow rate is set to 0 tonnes/hr initially.

2.2.3 Outputs of the Repulper Tank

The only output from the Repulper tank is the mix coming out from the Repulper tank. In order to ensure the quantity and the quality of the output mix, different output measurements are carried out. These output measurements are the total solids density of the mix, the height of the Repulper tank and the mass flow rate of the mix. Fortunately, the density sensor measures the solids density rather accurately. The height of the Repulper tank can be measured as well. However, since there is lots of turbulence caused by the stirring action of the stirrer in the mixing tank and the splashes of the pouring of the inputs, the height of the tank level can only be measured approximately. Hence, as will be seen in later chapters, the measurement of the weight of the tank is preferred. To measure the output mass flow rate, the system needs a new mass flow meter. Coriolis mass flow meter can be installed in this scenario. Also, the speed of the pump has to be controlled in order to produce the required output mass flow rate. However, this pump speed is not constant. This is because it is affected by the specific gravity of the mix solution in the Repulper tank. Since the specific gravity of Strathcona and Raglan vary, the specific gravity of the mix varies as well. Furthermore, pump characteristic constant can vary when the viscosity of the mix changes. Consequently, the speed that is needed differ accordingly as well. In this study, however, since the pump is outside of the mixing tank, the pump speed output can be manipulated in the sense of SISO. This manipulation is useful as it simplifies the MIMO mixing tank system. The other non-measurable but desirable parameter is the Raglan to Strathcona ratio. This ratio cannot be measured directly. It can only be deduced mathematically indirectly from the outputs of the measurements. In all, these output measurements are essential in establishing any feedback control schemes. Before going into the formulation of the systems, the respective symbols which represent different variables and parameters are presented in the next subsection. Also, the nominal values of the variables are included as well.

2.3 Notation and Nominal Operating Point

All units are in SI, e.g., t/h means *metric* tonnes per hour, unless otherwise specified.

Symbol		Variable	Nominal Values
D_{Rep}	:	diameter of Repulper tank (m)	2.5 m
f_f	:	density of Strathcona slurry from filters (% solids)	80%
f_m	:	mix slurry solids density in % in Repulper tank	70 %
f_s	:	input Strathcona slurry's solids density in %	65 %
H_{Rep}	:	height of Repulper tank (m)	3.0 m
h_{Rep}	:	pulp level in Repulper tank (m)	2.40 m (80% full)
M_{SR}	:	total mass of dry Strathcona in Repulper tank	13.39 t
M_{RR}	:	total mass of dry Raglan in Repulper tank	4.14 t
M_{WR}	:	total mass of water in Repulper tank	7.51 t
$\dot{M}_s$	:	dry mass flow rate of Strathcona feed (t/h) from pinch valve	27.5 t/h
$\dot{M}_f$	:	dry mass flow rate of Strathcona feed from filters	0 t/h
$\dot{M}_R$	:	dry mass flow rate of Raglan powder (t/h)	8.5 t/h
$\dot{M}_W$	:	mass flow rate of water	0.624 t/h
$\dot{M}_m$	:	dry mass flow rate of mix out of Repulper tank	36 t/h
$\dot{M}_{m+w}$	:	mass flow rate of mix out of Repulper tank	51.43 t/h
$\dot{M}_{Sm}$	:	dry mass flow rate of Strathcona in mix out of Repulper tank	27.5 t/h

$\dot{M}_{Rm}$	:	dry mass flow rate of Raglan in mix out of Repulper tank	8.5 t/h
$\dot{M}_{wm}$	:	mass flow rate of water in mix out of Repulper tank	15.43 t/h
r	:	ratio of dry Raglan/Strathcona in Repulper tank	0.309
SG_M	:	specific gravity of mix (t/m^3)	2.129 t/m^3
SG_R	:	specific gravity of Raglan powder (t/m^3)	3.9 t/m^3
SG_S	:	specific gravity of dry Strathcona feed (t/m^3)	4.2 t/m^3
V_{Rep}	:	active volume of Repulper tank (m^3)	14.3 m^3
x_v	:	Strathcona slurry pinch valve opening (%)	78.6%
ω_{pm}	:	velocity of transfer pump variable speed drive (rpm)	962 rpm

2.4 Dynamic Analysis

Since this study only concentrates on the dynamics of the Repulper tank of the whole process, only the Repulper tank and the transfer pump's dynamic equations are being considered.

2.4.1 Repulper Tank

The first order nonlinear differential and algebraic equations below describe the dynamic behaviour of the total masses of Strathcona, Raglan powder and water in the Repulper tank:

I. Conservation of Mass of Strathcona in Repulper tank

$$\dot{M}_{SR} = \dot{M}_S + \dot{M}_f - \frac{M_{SR}}{M_{SR} + M_{RR}} \dot{M}_m \tag{2.1}$$

II. Conservation of Mass of Raglan in Repulper tank

$$\dot{M}_{RR} = \dot{M}_R - \frac{M_{RR}}{M_{SR} + M_{RR}} \dot{M}_m \tag{2.2}$$

III. Conservation of Mass of Water in Repulper tank

$$\dot{M}_{WR} = \frac{(1 - f_s)}{f_s} \dot{M}_S + \dot{M}_W + \frac{(1 - f_f)}{f_f} \dot{M}_f - \frac{M_{WR}}{M_{SR} + M_{RR}} \dot{M}_m \tag{2.3}$$

IV. Density at the Output of the Repulper tank

$$f_m = \frac{M_{SR} + M_{RR}}{M_{SR} + M_{RR} + M_{WR}} \tag{2.4}$$

V. Raglan to Strathcona Ratio:

$$r = \frac{M_{RR}}{M_{SR}} \tag{2.5}$$

VI. Repulper tank Level

$$h_{\mathrm{Re}\,p} = \left(\frac{4}{\pi {D_{\mathrm{Re}\,p}}^2} \right) \left(\frac{M_{RR}}{SG_R} + \frac{M_{SR}}{SG_S} + M_{WR} \right) \tag{2.6}$$

2.4.2 Transfer Pump

The transfer pump characteristic from pump motor velocity to mass flow rate of mix, including water is as follows:

$$\dot{M}_{m+w} = SG_M \cdot k_{pump} \cdot \omega_p \qquad (2.7)$$

The specific gravity of the mix, SG_M relates to the specific gravity of Strathcona and Raglan. The k_{pump} is the pump characteristic constant.

2.4.3 Solutions of the Nonlinear Equations to Respective Set Points

The usual problem associated with the system of equations is to find the set of solutions, if feasible, to the equations. At a first glance this seems to be a very complicated problem. This is because the plant, which is composed of the equations (2.1)-(2.7), is a mix of differential and algebraic equations with five inputs, three states and four outputs.

The five inputs of the system are the input dry mass flow rate of Strathcona ($\dot{M}_s$), Raglan ($\dot{M}_R$), water ($\dot{M}_w$) and filter cakes ($\dot{M}_f$).

The three state variables of the system are the dry mass of Strathcona (M_{SR}), Raglan ($\dot{M}_R$) and water (M_{wR}) in the Repulper tank.

The four outputs of the system are the height of the Repulper tank (h_{Rep}), the ratio of dry mass of Raglan to Strathcona (r), the solids density of the output mix of the Repulper tank (f_m) and the speed of the pump which pumps the mixed solution out of the Repulper tank (ω_{pm}).

The dynamics of the state differential equations are desired to be equal to zero (equations (2.1)-(2.3)). This means that we require the derivatives of the changes of the masses of Strathcona, Raglan and water in the Repulper tank to be zero. This is required so that the tank's different components are in a state of equilibrium. The equilibrium pursued is a dynamic equilibrium in which though there are continuous flows in the system, the net changes are zero. In addition we want to achieve certain desired characteristics of the flow coming out from the Repulper tank. Since the tank is assumed to be well mixed, the characteristics of the mix inside the tank, such as total mass density, Raglan to Strathcona ratio should be the same as the flow of the slurry coming out from the tank. We want the mass density, f_m, to be kept at 70%, and we would like to keep the Raglan to Strathcona mass ratio at 0.309. These two requirements are the most important since it ensures the quality of mixed slurry. Besides, with a limited capacity of a tank, it is required to keep the tank level at a certain point where it is sufficiently large to handle any sudden increase of withdrawal on one hand, and on the other hand safe enough to handle any sudden surge of incoming inputs. Hence the set point for the Repulper tank level is to be kept at 80% full of the tank, at 2.4m. As the tank is three meters tall, this would give enough safety ground to accommodate a normal surge of inflow. Furthermore, it is specified to keep the output flow rate at 51.43 t/h by controlling the speed of the pump. Hence, ideally, the whole system should be in an equilibrium state. To find the equilibrium state of the system, which can be represented by the seven equations, is to find the inputs and the states which can satisfy all the seven equations of the plant concurrently. It is difficult to solve the equations analytically. Hence, in order to find the solution set of the problem, a brute-force like method is used: optimization. This method is to try to find the solution by searching through the whole R^{m+n} space, where m is the dimension of inputs and n is the dimensions of state variables. Fortunately, different optimization techniques can greatly help to find the solution effectively. The next chapter is devoted to optimization and its search results.

Chapter 3

Static Optimization with Inequality Constraints

Static optimization is used to search for the solutions of the system. The thinking was to treat all the state variables and inputs to be variables. We could form an objective function which composed of all the errors of the seven equations from (2.1) to (2.7) together in a $H_{2\text{-}norm}$ format. Since then if we minimize this new objective function called V with respective to the other variables, we could find the solutions which minimize the error of the cost function. If there is a solution that minimize all the errors to zero concurrently, then a solution, a set of state and input values, is found which can solve for all the equations (2.1) and (2.8). But first we need to ask ourselves: Does the solution exists? If it does exist, is it unique?

3.1 Existence and Uniqueness of the Solutions

This question turns out to be a difficult one. With a closer look at the system, we see that there are seven equations to be solved and there are eight unknowns: three state variables and five input variables. It is non-prudent to state that since there are more equations than unknown, the solutions exist and are not unique. This is because the set of equations could be inconsistent so that there is not enough information to solve for all the respective variables. Hence, this question of existence and uniqueness can only be answered after the results of the optimization.

3.2 Objective Function Formulation

We form the new cost function V, by moving the desired constants of the left-hand side of the equations to the right-hand side and then take the square of each of the new sub-function formed. We could put scalar weightings constants in front of each square term. Hence we have:

$$v_1(x) = \dot{M}_S + \dot{M}_f - \frac{M_{SR}}{M_{SR} + M_{RR}} \dot{M}_m - 0 \tag{3.1}$$

$$v_2(x) = \dot{M}_R - \frac{M_{RR}}{M_{SR} + M_{RR}} \dot{M}_m - 0 \tag{3.2}$$

$$v_3(x) = \frac{(1 - f_s)}{f_s} \dot{M}_S + \dot{M}_W + \frac{(1 - f_f)}{f_f} \dot{M}_f - \frac{M_{WR}}{M_{SR} + M_{RR}} \dot{M}_m - 0 \tag{3.3}$$

$$v_4(x) = \frac{M_{SR} + M_{RR}}{M_{SR} + M_{RR} + M_{WR}} - 0.70 \tag{3.4}$$

$$v_5(x) = \frac{M_{RR}}{M_{SR}} - 0.309 \tag{3.5}$$

$$v_6(x) = \left(\frac{4}{\pi D_{\mathrm{Re}\,p}}\right)\left(\frac{M_{RR}}{SG_R} + \frac{M_{SR}}{SG_S} + M_{WR}\right) - 2.4 \tag{3.6}$$

$$v_7(x) = SG_m k_{pump}\omega_p - 51.43 \tag{3.7}$$

Then we formulate the final objective function:

$$\begin{aligned} V(x) = {} & w_1 \cdot v_1(x)^2 + w_2 \cdot v_2(x)^2 + w_3 \cdot v_3(x)^2 + w_4 \cdot v_4(x)^2 \\ & + w_5 \cdot v_5(x)^2 + w_6 \cdot v_6(x)^2 + w_7 \cdot v_7(x)^2 \end{aligned} \tag{3.8}$$

Since the objective values of $v_4(x)$ and $v_5(x)$ are too small numerically compared to the other $v_i(x)$, hence we set w_4 and w_5 to be ten and the other w_i to be 1. Also,

$$x = \begin{bmatrix} x_1 = \dot{M}_S, x_2 = \dot{M}_f, x_3 = \dot{M}_R, x_4 = \dot{M}_W, x_5 = M_{SR}, \\ x_6 = M_{RR}, x_7 = M_{WR}, x_8 = \omega_p \end{bmatrix} \tag{3.9}$$

is composed of three state variables and five input variables respectively.

Since all the state and input variables are non-negative, the optimization is subject to a set of eight inequality constraints, namely:

$$A = \{x_1 \geq 0, x_2 \geq 0, x_3 \geq 0, x_4 \geq 0, x_5 \geq 0, x_6 \geq 0, x_7 \geq 0, x_8 \geq 0\} \tag{3.10}$$

The optimization was carried out using the optimization toolbox from Matlab
(The Matlab Function ‘constr’ is a constrained optimization routine. It is being used with inequality constraints being set at as all state variables have to be slightly bigger than

zeros.). The optimization is carried out to minimize the 2-norm of the errors of each of the equations.

The solution that was found is:

$$S = \{x_1 = 14.50, x_2 = 13, x_3 = 8.49, x_4 = 4.37, x_5 = 13.41, \\ x_6 = 4.14, x_7 = 7.52, x_8 = 961\} \quad (3.11)$$

This solution gives *V(x)* a value of 6.59E-6. Since the solution minimizes *V* to a very small value, it minimizes all the corresponding $v_i(x)$ as well. Hence *S* is a solution for our system.

3.3 Local Minimum or Saddle Point

The solution *S* only tells us that *S* is a stationary point of the cost function. Hence, in order to know if the solution *S* is stable or not, we need to determine whether *S* lies at a local minimum or merely at a saddle point. To verify that it is to determine if the Hessian of *V(x)* evaluated at *S* is positive definite or not.

We have also checked the gradient of *V(x)* ,

$$g(x) = \left[\frac{\partial V}{\partial x_1} \quad \frac{\partial V}{\partial x_2} \quad \frac{\partial V}{\partial x_3} \quad \frac{\partial V}{\partial x_4} \quad \frac{\partial V}{\partial x_5} \quad \frac{\partial V}{\partial x_5} \quad \frac{\partial V}{\partial x_6} \quad \frac{\partial V}{\partial x_7} \quad \frac{\partial V}{\partial x_8} \right]^T \quad (3.12)$$

evaluated at *S* is indeed very small, in the order of 10^{-3}. Then we evaluate the Hessian of *V(x)*,

$$h(x)=\begin{bmatrix} \frac{\partial V}{\partial x_1 \partial x_1} & \frac{\partial V}{\partial x_1 \partial x_2} & \frac{\partial V}{\partial x_1 \partial x_2} & \cdots & \frac{\partial V}{\partial x_1 \partial x_8} \\ \frac{\partial V}{\partial x_2 \partial x_1} & \cdot & \cdot & \cdots & \frac{\partial V}{\partial x_2 \partial x_8} \\ \cdot & & & & \cdot \\ \cdot & & & & \cdot \\ \cdot & & & & \cdot \\ \cdot & & & & \cdot \\ \cdot & & & & \cdot \\ \frac{\partial V}{\partial x_8 \partial x_1} & \frac{\partial V}{\partial x_8 \partial x_2} & \cdot & \cdots & \frac{\partial V}{\partial x_8 \partial x_8} \end{bmatrix} \qquad (3.13)$$

at *S*. In order to determine the positive definiteness of *h(x)*, we evaluate determinants of each of the sub-matrices of *h(x)*. Since the Hessian is an eight by eight matrix. It is easier to determine the determinant of the smaller sub-matrices. Moreover, since the four by four sub-matrix contains only numbers or constant, it is easier to just analyze the four-by-four sub-matrix and the smaller sub-matrices it includes: one by one, two by two and three by three. If one of these sub-matrices, (one by one, two by two, three by three or four by four) has determinant which is not positive definite, then the solution *S* is not a minimum. Moreover, since the determinant is the same for all the solutions of the cost function, it would imply that the Hessian of the function itself is intrinsically non-positive definite not only with *S*, but with all solution sets. First, let us denote *U* as the set that contains all solutions for the system, i.e.

$$U := \{x \in R_+ : V(x) = 0\} \qquad (3.14)$$

The four by four sub-matrix of the Hessian of the cost function is:

$$h_4(x)=\begin{bmatrix} 2+2\cdot r_S^2 & 2+2\cdot r_S\cdot r_f & 0 & 2\cdot r_S \\ 2+2\cdot r_S\cdot r_f & 2+2\cdot r_f^2 & 0 & 2\cdot r_f \\ 0 & 0 & 2 & 0 \\ 2\cdot r_S & 2\cdot r_f & 0 & 2 \end{bmatrix} \qquad (3.15)$$

$$, r_S=\frac{(1-f_S)}{f_S}; r_f=\frac{(1-f_f)}{f_f}$$

The four determinants of the four sub-matrices are:

$$\det(h_1(x))=2+2\cdot r_s^2>0 \qquad \because r_S\geq 0 \qquad (3.16)$$

$$\det(h_2(x))=(2+2\cdot r_S^2)(2+2\cdot r_S^2)-(2+2\cdot r_S\cdot r_f)^2=4(r_S-r_f)^2\geq 0 \qquad (3.17)$$

$$\begin{aligned}\det(h_3(x)) &= 2(2+2\cdot r_S^2)(2+2\cdot r_f^2)+0+0-0-0-2(2+r_S\cdot r_f)^2 \\ &= 8(r_S-r_f)^2\geq 0\end{aligned} \qquad (3.18)$$

$$
\begin{aligned}
\det(h_4(x)) &= (2+2\cdot r_S^2)\det\begin{bmatrix} 2+2\cdot r_f^2 & 0 & 2\cdot r_f \\ 0 & 2 & 0 \\ 2\cdot r_f & 0 & 2 \end{bmatrix} \\
&\quad -(2+2\cdot r_S\cdot r_f)\begin{bmatrix} 2+2\cdot r_S\cdot r_f & 0 & 2\cdot r_f \\ 0 & 2 & 0 \\ 2\cdot r_S & 0 & 2 \end{bmatrix} \\
&\quad +0-(2\cdot r_S)\det\begin{bmatrix} 2+2\cdot r_S\cdot r_f & 2+2\cdot r_f^2 & 0 \\ 0 & 0 & 2 \\ 2\cdot r_S & 2\cdot r_f & 0 \end{bmatrix} \\
&= (2+2\cdot r_S^2)\left\{4(2+2\cdot r_f^2)-8\cdot r_f^2\right\} \\
&\quad -(2+2\cdot r_S\cdot r_f)\left\{4(2+2\cdot r_S\cdot r_f)-8\cdot r_S\cdot r_f\right\} \\
&\quad -(2\cdot r_S)\left\{4r_S\cdot(2+2\cdot r_f^2)-4r_f(2+2r_S\cdot r_f)\right\} \\
&= 16(1+r_S^2)-16(1+r_S\cdot r_f)-16r_S\cdot(r_S-r_f) \\
&= 0
\end{aligned}
\qquad (3.19)
$$

Even though the determinants of the first sub-matrix is positive definite and the second and the third determinants of the sub-matrices could be positive definite if ($f_S<f_f$), we could see from (3.19) that the determinant of the four by four sub-matrix is always zero. This means that the stationary solution and all the solution sets in U are not local minimum. They are possibly saddle points. As we know then *h(x)* is at most positive semi-definite, it implies that our system plant *P* could just be marginally stable even at equilibrium points.

3.4 Finding the Solution Sets *U*

In normal circumstances, it would not be easy for us to find the rules which could generate the sets of solutions. However, taking a closer look at the equations (2.4)-(2.6), we have three algebraic equations and three unknowns. If we substitute the desired outputs with our set point values as we did for our optimization problem. Then we can

solve the three state variables that are needed to attain those output set points, ('f_m=0.7', 'r=0.309' and 'h_{rep}=2.4m') with ease. We have:

$$x_5 = M_{SR} = 13.413 \text{ tonnes} \tag{3.20}$$

$$x_6 = M_{RR} = 4.1446 \text{ tonnes} \tag{3.21}$$

$$x_7 = M_{WR} = 7.5247 \text{ tonnes} \tag{3.22}$$

For equation (2.7), it would seem to be easy if SG_M, specific gravity of the mix, would be merely a constant. But in fact SG_M is related to the three state variables and the specific gravities of Strathcona and Raglan in the following way:

$$SG_M = \frac{(x_5 + x_6 + x_7)}{(x_5 / SG_S + x_6 / SG_R + x_7)} \tag{3.23}$$

However, since now we have solved for x_5, x_6 and x_7 we can readily solve the desired pump speed with equation (2.7):

$$\dot{M}_{M+w} = \frac{k_p \cdot \omega_p \cdot (x_5 + x_6 + x_7)}{(x_5 / SG_S + x_6 / SG_R + x_7)} \tag{3.24}$$

and with the nominal values of the specific gravity of Strathcona and Raglan, we get:

$$x_8 = \omega_p = 962.0197 \; RPM \tag{3.25}$$

Therefore, for all solution sets, equations (3.21), (3.22), (3.23) and (3.25) are always valid. This implies that there is only one set of x_5, x_6, x_7 and x_8, which satisfy P and hence they are unique. But we stated earlier on that there might be more than one set of solution

as we have more variables than equations. The answer would lie into exploring the three state equations: (3.1)-(3.3).

There is a mysterious term in these three equations, the dry mass flow rate of mix out of Repulper tank. Fortunately, we could relate the dry mass flow rate out of the tank with total mass flow rate by multiplying itself with the density factor (2.4).

Hence we have:

$$\dot{M}_m = \left(\frac{M_{SR} + M_{RR}}{M_{SR} + M_{RR} + M_{WR}} \right) \cdot SG_M \cdot k_{pump} \cdot \omega_p \tag{3.26}$$

Since we know also SG_M from (3.23), and with (3.26), we have:

$$\dot{M}_m = \frac{SG_M \cdot k_{pump} \cdot \omega_p \cdot \left(M_{SR} + M_{RR} \right)}{\left(M_{SR} / SG_S + M_{RR} / SG_R + M_W \right)} \tag{3.27}$$

We are ready to transform our three state equations. After algebraic manipulation and cancellation, we have:

$$\dot{M}_{SR} = \dot{M}_S + \dot{M}_f - \frac{SG_M \cdot k_{pump} \cdot \omega_p \cdot M_{SR} \cdot \left(M_{SR} + M_{RR} \right)}{\left(M_{SR} / SG_S + M_{RR} / SG_R + M_W \right)} \tag{3.28}$$

$$\dot{M}_{RR} = \dot{M}_R - \frac{SG_M \cdot k_{pump} \cdot \omega_p \cdot M_{RR} \cdot \left(M_{SR} + M_{RR} \right)}{\left(M_{SR} / SG_S + M_{RR} / SG_R + M_W \right)} \tag{3.29}$$

$$\begin{aligned} \dot{M}_{WR} = {} & \dot{M}_S \frac{(1 - f_s)}{f_s} + \dot{M}_f \frac{(1 - f_f)}{f_f} + \dot{M}_W \\ & - \frac{SG_M \cdot k_{pump} \cdot \omega_p \cdot M_{WR} \cdot \left(M_{SR} + M_{RR} \right)}{\left(M_{SR} / SG_S + M_{RR} / SG_R + M_W \right)} \end{aligned} \tag{3.30}$$

Since we would like the dynamics of the state variables inside the tank be in equilibrium, we would set all the left hand of (3.28), (3.29) and (3.30) to be zeros. From (3.29), we could realize that x_3, the Raglan input, is unique as well:

$$\dot{M}_R = \frac{SG_M \cdot k_{pump} \cdot \omega_p \cdot M_{RR} \cdot (M_{SR} + M_{RR})}{(M_{SR}/SG_S + M_{RR}/SG_R + M_W)} \tag{3.31}$$

After substituting equations (3.20), (3.21), (3.22) and (3.25), we found the Raglan feed rate to be:

$$x_3 = \dot{M}_R = 8.4983\ tonnes \tag{3.32}$$

Also we have:

$$\dot{M}_S = -\dot{M}_f + \frac{SG_M \cdot k_{pump} \cdot \omega_p \cdot M_{SR} \cdot (M_{SR} + M_{RR})}{(M_{SR}/SG_S + M_{RR}/SG_R + M_W)} \tag{3.33}$$

and

$$\begin{aligned} \dot{M}_S \frac{(1-f_s)}{f_s} &= -\dot{M}_f \frac{(1-f_f)}{f_f} - \dot{M}_W \\ &+ \frac{SG_M \cdot k_{pump} \cdot \omega_p \cdot M_{WR} \cdot (M_{SR} + M_{RR})}{(M_{SR}/SG_S + M_{RR}/SG_R + M_W)} \end{aligned} \tag{3.34}$$

Now we have two equations and three unknowns left. We have freedom to choose one of the unknown to be the free variable. Since in our process, we would like to have maximum freedom of pouring in the filter cakes, we pick the mass flow rate of filter cakes as our free variable. After substituting in the equilibrium state values of (3.21), (3.22), (3.23) and (3.25), we have:

$$x_1 = \dot{M}_S = -\dot{M}_f + C_1 \tag{3.35}$$

where

$$C_1 = 27.5019 \text{ t/h} \tag{3.36}$$

and

$$x_4 = \dot{M}_W = \dot{M}_f \cdot \left(\frac{(1-f_S)}{f_S} - \frac{(1-f_f)}{f_f} \right) - C_1 \cdot \frac{(1-f_S)}{f_S} + C_2 \tag{3.37}$$

where

$$C_2 = 15.4249 \text{ t/h} \tag{3.38}$$

Therefore, we have our solution set

$$U=\left\{\begin{array}{l} x_1=\dot{M}_S=-\dot{M}_f+C_1 \quad ,C_1=27.5019 \\ x_2=\dot{M}_f=b\ ,b\in R, b\geq 0 \\ x_3=\dot{M}_R=8.4983 \\ x_4=\dot{M}_W=\dot{M}_f\cdot\left(\dfrac{(1-f_S)}{f_S}-\dfrac{(1-f_f)}{f_f}\right) \\ \qquad\qquad -C_1\cdot\dfrac{(1-f_S)}{f_S}+C_2 \quad ,C_2=15.4249 \\ x_5=M_{SR}=13.413 \\ x_6=M_{RR}=4.1446 \\ x_7=M_{WR}=7.5247 \\ x_8=\omega_p=962.0197 \end{array}\right\} \tag{3.39}$$

From the set *U*, we could see that there are infinite many equilibrium points. The filter flow rate is being chosen as a free variable to accommodate changes and disturbances of the system. As long as the dry filter mass flow rate is less than or equal to 27.5019 t/hr, the system would work fine. Mathematically, it means:

$$0\leq\dot{M}_{fdry}\leq 27.5019 \tag{3.40}$$

But one has to also note that the total volume of water from Strathcona slurry, filter cakes and water input could not exceed 15.4249 t/hr. Otherwise, the density % of the total amount of Strathcona and Raglan in the tank would be less than the optimal density set point, 70%. Hence we need to constrain the total amount of water given by Strathcona slurry and its filter cakes to the Repulper tank. We can separate the wet Strathcona slurry flow-rate and its solids density separately rather than just expressing the dry Strathcona flow rate as a result. We would do the same thing to the filter cakes as well. Then we have a set of new equations:

$$\tilde{x}_1 = \dot{M}_{Swet} = \frac{(-f_f \cdot \dot{M}_{fwet} + C_1)}{f_S} \quad , C_1 = 27.5019 \tag{3.41}$$

$$\frac{(-f_f \cdot \dot{M}_{fwet} + 27.5019)}{f_S} \geq 0 \tag{3.42}$$

$$f_f \cdot \dot{M}_{fwet} \leq 27.5019 \tag{3.43}$$

Multiplying on both sides with $\frac{(1-f_f)}{f_f}$, we get:

$$\frac{(1-f_f)\cdot f_f}{f_f} \cdot \dot{M}_{fwet} \leq \frac{(1-f_f)\cdot 27.5019}{f_f} \tag{3.44}$$

$$\frac{(1-f_f)\cdot 27.5019}{f_f \cdot \dot{M}_{fwet}} \geq (1-f_f) \tag{3.45}$$

Also, an alternative expression for the flow rate of water is given as follows:

$$\begin{aligned} x_4 = \dot{M}_W = (&\frac{(f_f \cdot M_{fwet} + f_s \cdot M_{Swet})\cdot(1-f_m)}{f_m}) \\ &-((1-f_f)\cdot \dot{M}_{fwet} + (1-f_S)\cdot M_{Swet}) \end{aligned} \tag{3.46}$$

Since the water flow rate needed is constant with respect to the fixed Raglan input. And we know the total dry mass of Strathcona has to be equal to (1/0.309) times the Raglan powder in order to keep the Raglan to Strathcona ratio the same. Moreover, we require the total dry solids density, f_m, to be set at 70%. Hence we can replace

$$(\frac{(f_f \cdot M_{fwet} + f_s \cdot M_{Swet}) \cdot (1 - f_m)}{f_m}) \tag{3.47}$$

with 15.4249 tonnes/hr. Then (3.46) is simplified to:

$$x_4 = 15.4249 - ((1 - f_f) \cdot \dot{M}_{fwet} + (1 - f_S) \cdot M_{Swet}) \geq 0 \tag{3.48}$$

There is one problem. Since the filter cakes are poured into the Repulper tank with a mechanical delivery system which could not guarantee the exact amount that it does pour into the tank. Moreover, the filter cake solid density, f_f, is estimated with a range only. No exact measurements on the amount of filter cake that is being put in or the percentage of solids in the cake are available. Under these circumstances, it would be unreliable to rely on filter cakes to compensate the changes of solid %, f_S, in Strathcona Slurry. To resolve this dilemma, we should revisit our equations and put the flow rate of Strathcona as the free variable instead, while eliminating the contribution from the filter cakes at all. The following section deals with this simplified case.

3.5 Feedforward Scheme with Zero Input from Filter Cake

We would have new a new set of equations evolved from (3.41) and (3.46).

$$\hat{x}_1 = \dot{M}_{Swet} = \frac{27.5019}{f_S} \tag{3.49}$$

$$x_4 = \dot{M}_W = \left(\frac{(f_s \cdot M_{Swet}) \cdot (1 - f_m)}{f_m} \right) - (1 - f_S) \cdot M_{Swet} \tag{3.50}$$

Again we would set

$$\frac{(f_s \cdot M_{Swet}) \cdot (1 - f_m)}{f_m} = 15.4249 \tag{3.51}$$

Then (3.50) would be simplified to:

$$x_4 = \dot{M}_W = 15.4249 - (1 - f_S) \cdot M_{Swet} \tag{3.52}$$

Let us replace the Strathcona slurry flow rate in (3.52) with (3.49) and we require that the flow of water from water pipe to be greater than or equal to zero. Hence, we have:

$$x_4 = \dot{M}_W = 15.4249 - \frac{27.5019 \cdot (1 - f_S)}{f_S} \geq 0 \tag{3.53}$$

Solving f_S from (3.53), then the range of the solids %, f_S, of Strathcona slurry as which satisfy the inequality is obtained and we have:

$$f_S \geq \frac{27.5019}{42.9268} = 0.6407 \tag{3.54}$$

Equation (3.54) has a significant meaning to our control problem. It greatly simplifies the whole control operation. We have succeeded in transforming solving mixed differential equations and algebraic equations at equilibrium into two simple algebraic control equations (3.51) and (3.52) and one inequality constraint (3.54).

In addition, (3.54) means that if the slurry solids %, f_S is greater than 64.07%, we have 100% control of the system to have the system always stay in its optimal and equilibrium states. Recall that our collection of equilibrium states is the set U. In our simplified case where flow of filter cakes is set to be zero, we form another subset:

$$\tilde{U} \subset U \tag{3.55}$$

and it contains:

$$\tilde{U} = \left\{ \begin{array}{l} x_1 = \dot{M}_{Sdry} = 27.5019 \\ x_2 = \dot{M}_f = 0 \\ x_3 = \dot{M}_R = 8.4983 \\ x_4 = \dot{M}_W = 15.4249 - \dfrac{27.5019 \cdot (1 - f_S)}{f_S} \quad ,1.0 \geq f_S \geq 0.6407 \\ x_5 = M_{SR} = 13.413 \\ x_6 = M_{RR} = 4.1446 \\ x_7 = M_{WR} = 7.5247 \\ x_8 = \omega_p = 962.0197 \end{array} \right\} \quad (3.56)$$

This further implies that as long as our Strathcona solids % is greater than 64.07%, we would able to achieve equilibrium always. This means we could always satisfy all the equations from (2.1) to (2.7) and thus meeting all the output set points requirements. That is, keeping output solid density %, f_m, at 70%; keeping the Repulper tank level at 2.4m, keeping the Raglan to Strathcona dry mass ratio at 0.309 and keeping output slurry flow rate at 51.43t/h.

However, in reality the Strathcona solids % varies from 58% to 68%. When f_S is below 64.07%, we have to turn on the unpredictable filter cake operations. But once we turn on the filters cakes, we need to consider the variability of the quality (f_f , the solids %) and the quantity inevitably. This is why we need to go into feedback control using the output measurements to estimate the amount of Strathcona that has contributed from the filter cakes and the amount of water it contributes to the total amount of water in the Repulper tank. This has made the whole analysis even more interesting.

Linear system analysis is a well-established rich area which can asses various characteristics of a linear system. To have a deeper understanding into a nonlinear system, it is also useful to linearize a nonlinear system at its operating points, and then subject it to linear system analysis. Moreover, there are well-established MIMO linear

control tools which is based on a linear system. In the next chapter, we are going to linearize the system at the system's operating points and hence, we can understand further the nonlinear system's characteristics through the point of a view of its linearized version.

Chapter 4

Linearization of Existing Repulper Tank Process

4.1 Introduction

To linearize a system, we need to determine the point of linearization. Most linear control strategies require linearization at an equilibrium point, else gain scheduling might need to be employed. But the stability of gain switching from one set of operating points to another is not well understood and defined. Hence, it is better to use linear control strategies at only one equilibrium point.

The original system has just a Repulper tank. Consequently, there are infinite sets of equilibrium points. Therefore, even though linearization can be carried out at one point, the parameter variations of the inputs can greatly disturb the final stability of the linear controller. This is because the linear controller at the end will be put into the nonlinear scenario as well for full simulation. Hence, if the parameters of the inputs vary significantly as they do, then the linear controller may fail.

Hence, it is important to position the system at only one set of equilibrium points. This is feasible only if the linearized system is not being subjected to parameter variations once it is put back in the nonlinear setting. As then the system's conditions do not vary with time, it then becomes a time invariant system. Then, lots of advanced control strategies that are based on linear time invariant models can be used, e.g. PID control, feedback pole placement, H_2 optimal control etc.

Before we establish the linear system, we should answer two fundamental questions:

1. Is the steady state reachable by the system? If it is reachable and hence exists, then is it unique?
2. The second important question to answer is the internal stability problem. It is important to know whether the linearized system at a particular equilibrium point is stable or not. If there exists more than one equilibrium point, how do we determine which equilibrium points are stable?

The answer to the first question has been answered by the optimization solution in Chapter 3. Yes, we do have steady state, that is all variables (state and input variables) are unchanged and yet maintain a dynamic balance. To see if the steady state is reachable or not, we simply operate our system inputs with the inputs in the solution set, U. Then we would be able to attain the steady state. From our solutions of the optimization, since we have 7 equations and 8 unknowns we have an infinite set of solutions and our solution set is stated in (3.39):

$$U = \left\{ \begin{array}{ll} x_1 = \dot{M}_S = -\dot{M}_f + C_1 & , C_1 = 27.5019 \\ x_2 = \dot{M}_f = b & , b \in R, b \geq 0 \\ x_3 = \dot{M}_R = 8.4983 & \\ x_4 = \dot{M}_W = \dot{M}_f \cdot \left(\frac{(1-f_S)}{f_S} - \frac{(1-f_f)}{f_f} \right) - C_1 \cdot \frac{(1-f_S)}{f_S} + C_2 & , C_2 = 15.4249 \\ x_5 = M_{SR} = 13.4130 & \\ x_6 = M_{RR} = 4.1446 & \\ x_7 = M_{WR} = 7.5247 & \\ x_8 = \omega_p = 962.0197 & \end{array} \right\}$$

To answer the second question, we need to study the stability of the *A* matrix of the liinearized system at a particular equilibrium point. The *A* matrix of a linearized system is obtained from the Jacobian of the nonlinear state equation evaluated at an equilibrium point. Since we do have an infinite number of equilibrium points, it is difficult to study the stability of each one of them. The calculations of the respective Jacobian and determination of the stability criteria are done in the next few sections.

Going back to our nonlinear system, if we linearize it at the equilibrium point, then we should be able to analyze the nonlinear system in the simplified form as long as our state variables are close to the set *U*, the solution set. We could also determine the effects of disturbances to the system.

If we allow the filter cakes dry mass to be a disturbance, we would like to design our linear system to counter balance any disturbance caused by the filter cakes. We could get perfect control if our Strathcona slurry density is above 64.07%. Our analysis in this chapter would only limit to these situations. When we have Strathcona slurry density bigger or equal to 64.07%, we would not need filter cake contribution at all. We would hence linearize our system with zero contribution from the filter cakes. Then any filter cakes contribution due to mechanical system error would then be regarded as disturbance

in the linear analysis. We should first visit some of the basic theories and justification of linearization. The next section is largely based on [Bélanger, 1995].

4.2 Theoretical Basics of Linearization

This subsection has lots of fundamental materials which could have been put at the appendix. However, since there are important points of discussions of the reachability of the system during the discussion of linearization, it is then decided to include this subsection so that the whole linearization issue can be discussed more thoroughly.

If we start with a set of nonlinear equations of states and outputs, expressed in vectors form, where $f, h, \dot{x}, x, u$ and y are vectors:

$$\dot{x} = f(x,u) \tag{4.1}$$

$$y = h(x,u) \tag{4.2}$$

For '$u=u^*$' and '$x=x^*$', the system is in an *equilibrium state* whenever

$$f(x^*, u^*) = 0 \tag{4.3}$$

which to our system, P, means we want the rate of changes of mass of the three state variables be zero. The equilibrium states exist if there exist x^*, and u^* which would satisfy (4.1). As we have already seen in Chapter 3, our solution for our plant P does exist. Also we would like to set our desired outputs, the respective set points, as y^*. We would require that the same x^* and u^* that manages to have the function f map to 0 also would have the function h map to y^*. This condition is stated as:

$$h(x^*, u^*) = y^* \tag{4.4}$$

If the states are reachable to x^* and the inputs are physically feasible to be in u^*, then we could state that the system has a feasible equilibrium. Now, with the reachability assumption of the states, we would like to devise a perturbed linear model of the nonlinear system by the incremental method. When the states are being perturbed by the corresponding increments of inputs, the outputs would be deviated as well. This could be shown as follows:

$$x(t) = x^* + \Delta x(t) \tag{4.5}$$

$$u(t) = u^* + \Delta u(t) \tag{4.6}$$

$$y(t) = y^* + \Delta y(t) \tag{4.7}$$

By substituting (4.5), (4.6) and (4.7) into (4.1), (4.2), and noting that $\dot{x}^* = 0$ we get:

$$\dot{x}(t) = f(x^* + \Delta x, u^* + \Delta u) \tag{4.8}$$

$$y(t) = h(x^* + \Delta x, u^* + \Delta u) \tag{4.9}$$

or we get:

$$\Delta\dot{x}(t) = f(x^* + \Delta x, u^* + \Delta u) \tag{4.10}$$

$$\Delta y(t) = h(x^* + \Delta x, u^* + \Delta u) - y^* \tag{4.11}$$

We could then expand $f(\cdot)$ by using Taylor series and we get

$$f_i(x^* + \Delta x, u^* + \Delta u) = f_i(x^*, u^*) + \frac{\partial f_i}{\partial x_1}|_* \Delta x_1 + \frac{\partial f_i}{\partial x_n}|_* \Delta x_n + \ldots \frac{\partial f_i}{\partial u_1}|_* \Delta u_1 + \frac{\partial f_i}{\partial u_r}|_* \Delta u_r + \textit{higher order terms in } \Delta x \textit{ and } \Delta u, i = 1, \ldots, n \quad (4.12)$$

Also, since $f_i(x^*, u^*) = 0$ then we could write (4.10) as :

$$\Delta \dot{x} = \frac{\partial f}{\partial x}|_* \Delta x + \frac{\partial f}{\partial u}|_* \Delta u \quad (4.13)$$

where $\frac{\partial f}{\partial x}$ *is the Jacobian of* f *with respect to* x and is equal to:

$$\frac{\partial f}{\partial x} = \begin{bmatrix} \frac{\partial f_1}{\partial x_1} & \frac{\partial f_1}{\partial x_2} & \cdots & \frac{\partial f_1}{\partial x_n} \\ \frac{\partial f_2}{\partial x_1} & \frac{\partial f_2}{\partial x_2} & \cdots & \frac{\partial f_2}{\partial x_n} \\ \vdots & & & \\ \frac{\partial f_n}{\partial x_1} & \cdots & \cdots & \frac{\partial f_n}{\partial x_n} \end{bmatrix} \quad (4.14)$$

Similarly, $\frac{\partial f}{\partial u}$ *is the Jacobian of* f *with respect to* u.

In the same way as *f(·)*, when we expand *h(·)* , we will get the same Jacobian terms, $(\frac{\partial h}{\partial x}, \frac{\partial h}{\partial u})$, as well.

$$h_i(x^* + \Delta x, u^* + \Delta u) = h_i(x^*, u^*) + \frac{\partial h_i}{\partial x_1}|_* \Delta x_1 + \frac{\partial h_i}{\partial x_n}|_* \Delta x_n + \\ + \ldots \frac{\partial h_i}{\partial u_1}|_* \Delta u_1 + \frac{\partial h_i}{\partial u_r}|_* \Delta u_r \qquad (4.15) \\ + \textit{higher order terms in } \Delta x \textit{ and } \Delta u, i = 1, \ldots p$$

But since $y^* = h_i(x^*, u^*)$, we have the following when we substitute (4.15) into (4.11):

$$\Delta y = \frac{\partial h}{\partial x}|_* \Delta x + \frac{\partial h}{\partial u}|_* \Delta u \qquad (4.16)$$

again where $\frac{\partial h}{\partial x}$ *is the Jacobian of h with respect to x* and,

$\frac{\partial h}{\partial u}$ *is the Jacobian of h with respect to u*.

In the following subsection, the original system's state equations and the modified output equations will form the modified equations. The modified equations are the same as those used in the nonlinear formulation in the previous chapter.

The changes between the original output equations (2.4) to (2.7) and the new output equations are many. Although the first output, the total solids density output is the same, the second output equation, the ratio of Raglan and Strathcona, is not used as it is not measurable. Also since measuring the tank level is subject to errors caused by the turbulence at the surface of the solution in the tank, total masses of the tank is used as the output instead. Total masses, as mentioned before in the nonlinear formulation, can be measured easily by the appropriate weight sensor. In addition, the specific gravity of the mixed mass of the solution is used as an output as well. The reasons behind this because it can be readily measured by getting the ratio of the total mass flow rate and the output

volumetric flow rate. Lastly, the output flow equation is being kept unchanged. Hence, it is interesting to see if linear control at the desired operating conditions does perform as required.

Linearization will be carried out with this new set of equations. These equations forms the system *P*.

4.3 Linearizing System *P*

In order to express the state equations more explicitly with its relations to its respective solid densities, we present the state equations of *P* using the Strathcona wet mass flow rate and the filter cakes wet mass flow rate. Hence:

$$\dot{M}_{SR} = f_S \cdot \dot{M}_S + f_f \cdot \dot{M}_f - \frac{k_{pump} \cdot \omega_p \cdot M_{SR}}{(M_{SR}/SG_S + M_{RR}/SG_R + M_{WR})} \tag{4.17}$$

$$\dot{M}_{RR} = \dot{M}_R - \frac{k_{pump} \cdot \omega_p \cdot M_{RR}}{(M_{SR}/SG_S + M_{RR}/SG_R + M_{WR})} \tag{4.18}$$

$$\dot{M}_{WR} = (1-f_S) \cdot \dot{M}_S + (1-f_f) \cdot \dot{M}_f - \frac{k_{pump} \cdot \omega_p \cdot M_{WR}}{(M_{SR}/SG_S + M_{RR}/SG_R + M_{WR})} \tag{4.19}$$

and the modified set of output equations are:

$$f_m = \frac{M_{SR} + M_{RR}}{M_{SR} + M_{RR} + M_{WR}} \tag{4.20}$$

$$M_{Tot\_Mass} = M_{SR} + M_{RR} + M_{WR} \tag{4.21}$$

$$SG_M = \frac{\left(M_{SR} + M_{RR} + M_{WR}\right)}{\left(M_{SR}/SG_S + M_{RR}/SG_R + M_{WR}\right)} \tag{4.22}$$

$$\dot{M}_{M+W} = \frac{k_p \cdot \omega_P \cdot \left(M_{SR} + M_{RR} + M_{WR}\right)}{\left(M_{SR}/SG_S + M_{RR}/SG_R + M_{WR}\right)} \tag{4.23}$$

The variables for this new set of equations are defined as follows in the next page:

$$\begin{aligned} &x_1 = M_{SR}; \quad x_2 = M_{RR}; \quad x_3 = M_{WR} \\ &u_1 = \dot{M}_S; \quad u_2 = \dot{M}_R; \quad u_3 = \dot{M}_f; \quad u_4 = \dot{M}_W; \quad u_5 = \omega_p \\ &y_1 = f_m; \quad y_2 = M_{Total}; \quad y_3 = SG_M; \quad y_4 = \dot{M}_{M+W} \end{aligned} \tag{4.24}$$

Then the nonlinear state space matrix format is:

$$\begin{bmatrix} \dot{x}_1 \\ \dot{x}_2 \\ \dot{x}_3 \end{bmatrix} = \begin{bmatrix} f_S \cdot u_1 + f_f \cdot u_2 - \dfrac{k_p \cdot u_5 \cdot x_1}{(x_1/SG_S + x_2/SG_R + x_3)} \\ u_3 - \dfrac{k_p \cdot u_5 \cdot x_2}{(x_1/SG_S + x_2/SG_R + x_3)} \\ \left(1 - f_S\right) \cdot u_1 + \left(1 - f_f\right) \cdot u_2 + u_4 - \dfrac{k_p \cdot u_5 \cdot x_3}{(x_1/SG_S + x_2/SG_R + x_3)} \end{bmatrix}$$

$$\begin{bmatrix} y_1 \\ y_2 \\ y_3 \\ y_4 \end{bmatrix} = \begin{bmatrix} \dfrac{x_1 + x_2}{x_1 + x_2 + x_3} \\ x_1 + x_2 + x_3 \\ \dfrac{\left(x_1 + x_2 + x_3\right)}{\left(x_1/SG_S + x_2/SG_R + x_3\right)} \\ \dfrac{k_p \cdot u_5 \cdot \left(x_1 + x_2 + x_3\right)}{\left(x_1/SG_S + x_2/SG_R + x_3\right)} \end{bmatrix} \tag{4.25}$$

Then the following partial derivatives $\frac{\partial f}{\partial x}, \frac{\partial f}{\partial u}, \frac{\partial h}{\partial x}, \frac{\partial h}{\partial u}$ are calculated:

$$\frac{\partial f}{\partial x} =$$

$$\begin{bmatrix} \dfrac{\left\{-k_p \cdot u_5 \cdot \left(x_2 / SG_R + x_3\right)\right\}}{\left(x_1 / SG_S + x_2 / SG_R + x_3\right)^2} & \dfrac{\left\{k_p \cdot u_5 \cdot x_1 / SG_R\right\}}{\left(x_1 / SG_S + x_2 / SG_R + x_3\right)^2} & \dfrac{\left\{k_p \cdot u_5 \cdot x_1\right\}}{\left(x_1 / SG_S + x_2 / SG_R + x_3\right)^2} \\ \dfrac{k_p \cdot u_5 \cdot x_2 / SG_S}{\left(x_1 / SG_S + x_2 / SG_R + x_3\right)^2} & \dfrac{\left\{-k_p \cdot u_5 \cdot \left(x_1 / SG_S + x_3\right)\right\}}{\left(x_1 / SG_S + x_2 / SG_R + x_3\right)^2} & \dfrac{k_p \cdot u_5 \cdot x_2}{\left(x_1 / SG_S + x_2 / SG_R + x_3\right)^2} \\ \dfrac{k_p \cdot u_5 \cdot x_3 / SG_S}{\left(x_1 / SG_S + x_2 / SG_R + x_3\right)^2} & \dfrac{\left\{k_p \cdot u_5 \cdot x_3 / SG_R\right\}}{\left(x_1 / SG_S + x_2 / SG_R + x_3\right)^2} & \dfrac{\left\{-k_p \cdot u_5 \cdot \left(x_1 / SG_S + x_2 / SG_R\right)\right\}}{\left(x_1 / SG_S + x_2 / SG_R + x_3\right)^2} \end{bmatrix} \tag{4.26}$$

$$\frac{\partial f}{\partial u} =$$

$$\begin{bmatrix} f_S & f_f & 0 & 0 & \dfrac{-k_p \cdot x_1}{\left(x_1 / SG_S + x_2 / SG_R + x_3\right)} \\ 0 & 0 & 1 & 0 & \dfrac{-k_p \cdot x_2}{\left(x_1 / SG_S + x_2 / SG_R + x_3\right)} \\ 1 - f_S & 1 - f_f & 0 & 1 & \dfrac{-k_p \cdot x_3}{\left(x_1 / SG_S + x_2 / SG_R + x_3\right)} \end{bmatrix} \tag{4.27}$$

$$\frac{\partial h}{\partial x} =$$

$$\begin{bmatrix} \frac{x_3}{(x_1+x_2+x_3)^2} & \frac{x_3}{(x_1+x_2+x_3)^2} & \frac{-(x_1+x_2)}{(x_1+x_2+x_3)^2} \\ 1 & 1 & 1 \\ \frac{\left\{\begin{matrix} x_2 \cdot \\ \begin{pmatrix} 1/SG_R \\ -1/SG_S \end{pmatrix} \\ +x_3 \cdot (1-1/SG_S) \end{matrix}\right\}}{\begin{pmatrix} x_1/SG_S + \\ x_2/SG_R + x_3 \end{pmatrix}^2} & \frac{\left\{\begin{matrix} x_1 \\ \cdot \begin{pmatrix} 1/SG_S \\ -1/SG_R \end{pmatrix} \\ +x_3 \\ \cdot (1-1/SG_R) \end{matrix}\right\}}{\begin{pmatrix} x_1/SG_S + \\ x_2/SG_R + x_3 \end{pmatrix}^2} & \frac{\left\{\begin{matrix} x_1 \cdot \\ (1/SG_S - 1) \\ +x_2 \cdot \\ (1/SG_R - 1) \end{matrix}\right\}}{\begin{pmatrix} x_1/SG_S + \\ x_2/SG_R + x_3 \end{pmatrix}^2} \\ \frac{\left\{\begin{matrix} k_p \cdot u_5 \cdot \\ \left\{\begin{matrix} x_2 \cdot \begin{pmatrix} 1/SG_R - \\ 1/SG_S \end{pmatrix} \\ +x_3 \cdot \begin{pmatrix} 1- \\ 1/SG_S \end{pmatrix} \end{matrix}\right\} \end{matrix}\right\}}{\begin{pmatrix} x_1/SG_S + \\ x_2/SG_R + x_3 \end{pmatrix}^2} & \frac{\left\{\begin{matrix} k_p \cdot u_5 \cdot \\ \left\{\begin{matrix} x_1 \cdot \begin{pmatrix} 1/SG_S \\ -1/SG_R \end{pmatrix} \\ +x_3 \cdot \begin{pmatrix} 1- \\ 1/SG_R \end{pmatrix} \end{matrix}\right\} \end{matrix}\right\}}{\begin{pmatrix} x_1/SG_S + \\ x_2/SG_R + x_3 \end{pmatrix}^2} & \frac{\left\{\begin{matrix} k_p \cdot u_5 \\ \cdot \left\{\begin{matrix} x_1 \cdot \\ \begin{pmatrix} 1/SG_S - \\ 1 \end{pmatrix} \\ +x_2 \cdot \\ (1/SG_R - 1) \end{matrix}\right\} \end{matrix}\right\}}{\begin{pmatrix} x_1/SG_S + \\ x_2/SG_R + x_3 \end{pmatrix}^2} \end{bmatrix} \quad (4.28)$$

$$\frac{\partial h}{\partial u} =$$

$$\begin{bmatrix} 0 & 0 & 0 & 0 & 0 \\ 0 & 0 & 0 & 0 & 0 \\ 0 & 0 & 0 & 0 & 0 \\ 0 & 0 & 0 & 0 & \frac{k_p \cdot (x_1+x_2+x_3)}{(x_1/SG_S + x_2/SG_R + x_3)} \end{bmatrix} \quad (4.29)$$

Since we are linearizing the system at the desired operating set points, the partial derivatives are evaluated at those points to get the equivalent system matrices:

A, *B*, *C*, *D*.

$$A = \frac{\partial f}{\partial x}|_{*} \tag{4.30}$$

$$B = \frac{\partial f}{\partial u}|_{*} \tag{4.31}$$

$$C = \frac{\partial h}{\partial x}|_{*} \tag{4.32}$$

$$D = \frac{\partial h}{\partial u}|_{*} \tag{4.33}$$

Note that the notation '$|_{*}$' in the above equations means that the partial derivatives are evaluated at the equilibrium point. Then, the perturbed state space model can be formed:

$$\Delta\dot{x} = A \cdot \Delta x + B \cdot \Delta u \tag{4.34}$$

$$\Delta y = C \cdot \Delta x + D \cdot \Delta u \tag{4.35}$$

$$\begin{bmatrix}\Delta\dot{x}_1\\ \Delta\dot{x}_2\\ \Delta\dot{x}_3\end{bmatrix}=\begin{bmatrix}-1.4972 & 0.5997 & 2.3389\\ 0.1732 & -1.8687 & 0.7232\\ 0.3123 & 0.3364 & -0.7423\end{bmatrix}\begin{bmatrix}\Delta x_1\\ \Delta x_2\\ \Delta x_3\end{bmatrix}$$

$$+\begin{bmatrix}0.6500 & 0.8000 & 0 & 0 & -0.0286\\ 0 & 0 & 1.0000 & 0 & -0.0088\\ 0.3500 & 0.2000 & 0 & 1.0000 & -0.0088\end{bmatrix}\begin{bmatrix}\Delta u_1\\ \Delta u_2\\ \Delta u_3\\ \Delta u_4\\ \Delta u_5\end{bmatrix}$$

$$\begin{bmatrix}y_1\\ y_2\\ y_3\\ y_4\end{bmatrix}=\begin{bmatrix}0.0120 & 0.0120 & -0.0280\\ 1.0000 & 1.0000 & 1.0000\\ 0.0419 & 0.8386 & -0.096\\ 1.0127 & 0.9326 & -2.3198\end{bmatrix}\begin{bmatrix}\Delta x_1\\ \Delta x_2\\ \Delta x_3\end{bmatrix}$$

$$+\begin{bmatrix}0 & 0 & 0 & 0 & 0\\ 0 & 0 & 0 & 0 & 0\\ 0 & 0 & 0 & 0 & 0\\ 0 & 0 & 0 & 0 & 0.0535\end{bmatrix}\begin{bmatrix}\Delta u_1\\ \Delta u_2\\ \Delta u_3\\ \Delta u_4\\ \Delta u_5\end{bmatrix} \tag{4.36}$$

This new perturbed model forms the perturbed plant system:

$$Z=\begin{bmatrix}A & B\\ C & D\end{bmatrix} \tag{4.37}$$

With:

$$A=\begin{bmatrix}-1.4972 & 0.5997 & 2.3389\\ 0.1732 & -1.8687 & 0.7232\\ 0.3123 & 0.3364 & -0.7423\end{bmatrix} \tag{4.38}$$

$$B = \begin{bmatrix} 0.6500 & 0.8000 & 0 & 0 & -0.0286 \\ 0 & 0 & 1.0000 & 0 & -0.0088 \\ 0.3500 & 0.2000 & 0 & 1.0000 & -0.0088 \end{bmatrix} \quad (4.39)$$

$$C = \begin{bmatrix} 0.0120 & 0.0120 & -0.0280 \\ 1.0000 & 1.0000 & 1.0000 \\ 0.0419 & 0.8386 & -0.096 \\ 1.0127 & 0.9326 & -2.3198 \end{bmatrix} \quad (4.40)$$

$$D = \begin{bmatrix} 0 & 0 & 0 & 0 & 0 \\ 0 & 0 & 0 & 0 & 0 \\ 0 & 0 & 0 & 0 & 0 \\ 0 & 0 & 0 & 0 & 0.0535 \end{bmatrix} \quad (4.41)$$

Since, now our perturbed Z model is linear, it is then needed to further confirm that Z is time invariant as well. Since the original system P is a time invariant system, that is as described in [Oppenheim et al, 96], a time shift in the input signal results in an identical time shift in the output signal, the perturbed Z model shall be time invariant as well. This is because the process of mixing does not change from one day to another. The results of the mixing depend solely on the inputs and the state values in the tank. Hence, Z is a time invariant system. With a time invariant system, there are lots of tools to uncover the intrinsic properties of Z. These properties include observability, controllability, stability etc. They are discussed in the next subsection.

4.4 Properties of *Z*

i) Observability:

According to [Bélanger,1995], the theorem states that an LTI system is observable if and only if it has unobservable states. This implies that non-zero states should be mapped to

non-zero outputs. To determine if a system is observable, it is to determine, by theorem, if there is a state x^* such that

$$\begin{bmatrix} C \\ CA \\ \vdots \\ CA^{n-1} \end{bmatrix} x^* = 0 \qquad (4.42)$$

The above theorem has an important geometric interpretation. As stated in [Belanger, 1995], it is feasible to find such a state which is orthogonal to all rows of the above matrices. However, this is possible only if the rows of (4.42), considered as n-vectors, do not span the full *n*-dimensional space. This means that if the row vectors (4.42) has rank less than *n*, then it is possible to find such a vector which is orthogonal to all rows. Hence, the necessary and sufficient condition for observability is:

$$rank \begin{bmatrix} C \\ CA \\ \vdots \\ CA^{n-1} \end{bmatrix} = n \qquad (4.43)$$

Following the above test (4.43), it is found that the *Z* does have a full rank, three. Hence, *Z* is observable.

ii) Controllability

As stated in [Bélanger, 1995], if there is any state which cannot be obtained by the appropriate mapping of the input, as in the case of zero-state response, then the LTI system is deemed be uncontrollable. Similar to the idea of observability, to determine controllability of an LTI system is to find a state x^*, which is orthogonal to all the row vectors of the following matrix:

$$\begin{bmatrix} B^T \\ B^T A^T \\ \vdots \\ B^T \left(A^T\right)^{n-1} \end{bmatrix} x^* = 0 \qquad (4.44)$$

Hence, by transposing, with the similar reasoning as in the observability test in (4.43), the system is controllable if

$$rank\begin{bmatrix} B & AB & \ldots & A^{n-1}B \end{bmatrix} = n \qquad (4.45)$$

Following the above test (4.45), it is found that Z does have a full rank, three. Hence, Z is controllable.

iii) Stability

a) Internal Stability

As from [Sarachik, 1997], there are two types of internal stability, (uniformly) stable which is defined as:

$$\exists \gamma > 0 \rightarrow \left\{ \forall x_0 \in R^n : \| x(t) \| \leq \gamma \| x_0 \| \right\} \qquad (4.46)$$

Also as in [Sarachik, 1997], an LTI system is stable if and only if all eigenvalues of A are in closed left half plane. In addition, if there is any eigenvalue on the jω-axis, the multiplicity of the zero eigenvalue can only be one. If all eigenvalues of A are in the open left plane, i.e. all eigenvalues have their real parts strictly less than zero, then the system is said to be asymptotically stable. Asymptotically

stability requires both Lyapunov stability and convergence. That is all states are vanishing to zero as time goes to infinity, when there are no inputs. Internal stability requires asymptotic stability. Hence, if a system is not asymptotically stable, it is not internally stable. Coming back to the process system itself, *P* is a nonlinear system. It is important to remember that the system inputs includes both the incoming mass flow rates of the substrates and the pump speed of the pump which pumps the mixed substrate out of the Repulper tank. Hence if the inputs are zero, this means nothing coming in and nothing going out, then the changes of the state variables are definitely zero. Hence, in zero-input situation, the system should be Lyapunov stable. It is not asymptotically stable however as the masses in the mixing tank does not vanish if there are no inputs and the pump does not draw any output. Intuitively, the uniform stability of *P* shall pass on to its perturbed model, *Z*. That is the perturbed model should be uniformly stable as well. The eigenvalues of our perturbed Z are:

$$eig(A) = \begin{bmatrix} -2.0541 \\ 0 \\ -2.0541 \end{bmatrix} \qquad (4.47)$$

By the above theorem, this system is deemed as uniformly stable in the Lyapunov sense as two eigenvalues are strictly less than zero and the eigenvalue located at the jω-axis does not have multiplicity more than one. This matches with our intuitive hypothesis before. However, system *Z* is not asymptotically stable, and hence is not internally stable. Also, note that there is an interesting fact about the system where two negative eigenvalues are equal. There are many hypothesis of this interesting founding, however they do not give a conclusive property of the system and has yet to be discovered.

b) Input-Output Stability

As stated in [Bélanger, 1995], by definition, an LTI system is input-output stable if the zero-state output is bounded for all bounded inputs. Further, a system is input output stable if its transfer function has all its poles in the open left half plane. However, there can be pole-zero cancellations in the transfer functions. Unstable poles might be cancelled out by the zeros and thus 'hidden' in the transfer function. This refers to the cases of non-minimal realization. Hence if the realization is not minimal, then a system is input-output stable if the unstable poles can be cancelled out by the zeros of its transfer function. In terms of a multi-input multi-output system, the necessary and sufficient condition for the system to be input-output stable is that all the individual elements of the transfer function have all their poles in the open left half-plane. In fact, if an 'LTI' system is internally stable, it is also input-output stable. Since Z is internally unstable and minimal, it should then be input-output unstable. This fact is being further confirmed from the analysis of the elements of the transfer function.

In conclusion of this section (4.4), from all the above discussion, it is found that the perturbed system Z is uniformly stable, observable and controllable. But, unfortunately, Z is not internally stable. After we investigated the stability of the linearized system, Z of plant P**,** we have a deeper understanding in the intrinsic stability properties of the solution. Now, we shall be in better position in controller design. First of all, we are going to do the nonlinear control design, then linear control design would follow at the end. Meanwhile, we are going to visit the introductory theory of nonlinear control design, input-output linearization and switching control in the next chapter.

Chapter 5

Nonlinear Control Theory & System Analysis

5.1 Nonlinear Control Theory Overview

After understanding more deeply the nature of the system by linearizing our nonlinear system in the last chapter, we are going to establish the basics of nonlinear control theory. Moreover, nonlinear analysis of the existing Repulper tank process is addressed in this chapter.

In the original Falconbridge report, three independent SISO (Single-Input-Single-Output) linear controllers are used to control the system. There are Repulper tank level PI controller, Raglan to Strathcona ratio PI controller and density PI controller. The PI

controllers are designed by using the linearized plant *P* operated at the nominal operating points. The PI controllers are designed in Laplace domain to have good stability properties and satisfactory performance.

This original design has attained success in achieving the design objectives. However, when Strathcona slurry density's incoming density is lower than the critical point, 64.067%, the controllers cannot operate in this situation. Besides, since the system has multiple inputs and multiple outputs in nature, independent controllers might cause conflicts. It is then a dilemma to decide on the respective control decisions to satisfy all tracking objectives. Moreover, stability of the MIMO system using SISO independent controllers has not been proved and hence might be jeopardized. Consequently, it is desirable to design a MIMO (Multi-Input-Multi-Output) controller which can take into account the complexities of the system and produce control actions which can attain all control objectives at the same time. There are MIMO control techniques in both nonlinear and linear settings.

The original SISO controllers are linear and they are based on linearizing the original nonlinear system at a specific set of operating conditions. However, this linearization has neglected the fact that the original nonlinear system has uncertain values such as the specific gravities of Strathcona and Raglan. Hence, to control the system in a more basic way is to return back to the original nonlinear system. To be able to control a system at its original nonlinear nature is a challenge. Since nonlinear systems are non-uniform, there is hardly any unified theory which could completely characterize nonlinear systems in general. The development of Lyapunov theory was a major breakthrough in determining the stability of a very large class of nonlinear systems. However, it is difficult to have one single nonlinear control method which can apply successfully in all nonlinear circumstances.

Nevertheless, the advantage of a nonlinear control formulation is that it does not require the system to operate at a specific set of operating points. Due to the varied parametric nature of the density of the incoming Strathcona slurry, nonlinear controllers seem to be

more advantageous. But the drawback of utilizing nonlinear controllers is that it is often difficult to formulate the controllers systematically.

On the other hand, linear controllers have been developed much more systematically in the last thirty years. From the development of H_∞ theory by George Zames to its continuation in the development of μ-synthesis, linear systems control theory has had a great success. One of the crucial propelling forces behind the advancement of linear control theory is the advance of the development of linear systems theory. However, as most real systems are nonlinear in nature, linearizing a nonlinear system at a specific operating point can only stabilize the system at that specific set of operating conditions with small perturbations. Even though "Gain-Scheduling" seems to work properly if the operating sets are finite, there is not yet mathematical proof of the stability of using gain scheduling when the system switches from one control scheduler to another.

In the past twenty years, there is a new prominent nonlinear control methods which tries to build the link between inputs to state and inputs to outputs. The more popular one is "Input-Output linearization". In this study this nonlinear control analysis and design method is being used. In addition, this is to compare with a simple nonlinear feedback control scheme which is being developed in this study. The general theory of these two nonlinear control design strategies is introduced in the next section. Robustness capabilities are also evaluated and developed to overcome model uncertainties when applicable. Linear control design issues are dealt with afterwards.

5.1.1 Theory of Input-Output Linearization

5.1.1.1 Introductory Theory of Input-Output Linearization

Prof. Alberto Isidori developed "Input-to-state linearization and input-to-output linearization" in the 1980's, at the University of Rome in Italy. Input-to-state linearization is essentially a coordinate transformation which present inputs with respect

to states. That is, it tries to express the inputs explicitly in terms of the states. However, generally, due to the rich characteristics of nonlinear equations, the existence of such a transformation is not guaranteed. Hence, in the scope of this study, the focus is to utilize input-output linearization. It comes as a further development of input-to-state linearization. From the paper of [A. Isidori, 1995], the idea is to develop a mapping, or a coordinate transformation which states the relationships between input and output explicitly with the states being eliminated. Since this transformation involves the gradients of the output functions, it is called a differential diffeomorphism. If this transformation is valid for the whole space spanned by the states, then it is called "global diffeomorphism", otherwise it is called "local diffeomorphism". Another important consequence of this transformation is that it relates the new state equations to the new input *v*. Hence nonlinear system equations are transformed into linear equations in the respective valid region. Hereafter, the respective theoretical formulation of input-output linearization is presented. For ease of understanding the basic concept, the SISO case is presented first and the MIMO formulation follows. The paper of [Sastry & Isidori, 1989] is used to describe the basic theory and formulation of SISO and MIMO formulation.

5.1.1.2 SISO Case

Firstly, considering the single-input, single-output, time-invariant state space system:

$$\begin{aligned} \dot{x} &= f(x) + g(x) \cdot u \\ y &= h(x) \end{aligned} \qquad (5.1.1.2.1)$$

with $x \in R^n$; f, g, h being smooth functions. In order to obtain a direct relationship between the respective outputs and the inputs, we differentiate y with respect to time until the inputs appear:

$$\dot{y} = L_f h + L_g h u \qquad (5.1.1.2.2)$$

where

$$L_f h(x) = \sum_{i=1}^{n} \frac{\partial h}{\partial x_i} \cdot f_i(x) \qquad (5.1.1.2.3)$$

$$L_g h(x) = \sum_{i=1}^{n} \frac{\partial h}{\partial x_i} \cdot g_i(x) \qquad (5.1.1.2.4)$$

(5.1.1.2.3) and (5.1.1.2.4) is the exact differential which is the derivative of the output functions *h(x)* along *f* and *g*. They are also called "*Lie derivatives*". In fact, what it is trying to do is to use the outputs as the new states. Hence, when the output is differentiated with respect to time, by chain rule, we get the respective new state equation:

$$\dot{y}(t) = \frac{dy}{dt} = \frac{\partial h}{\partial x} \cdot \frac{dx}{dt} = \frac{\partial h}{\partial x} \cdot [f(x(t)) + g(x(t)) \cdot u(t)] \qquad (5.1.1.2.5)$$

Then the respective control law to make (5.1.1.2.5) linear is:

$$u = \frac{1}{L_g h}\left(-L_f h + v\right) \qquad (5.1.1.2.6)$$

The above control law hence yields the linear system:

$$\dot{y} = v \qquad (5.1.1.2.7)$$

However when:

$$L_g h = 0 \qquad (5.1.1.2.8)$$

as when there is any singularity in (5.1.1.2.8), it is necessary to further differentiate the output equation to obtain:

$$\ddot{y} = L^2{}_f h + \left(L_g L_f h\right) u \tag{5.1.1.2.9}$$

where

$$L^2{}_f h = L_f \left(L_f h\right) \tag{5.1.1.2.10}$$

$$L_g L_f h = L_g \left(L_f h\right) \tag{5.1.1.2.11}$$

If (5.1.1.2.11) is not equal to zero, then the control law will become

$$u = \frac{1}{L_g L_f h}\left(-L^2{}_f h + v\right) \tag{5.1.1.2.12}$$

and the linearized system is:

$$\ddot{y} = v \tag{5.1.1.2.13}$$

One then can state the system has relative degree γ at x^o if it satisfies two conditions:

$$\begin{aligned} &i)\ L_g L^i{}_f h = 0 \ \textit{for} \forall x \ \textit{in a neighborhood of} \ x^o \\ &\quad \textit{and for} \ i = 0,...\gamma - 2 \end{aligned} \tag{5.1.1.2.14}$$

$$ii)\ L_g L^{\gamma-1}{}_f h(x^o) \neq 0 \tag{5.1.1.2.15}$$

If both (5.1.1.2.14) and (5.1.1.2.15) are valid for all x belonging to R^n, then the system is said to have a strong relative degree. Then the control law and the linear equation can be expressed generally as:

$$u = \frac{1}{L_g L^{\gamma-1}{}_f h}\left(-L^{\gamma}{}_f h + v\right) \qquad (5.1.1.2.16)$$

$$y^{(\gamma)} = v \qquad (5.1.1.2.17)$$

Now then, there exists a neighborhood U^o of x^o such that the mapping

$$T : U^o \rightarrow R^n \qquad (5.1.1.2.18)$$

has to satisfy the following two conditions:

i) T is smooth. (5.1.1.2.19)

ii) T^{-1} exists and is smooth as well. (5.1.1.2.20)

Henceforth the mapping is defined as:

$$\begin{aligned} &T_1(x) = \xi_1 \equiv h(x) = y \\ &T_2(x) = \xi_2 \equiv L_f h(x) \\ &\vdots \\ &T_\gamma(x) = \xi_\gamma \equiv L_f^{\gamma-1} h(x) \end{aligned} \qquad (5.1.1.2.19)$$

such that the mapping stated above (5.1.1.2.18) is a diffeomorphism onto its image. Moreover, if the relative degree is less than the dimensions of x, n, then in order to replenish the rest of the n-γ states, we require the mapping:

$$T_i(x) = \eta_i \quad for\ i = \gamma + 1, \ldots . n \qquad (5.1.1.2.20)$$

to be smooth and satisfies the conditions below

$$dT_i(x)g(x) = 0 \quad for\ i = \gamma + 1, \ldots . n \qquad (5.1.1.2.21)$$

It might seem that there are lots of choices of choosing the functions η_i, but indeed it is not as easy as it seems to be especially if it has to satisfy all the partial derivatives' equations as in (5.1.1.2.21). Hence they are defined as:

$$\begin{aligned} &T_{r+1}(x) = \eta_1 \\ &\vdots \\ &T_n(x) = \eta_{n-r} \end{aligned} \qquad (5.1.1.2.25)$$

The mapping can then be said to be:

$$T(x) \equiv [\xi_1, \xi_2 ..., \xi_r, \eta_1, ..., \eta_{n-r}] \qquad (5.1.1.2.26)$$

Hence then the diffeomorphism undertaken by the mapping has enabled the original nonlinear state equations (5.1.1.2.1) to be rewritten as the following new state equations, the "normal form":

$$\begin{bmatrix} \dot{\xi}_1 \\ \vdots \\ \dot{\xi}_r \\ \dot{\eta}_{n-r} \end{bmatrix} = \begin{bmatrix} \xi_2 \\ \vdots \\ \alpha(\xi,\eta) + \beta(\xi,\eta) \cdot u \\ w(\xi,\eta) \end{bmatrix} \begin{Bmatrix} \xi \equiv [\xi_1, ... \xi_r]^T, \\ \eta \equiv [\eta_1, ... \eta_{n-r}]^T \end{Bmatrix} \qquad (5.1.1.2.27)$$

To define the region of the validity of diffeomorphism is to verify the region where,

$$x = T^{-1}(T(x)), x \in U^o \qquad (5.1.1.2.28)$$

exists. If the validity region, U^o, does not contain the whole R^n, then it is a local diffeomorphism. Otherwise, it is a global diffeomorphism.

When the relative degree is less than n, the problem of "zero dynamics" needs to be verified. This is the case as when:

$$\{\xi_1,...,\xi_r\}=0 \Rightarrow \{\dot{\xi}_1,...,\dot{\xi}_r\}=0, \quad but\ \{\dot{\eta}_1,...,\dot{\eta}_{n-r}\}\neq 0 \qquad (5.1.1.2.29)$$

The above problem is partly due to the new state variables, η_i, which can be unobservable. This is because these states are created to satisfy the requirement of (5.1.1.2.21), they do not necessarily need to have any actual meanings and hence they could be non-measurable in reality. Also, from [Sastry and Isidori, 1989], if the zero-dynamics are asymptotically stable, i.e. both convergent and stable in Lyapunov sense, then the nonlinear system is said to be at minimum phase.

5.1.1.3 MIMO Case

The MIMO state space system can be presented as:

$$\dot{x}=f(x)+\sum_{i=1}^{m} g_i(x)\cdot u_i \quad x\in R^n \qquad y_j=h_j(x)\ \ j=1.....p \qquad (5.1.1.3.1)$$

There are complexities implied when there is a freedom of choice of number of inputs and outputs. First of all, there are conditions under which the input-output linearization is feasible. For a MIMO system which has n states, m inputs and p outputs, there are two basic criteria that need to be fulfilled:

(1) $p \geq n$ (5.1.1.3.2)

As stated in the paper of [Sastry & Isidori, 1989], the most important condition for input-output linearization to be feasible is the states' information be available. If the states

cannot be measured directly, information must be obtained from the output measurements. This requires the number of outputs to be greater than or at least equal to the number of states so that full state 'injective' information could be obtained.

(2) $m \geq p$ (5.1.1.3.3)

From [Kolavennu et al., 2001], if the number of outputs is greater than the number of inputs, then the system is uncontrollable.

Following the approach in [Sastry and Isidori, 1989], consider the "*n*-state", "*m*-input" and "*p*-output" nonlinear system of the form:

$$\left\{\begin{array}{l} \dot{x} = f(x) + g_1(x)u_1 + \ldots + g_m(x)u_m \\ y_1 = h_1(x) \\ \vdots \\ y_p = h_p(x) \end{array}\right\} \left\{\begin{array}{l} x \in R^n, u \in R^m, y \in R^p; \\ and\ f, g_i\ and\ h_i \\ are\ assumed\ to\ be\ smooth \end{array}\right\} \quad (5.1.1.3.4)$$

For ease of manipulation, we consider here the case of exact input-output linearization of which the number of inputs is equal to the number of outputs. Hence, *m* is equal to *p*. Then, each individual output equation, y_j, is differentiated with respect to time:

$$\dot{y}_j = L_f h_j + \sum_{i=1}^{p} \left(L_{g_i} \cdot h_j \right) u_i \quad (5.1.1.3.5)$$

Then, we define γ_j to be the smallest integer such that each individual output equation, $y^{(\gamma_j)}{}_j$, has at least one of the input terms in the equation:

$$y^{(\gamma_j)}{}_j = L^{\gamma_j}{}_f h_j + \sum_{i=1}^{p} L_{g_i} \left(L^{\gamma-1}{}_{f_i} \cdot h_j \right) u_i \quad (5.1.1.3.6)$$

Henceforth, the second term on the R.H.S. of (5.1.1.3.6) defines the following square matrix:

$$M(x)=\begin{bmatrix} L_{g_1}\left(L^{\gamma_1-1}{}_f\cdot h_1\right) & .... & L_{g_p}\left(L^{\gamma_1-1}{}_f\cdot h_1\right) \\ \vdots & & \vdots \\ L_{g_1}\left(L^{\gamma_p-1}{}_f\cdot h_p\right) & ... & L_{g_p}\left(L^{\gamma_p-1}{}_{f_i}\cdot h_p\right) \end{bmatrix}\left\{M(x)\in R^{p\times p}\right\} \qquad (5.1.1.3.7)$$

Then (5.1.1.3.6) can be written as:

$$\begin{bmatrix} y^{(\gamma_1)}{}_1 \\ \vdots \\ y^{(\gamma_p)}{}_p \end{bmatrix}=\begin{bmatrix} L^{\gamma_1}{}_f h_1 \\ \vdots \\ L^{\gamma_p}{}_f h_p \end{bmatrix}+M(x)\begin{bmatrix} u_1 \\ \vdots \\ u_p \end{bmatrix} \qquad (5.1.1.3.8)$$

As stated in [Isidori, 1995], the nonlinear system (5.1.1.3.4) has a vector of relative degree:

$$\left\{\gamma_1,....,\gamma_p\right\} \qquad (5.1.1.3.9)$$

if it satisfies the two conditions below:

i) $L_{g_i}L^k{}_{f_i}\cdot h_j(x)=0\left\{1\le i\le m;1\le j\le p;k<\gamma_i-1;\forall x\in U^o of\, x^o\right\}$ (5.1.1.3.10)

ii) The matrix (5.1.1.3.7) is nonsingular at '$x=x^o$' (5.1.1.3.11)

If the MIMO nonlinear does satisfy the above two conditions, then *M(x)* is bounded away from singularity for the neighborhood of U^o of x^o. Henceforth, the state feedback control law is:

$$u = -M^{-1}(x)\cdot\begin{bmatrix} L^{\gamma_1}{}_f h_1 \\ \vdots \\ L^{\gamma_p}{}_f h_p \end{bmatrix} + M^{-1}(x)\cdot v \qquad (5.1.1.3.12)$$

It is valid for x belongs to U^o, which is a neighborhood of x^o.

The above control law is called static-state feedback linearizing control law. It is called static-state because it does not depend on other states. It then yields the corresponding linear closed loop system:

$$\begin{bmatrix} y^{(\gamma_1)}{}_1 \\ \vdots \\ y^{(\gamma_p)}{}_p \end{bmatrix} = \begin{bmatrix} v_1 \\ \vdots \\ v_p \end{bmatrix} \qquad (5.1.1.3.11)$$

The total relative degree, γ of the system is the sum of the respective relative degrees of each output equation, i.e.:

$$\gamma = \gamma_1 + \gamma_2 + ...\gamma_p \qquad (5.1.1.3.12)$$

Now, similar to the case of the SISO case, if there exists a neighborhood U^o of x^o such that the mapping

$$T : U^o \rightarrow R^n \qquad (5.1.1.3.13)$$

does satisfy the conditions below

iii) T is smooth. (5.1.1.3.14)

iv) T^{-1} exists and is smooth as well. (5.1.1.3.15)

Henceforth the mapping is defined as for each of the y_j:

$$\begin{Bmatrix} T^{j}{}_{1}(x) = \xi^{j}{}_{1} \equiv h_j(x) = y_j \\ T^{j}{}_{2}(x) = \xi^{j}{}_{2} \equiv L_f h_j(x) \\ \vdots \\ T^{j}{}_{\gamma}(x) = \xi^{j}{}_{\gamma} \equiv L_f^{\gamma_j - 1} h_j(x) \end{Bmatrix} \{1 \le j \le p\} \qquad (5.1.1.3.16)$$

such that the mapping stated above is a diffeomorphism onto its image. Moreover, if the total relative degree γ, which is the sum of the respective relative degrees of each output equation is less than the dimensions of *x*, *n*, then in order to replenish the rest of the n-γ states, we require the mapping:

$$T_i(x) = \eta_i \quad for\ i = \gamma + 1, ...n \qquad (5.1.1.3.17)$$

to be smooth. However, this time, unlike in the case of SISO, we cannot expect (5.1.1.3.17) to have any special form as the distributions spanned by the vector field of g:

$$\{g_1(x), ..., g_p(x)\} \qquad (5.1.1.3.18)$$

is not involutive. Involutive means that a distribution is closed under the Lie bracket. By Frobenies' Theorem, involutivity equates integrability. Thus with any involutive distribution, there exists a unique surface (submanifold). Hence, the involutivity of g as defined in (5.1.1.3.18) has prohibited it to have any existence of a unique surface, and hence no special form is available for (5.1.1.3.17). Finally, the mapping can be defined in short as:

$$T(x) \equiv \left[\xi^{1}{}_{1}, \xi^{1}{}_{2} ..., \xi^{1}{}_{r_1}, ... \xi^{p}{}_{1}, \xi^{p}{}_{2} ..., \xi^{p}{}_{r_p}, \eta_1, ..., \eta_{n-r} \right] \qquad (5.1.1.3.19)$$

Before going to write the normal form of the diffeomorphic MIMO system, it is noted that due to the reason that the differential equations of the remaining states of (5.1.1.3.17) do not have any special form, we can only express them as:

$$\dot{\eta}_i = q(\xi,\eta) + \sum_{i=1}^{m} p_i(\xi,\eta)u_i = q(\xi,\eta) + p(\xi,\eta)u \qquad (5.1.1.3.20)$$

Hence then the diffeomorphism has enabled the original MIMO nonlinear state space system (5.1.1.3.4) to be rewritten as the following new state equations, the "normal form":

$$\begin{bmatrix} \dot{\xi}^1{}_1 \\ \vdots \\ \dot{\xi}^1{}_r \\ \vdots \\ \dot{\xi}^p{}_1 \\ \vdots \\ \dot{\xi}^p{}_r \\ \dot{\eta}_{n-r} \end{bmatrix} = \begin{bmatrix} \xi^1{}_2 \\ \vdots \\ \alpha_1(\xi,\eta) + \beta_1(\xi,\eta)\cdot u \\ \vdots \\ \xi^p{}_2 \\ \vdots \\ \alpha_p(\xi,\eta) + \beta_p(\xi,\eta)\cdot u \\ q(\xi,\eta) + p(\xi,\eta)\cdot u \end{bmatrix} \begin{Bmatrix} \xi \equiv \left[\xi^1{}_1,\ldots\xi^1{}_{r_1},\ldots\xi^p{}_1,\ldots\xi^p{}_{r_p}\right]^T, \\ \eta \equiv \left[\eta_1,\ldots\eta_{n-r}\right]^T \end{Bmatrix} \qquad (5.1.1.3.21)$$

Similarly as in SISO case, the region of the validity of diffeomorphism is to verify the region where,

$$x = T^{-1}(T(x)), x \in U^o \qquad (5.1.1.2.22)$$

exists. If the validity region, U^o, does not contain the whole R^n, then it is a local diffeomorphism. Otherwise, it is a global diffeomorphism. Again, similar to the SISO case, the problem of zero dynamics needs to be verified in the case of the relative degree less than the dimension of the states. It is to see if

$$\begin{aligned} &\left\{\xi^j{}_1,\ldots,\xi^j{}_r\right\} = 0 \Rightarrow \left\{\dot{\xi}^j{}_1,\ldots,\dot{\xi}^j{}_r\right\} = 0, \; for \left\{1 \le j \le p\right\} \\ &but \left\{\dot{\eta}_1,\ldots,\dot{\eta}_{n-r}\right\} \ne 0 \end{aligned} \qquad (5.1.1.3.23)$$

If the above condition is not satisfied, then the diffeomorphism of MIMO system has to consider the problem of zero-dynamics which can lead to instability.

The question left now is to decide on the control methods used with the new control v_j. With the common pole placement method in place, this means:

$$v = \begin{bmatrix} v_1 \\ \vdots \\ v_p \\ v_{\gamma+1} \\ \vdots \\ v_{n-\gamma} \end{bmatrix} = A \cdot T(\xi,\eta)^T = \begin{bmatrix} a_{11} & \dots & a_{1n} \\ \vdots & & \vdots \\ a_{n1} & \dots & a_{nn} \end{bmatrix} \cdot \begin{bmatrix} \xi^1{}_1 \\ \vdots \\ \xi^1{}_{\gamma_1} \\ \vdots \\ \xi^p{}_1 \\ \vdots \\ \xi^p{}_{\gamma_p} \\ \eta_1 \\ \vdots \\ \eta_{n-\gamma} \end{bmatrix} \qquad (5.1.1.3.24)$$

Henceforth, the challenging question in this study is to determine an A matrix which would result in asymptotic tracking behavior. However, most of the theorems available in the literature only deal with SISO cases. However, there is a theorem stated by [Isidori, 1995], which says that if the MIMO system has a Hurwitz A matrix, then we can attain asymptotic stability. Henceforth, the simplest Hurwitz matrix is a diagonal matrix with all negative entries, which are also its eigenvalues. This is feasible as our new transformed system is decoupled. We shall try this approach to see if it does lead to stability.

Moreover, it is also interesting to see if the constraints in inputs and/or states can be integrated into the formulation of the control law. Furthermore, since input-output linearization is based on the exact cancellation of the non-linearity of the system by the design of the control inputs, if there are model uncertainties, such as parametric uncertainties, then the stability of the system cannot be guaranteed. Since there is so much freedom in choosing A, there seems to be room to study the existence of stable solutions, the solutions themselves and the corresponding robustness and the optimality issues.

5.1.2 Switching Control

5.1.2.1 Switching Control

The switching control is a simple scheme, which is developed by the author, to use the errors of the state to compute the input efforts which can turn the respective states into the opposite directions of the errors. It can be looked at as a variant of sliding control.

In general, let us look at a multiple-ordered nonlinear differential system:

$$x^{(n)} = f(x) + b(x) \cdot u, u \in R; x \in R^n \qquad (5.1.2.1.1)$$

In order to view the difference between the switching control and general sliding control. A review of basic sliding control theory is given. In sliding control, as stated in [Michalska, 2001], the problem is then to construct the input control effort which would make:

$$x \equiv \left[x, \dot{x}, ..., x^{(n-1)} \right] \to \left[x_{des}, \dot{x}_{des}, ..., x_{des}{}^{(n-1)} \right] \qquad (5.1.2.1.2)$$

This is to say that we try to enforce the state tracking error, which is defined as:

$$e \equiv x - x_{des} \qquad (5.1.2.1.3)$$

equals to zero at a certain time t_1. More rigorously, it means:

$$\left\{ \exists t_1 : e^{(i)}(t_1) = 0, for\ i = 1, ..., n-2 \right\} \qquad (5.1.2.1.4)$$

n is the dimension of *x*. Also, it requires that the errors in *Laplace* domain follow the equation below:

$$(s+\lambda)^{n-1}\cdot e(s)=0,\lambda>0 \qquad (5.1.2.1.5)$$

In time domain, for example, for dimension of *x*, *n*, equal to two, it means:

$$\dot{e}+\lambda e=0 \qquad (5.1.2.1.6)$$

A sliding surface can be defined from the above equation:

$$S(t)=\dot{e}(t)+\lambda e(t) \qquad (5.1.2.1.7)$$

Then the equivalent problem for sliding control is to construct *u(x)* such that:

a) *S(t)* is reached in finite time t_1. (5.1.2.1.8)

b) $S(t)=0\,;\forall t\geq t_1$ (5.1.2.1.9)

The solution for the equivalent problem is to choose *u(x)* such that:

$$\frac{1}{2}\frac{dx}{dt}S^2(t)\leq-\eta\,|\,S(t)\,|\,;\forall t\geq 0,\eta>0 \qquad (5.1.2.1.10)$$

For example, for a second order differential system:

$$\ddot{x}=f+u \qquad (5.1.2.1.11)$$

Choosing the sliding function *S* to be:

$$S\equiv\dot{e}+\lambda\cdot e \qquad (5.1.2.1.12)$$

The equivalent control which will satisfy the two conditions about *S*, (5.1.2.1.8) and (5.1.2.1.9), is:

$$u = -f + \ddot{x}_d - \lambda \cdot (\dot{x} - \dot{x}_d) - \eta \cdot sign(S(t)); for \forall t \qquad (5.1.2.1.13)$$

The sliding control solution above resembles the switching control in this study. The control efforts of the switching control in this study also tries to minimize the errors to zero, the same condition (5.1.2.1.8) for sliding control, but it does not require the errors be zero within a certain time, condition (5.1.2.1.9). This is because the state errors can be made to zero in only one time step, theoretically if there are no constraints on inputs. This is similar to one dimensional case of sliding control. Hence, switching control used in this study can be looked at as the state space variant of sliding control.

Switching control is much simpler to formulate than the previous input-output linearization when it can work. This is because switching control requires the *g(x,t)* matrix of the nonlinear state space system

$$\begin{aligned} \dot{x} &= f(x,t) + g(x,t) \cdot u \\ y &= h(x,t) \end{aligned} \qquad (5.1.2.1.14)$$

to be invertible. Otherwise, switching control does guarantee the diminishing of the errors. On the other hand, it has the same problem as sliding control [Michalska, 2000], it brings the system to a chattering behavior which can wear out the actuators, and hence make the system easier subject to breakdowns due to equipment failures. Switching control is a discrete control. It is based on setting the control efforts acting against the direction of the state errors at each sampling time instant. Hence, it is especially suitable for systems which are controlled by computer. The state error varies with time and is defined as:

$$e(x,t) \equiv x(t) - x_{des} = dx(t) \qquad (5.1.2.1.15)$$

Then according to the state differential equations in a sampling time instant, which relates the incremental state movements with the respective contribution from inputs, we have

$$\frac{dx(t)}{dt} = f(x,t) + g(x,t) \cdot u \qquad (5.1.2.1.16)$$

In discrete time case, (5.1.2.1.16) becomes:

$$dx(k) = f(x,k) + g(x,k) \cdot u(k) \qquad (5.1.2.1.17)$$

Hence, it is possible to solve for the required control efforts which result in acting in the opposite direction of the errors at the next sampling time '*k+1*', and thus achieves the objective of tracking:

$$u(k+1) = g(x,k)^{-1} \cdot (-dx(k) - f(x,k)) \qquad (5.1.2.1.18)$$

The formulation (5.1.2.1.18) is feasible only with two necessary conditions. Firstly, it requires that *g(x,k)* to be invertible at all times. This is because if *g(x,k)* is invertible, the inverse of *g(x,k)* is feasible. Then when applying into the simulation system, the multiplication of *g(x,k)* and the inverse of it will form the identity matrix. Thus the final consequence of the control efforts will get decoupled again:

$$\begin{aligned} x(k+1) &= f(x,k) + g(x,k) \cdot g(x,k)^{-1} \cdot (-dx(k) - f(x,k)) \\ &= f(x,k) + (-dx(k) - f(x,k)) \end{aligned} \qquad (5.1.2.1.19)$$

In the case of robust switching control, unfortunately, since then the real system's *g* which contains uncertainties, differs with the *g* that is being used to obtain the control effort. Hence, we require *g* to be in a diagonal or triangular form. The reason behind this restriction would be dealt with in the following subsection of robust switching control.

Meanwhile, if the system is time invariant, then it is easy to determine algebraically whether *g(k)* can be singular or not, and if it does when it will be. Otherwise, in the time variant case, it can be very difficult to conclude when the *g(x,k)* is invertible or not. The second necessary condition for the control formula to be feasible is that the states' information is obtainable from the output measurements. Alternatively, the states can be measured directly if possible. The principle is to control the state errors to zeros. Then the corresponding output errors will go to zero as well.

5.1.2.2 Robust Switching Control

Originally, input-output linearization and its controller design have not taken the model uncertainties into account. Indeed, according to the paper by [Sastry & Isidori, 1989], it had stated that the major drawback of exact linearization is that it is based on the exact cancellation of nonlinear terms. If there is any uncertainty in the nonlinear function terms of *f* and *g*, the cancellation would hence be not exact and the resulting input-output equation is nonlinear.

In the literature, there has been quite a discussion about adaptive and robust input-output linearization. An early attempt by [Sastry & Isidori, 1989] deals with parametric adaptive control. Other efforts have also been using H_2 and/or H_∞ methods to evaluate the coefficients which would bound the outputs and hence the inputs. In a recent paper by [Kolavennu, et. al., 2001], a systematic approach of developing a H_2/ H_∞ stabilizing controller, which is formulated as a minimization problem and then solved with 'LMI' tools. All these approaches are based on sophisticated theories and complicated numerical procedures.

Based on the above considerations, with the basic idea of the switching control, the author has realized an alternative condition, which would ensure that the sliding control efforts act against the direction of errors with the uncertainties. However, the

uncertainties need to be bounded and parametric. This is usually feasible as physical systems usually have a finite range of variation of the parameters.

Nevertheless, in general, the basic criteria of having the control effort which would result in robust sliding tracking for a general state space system is:

$$-dx(k-1) \le \begin{Bmatrix} (f+\Delta f)(x,k) \\ +(g+\Delta g)(x,k) \\ \cdot(u+\Delta u)(x,k) \end{Bmatrix} < 0 ; \left(for\, dx(k-1) \ge 0 \right) \qquad (5.1.2.2.1)$$

$$-dx(k-1) \ge \begin{Bmatrix} (f+\Delta f)(x,k) \\ +(g+\Delta g)(x,k) \\ \cdot(u+\Delta u)(x,k) \end{Bmatrix} > 0 ; \left(for\, dx(k-1) < 0 \right) \qquad (5.1.2.2.2)$$

The above two conditions would ensure that the control efforts always bring the system to the direction of lesser errors. The above conditions are an adaptive procedure as the previous time instant's errors in states are used to calculate the new control efforts. Also, from the two equations above, it is needed to recognize the fact that the uncertainty could be nonlinear and it is not necessarily parametric. To demonstrate the uncertainty which is non-parametric, for example:

$$\begin{aligned} \dot{x}_1 &= x_1 + x_2 \\ (\dot{x}_1 + \Delta\dot{x}_1) &= \frac{(x_1 + x_2)}{x_3} \end{aligned} \qquad (5.1.2.2.3)$$

While the usual known parametric uncertainty could be also either linear or nonlinear as:

$$\begin{aligned} \dot{x}_1 &= x_1 + x_2 + k_3 \cdot u_1 \\ (\dot{x}_1 + \Delta\dot{x}_1) &= \frac{x_1}{k_1} + k_2 \cdot x_2 \end{aligned} \qquad (5.1.2.2.4)$$

Also, (5.1.2.2.4) has included an uncertainty which is rarely considered, the input uncertainty. Although in usual physical or industrial systems, this situation rarely happens, it does happen in some cases such as the study system' filter cakes' input mechanism. Seeing the complexity of the problem, this study does not deal with its analytical solution of the whole problem. Fortunately, our system's uncertainty is far simpler, and it is linear as well. Hence, only linear parametric bounded uncertainties are studied.

Although the above robust switching control effort works perfectly in SISO cases, there is one limitation if it is to extend the idea to MIMO situations. It is required that the state equations' *g* matrices in a de-coupled format or in a diagonal format.

This is because when we apply robust switching control, the *g(x,k)* matrix calculated with (5.1.2.2.1) and (5.1.2.2.2) contains bounded values:

$$u(k+1) = g_{\Delta extreme}{}^{-1} \cdot (-dx(k) - f_{\Delta extreme}(x,k)) \qquad (5.1.2.2.5)$$

where

$$f_{\Delta extrem}(x,k) = f(x,k) + \Delta_{extremum} f(x,k) \qquad (5.1.2.2.6)$$

$$g_{\Delta extrem}(x,k) = g(x,k) + \Delta_{extremum} g(x,k) \qquad (5.1.2.2.7)$$

while in real system, the perturbation of the matrix *g(x,k)* is randomly distributed within the bounded values. Hence, cancellation of the perturbed *g(x,k*) of the real system by the inverse of (5.1.2.2.7) is not feasible:

$$\begin{aligned} x(k+1) = {} & f(x,k) + \left(g(x,k) + \Delta g(x,k)\right) \cdot g_{\Delta extreme}(x,k)^{-1} \\ & \cdot (-dx(k) - f_{\Delta extreme}(x,k)) \\ & \left(where\ \Delta g_{\min}(x,k) \le \Delta g(x,k) \le \Delta g_{\max}(x,k)\right) \end{aligned} \qquad (5.1.2.2.8)$$

Hence, we have to rely on the basic structure of *g(x)* to obtain a decoupled one to one mapping between state errors and the control efforts. This is because, with a decoupled or diagonal or triangular g matrix, first input can be solved. Then with the solved first input, the subsequent inputs can be solved as well.

For example, if there are two state equations and both of them contains the same two control inputs, then it is very difficult to derive a solution which can drive the two state errors simultaneously to the negative direction of the errors. To illustrate this problem, let us consider two state equations at a time instant of a continuous uncertain system:

$$\begin{bmatrix} dx_1 \\ dx_2 \end{bmatrix} = \begin{bmatrix} f_1 + \Delta f_1 \\ f_2 + \Delta f_2 \end{bmatrix} + \begin{bmatrix} g_{11} + \Delta g_{11} & g_{12} + \Delta g_{12} \\ g_{21} + \Delta g_{21} & g_{22} + \Delta g_{22} \end{bmatrix} \cdot \begin{bmatrix} u_1 \\ u_2 \end{bmatrix} \qquad (5.1.2.2.9)$$

Even though it seems possible to solve for the two respective input control actions with the two respective state errors by the control effort:

$$u = \begin{bmatrix} u_1 \\ u_2 \end{bmatrix} = \begin{bmatrix} g_{11_{\Delta extreme}} & g_{12_{\Delta extreme}} \\ g_{21_{\Delta extreme}} & g_{22_{\Delta extreme}} \end{bmatrix}^{-1} \cdot \left(- \begin{bmatrix} dx_1 \\ dx_2 \end{bmatrix} - \begin{bmatrix} f_{1_{\Delta extreme}} \\ f_{2_{\Delta extreme}} \end{bmatrix} \right) \qquad (5.1.2.2.10)$$

in fact, it needs two state errors to formulate any one control effort. Hence, if the two state errors does not have the same sign, or even with the same sign, there is no guarantee that the respective control actions can steer the system's two states together to be in the opposite directions respectively of the previous direction of the state errors. Also, remember that this time we cannot cancel out the bounded *g* matrix, as we explain before by (5.1.2.2.8). Hence, the system with full g matrix, with entries in every element, cannot be controlled by robust switching control. On the other hand, if the system' inputs exists in such a format:

$$\begin{bmatrix} dx_1 \\ dx_2 \end{bmatrix} = \begin{bmatrix} f_1 + \Delta f_1 \\ f_2 + \Delta f_2 \end{bmatrix} + \begin{bmatrix} g_{11} + \Delta g_{11} & 0 \\ 0 & g_{22} + \Delta g_{22} \end{bmatrix} \cdot \begin{bmatrix} u_1 \\ u_2 \end{bmatrix} \qquad (5.1.2.2.11)$$

Then the control actions would become a one-to-one mapping with the respective state errors:

$$u = \begin{bmatrix} u_1 \\ u_2 \end{bmatrix} = \begin{bmatrix} g_{11_{\Delta extreme}} & 0 \\ 0 & g_{22_{\Delta extreme}} \end{bmatrix}^{-1} \cdot \left(- \begin{bmatrix} dx_1 \\ dx_2 \end{bmatrix} - \begin{bmatrix} f_{1_{\Delta extreme}} \\ f_{2_{\Delta extreme}} \end{bmatrix} \right) \qquad (5.1.2.2.12)$$

At the above equation, there is no ambiguity that each of the respective control actions is responsible to steer only its own state errors to zero. Alternative, if the inputs are in a lower triangular format as such:

$$\begin{bmatrix} dx_1 \\ dx_2 \end{bmatrix} = \begin{bmatrix} f_1 + \Delta f_1 \\ f_2 + \Delta f_2 \end{bmatrix} + \begin{bmatrix} g_{11} + \Delta g_{11} & 0 \\ g_{21} + \Delta g_{21} & g_{22} + \Delta g_{22} \end{bmatrix} \cdot \begin{bmatrix} u_1 \\ u_2 \end{bmatrix} \qquad (5.1.2.2.13)$$

Then the solution for this case is also feasible:

$$u = \begin{bmatrix} u_1 \\ u_2 \end{bmatrix} = \begin{bmatrix} g_{11_{\Delta extreme}} & 0 \\ g_{21_{\Delta extreme}} & g_{22_{\Delta extreme}} \end{bmatrix}^{-1} \cdot \left(- \begin{bmatrix} dx_1 \\ dx_2 \end{bmatrix} - \begin{bmatrix} f_{1_{\Delta extreme}} \\ f_{2_{\Delta extreme}} \end{bmatrix} \right) \qquad (5.1.2.2.14)$$

Then the first input can be solved readily. The second input also, can be solved easily when the 'negative' of the first state error, $-dx_1$, being replaced by the first calculated control input. Hence, it can be sure that the second control input is computed optimally to steer the second state error to zero. This assurance is based on the fact that the first state error has been dealt proficiently by the first control input already. Certainly, similar to the lower triangular format of *g*, upper triangular format of *g* is feasible as well.

In all, although robust switching control works promptly, it is being greatly confined of its applicability to those systems with g matrix in diagonal or triangular form.

5.1.2.3 Robust Switching Control for Linear Parametric Bounded Uncertainty

If the model uncertainty is linear, state-dependent, time varying and bounded, then (5.1.2.2.1) and (5.1.2.2.2) can be rewritten as:

$$-dx(k-1) \le \left\{ \begin{array}{l} (f(x,k)+\Delta f(x,k)) \\ +(g(x,k)+\Delta g(x,k)) \\ \cdot(u(x,k)+\Delta u(x,k)) \end{array} \right\} < 0 \,; \left(for\, dx(k-1) \ge 0 \right) \qquad (5.1.2.3.1)$$

$$\left(\Delta f_{\min} \le \Delta f \le \Delta f_{\max}, \Delta g_{\min} \le \Delta g \le \Delta g_{\max}, \Delta u_{\min} \le \Delta u \le \Delta u_{\max} \right)$$

$$-dx(k-1) \ge \left\{ \begin{array}{l} (f(x,k)+\Delta f(x,k)) \\ +(g(x,k)+\Delta g(x,k)) \\ \cdot(u(x,k)+\Delta u(x,k)) \end{array} \right\} > 0 \,; \left(for\, dx(k-1) < 0 \right) \qquad (5.1.2.3.2)$$

The solution to the above problem is to use the extreme bounded uncertainty values to obtain the control efforts which would satisfy (5.1.2.3.1). Since it is not possible to predict the uncertainty parameter for the next instant, we have to assume the worst cases so that all cases of uncertainties do not violate (5.1.2.3.1).

The above strategy can apply to SISO systems successfully. However, it can only apply to the restricted class of MIMO systems, which has an invertible *g(x,k)* matrix, as described before.

The subsequent sections deal with the system's dynamics formally and strategize the appropriate control methods.

5.2 System Uncertainties and Dynamics

5.2.1 Model Uncertainties

Model uncertainties are one of the most essential critical features of the system, therefore it is to be considered in detail first of all. The uncertainties includes input, state and output uncertainties:

a) Input Uncertainties:
The filter cakes' actual mass flow rate varies unpredictably and its actual solid density varies between 75% to 90%.

b) State Uncertainties:
The specific gravity of Strathcona slurry varies from 4.0 to 4.3 tonnes/m^3, while the specific gravity of Raglan varies from 3.8 to 4.0 tonnes/m^3 .

c) Output Uncertainty:
The pump characteristics curve constant can change nonlinearly if the output mix density and viscosity vary considerably.

Since the uncertainties of the system are quite significant, it is not easy to resolve these fuzziness while being able to attain the design objectives:

i) Maintain the solid density out of the Repulper tank to be 70%
ii) Maintain the Raglan to Strathcona ratio as 0.309.
iii) Maintain the tank level at 2.4m (80% full).
iv) Maintain the Repulper tank's output mass flow rate to be 51.43 tonnes/h.

It is preferable to design a controller which will not increase substantially the equipment costs. Hence, the initial effort is to try to use the original system, which uses only one tank, the Repulper tank, to accomplish all the design and tracking objectives.

Hereinafter, for the study purpose, it is interesting to see if different physical layout of the system can make the system perform more satisfactorily. Although this new layout might cost more in terms of the equipment and installation, it is more important, for the study purpose, to see if the new design layout can satisfy the design objectives even with significant model uncertainties.

Since the original Repulper tank system has the same operations, there is no specific part about the design philosophy of the original system. On the other hand, it is important to address the evolution of the ideas of how the alternative control design comes about. Hence, the next subsection is the design philosophy of the new alternative layout: three-phases-design instead of the original design of using one tank to resolve all dilemmas.

5.2.2 Alternative Control Design: 3 phases Design

As when Strathcona slurry density is above 64.067%, only water is needed to satisfy the final mixed slurry density requirement. But when the Strathcona slurry density is below 64.067%, then unpredictable contribution of filter cakes is required. However, since the process is continuous, it is impossible to guarantee that the freely dropped filter cakes can be immediately corrected of its deviation of solid density and mass flow rates. Therefore, its random deviation effect can only be seen once it is being diluted.

Phase I: Filter Cakes' Normalization Tank

Then, it is needed to normalize the filter cakes' solid density so that it can be used to increase the concentration of the Repulper tank accurately should the Strathcona slurry fall below 64.067%. It would be ideal for us to use the less dense incoming Strathcona slurry to normalize the filter cakes as this is our goal also. However, this can largely affect the final concentration of the mixed Strathcona slurry when it goes into the Repulper tank. This is because, there are large variations and fluctuations of the filter cakes, as these fluctuations can only be corrected after being detected at the output stream,

these fluctuations can greatly disturb the Repulper tank's mass balance. Hence, it is dangerous to use the incoming Strathcona slurry to dilute the filter cakes. Therefore, water is required to normalize or dilute the filter cakes. Since the filter cakes' lowest solid density is 75% and this is the nominal value, 75% is used as a set point to normalize the filter cakes. Consequently, a separate tank is required for stabilizing the filter cakes.

Phase II: Strathcona Normalizing Tank

Now, should we pour the stabilized filter cakes, Strathcona slurry with a variable known solid density, Raglan and water directly into the Repulper tank? To answer this question, it is important to see if the three state variables are readily available for controller design. To have the three state values, if the states cannot be measured directly, then the system needs to have at least three appropriate output equations which can be solved for the state information.

By "appropriate output" equations, it means that the equations should be invertible and as "robust" as possible against the model uncertainties. This in turn implies that the system designer should try the very best to avoid using the output measurements which depend upon the uncertain parameters. In our system, these output uncertain parameters means output uncertainty, the pump characteristic constant, and since the output equations are composed of state variables as well, the state uncertainties, the specific gravities of Strathcona and Raglan should be considered as well. Hence, to answer the earlier question of whether there is a need of a second stabilizing tank, it is then to see if there are three output measurable equations which do not include the pump characteristic constant and the specific gravities of Strathcona and Raglan.

As there are three states, this means three appropriate output equations are needed to solve for the state information. The original output equations are repeated here: (3.4), (3.5), (3.6) and (4.24):

$$f_m = \frac{M_{SR} + M_{RR}}{M_{SR} + M_{RR} + M_{WR}} \tag{3.4}$$

$$r = \frac{M_{RR}}{M_{SR}} \tag{3.5}$$

$$h_{\mathrm{Re}\,p} = \left(\frac{4}{\pi D_{\mathrm{Re}\,p}} \right) \left(\frac{M_{RR}}{SG_R} + \frac{M_{SR}}{SG_S} + M_{WR} \right) \tag{3.6}$$

$$\dot{M}_{m+w} = \frac{SG_R \cdot SG_S \cdot k_{pump} \cdot \omega_p \cdot (M_{SR} + M_{RR} + M_W)}{(SG_S \cdot M_{SR} + SG_R \cdot M_{RR} + SG_R \cdot SG_S \cdot M_W)} \tag{3.24}$$

However, (3.5) cannot be measured directly. The information of the ratio can only be derived once each of the state variables is being solved from the remaining output equations.

Looking at (3.6), this is an output which measures the tank level. However, as the specific gravities of both Strathcona and Raglan vary naturally, it is difficult to control the system at a specific tank level. However, there is definitely a need to control the tank level so that it will not overflow. To solve this dilemma, a modified control output can be put into place: total masses. Total masses can be measured easily by various commercial weight sensors. Hence, then by controlling the total masses of the system, even though the tank's level fluctuates slightly, it can be kept at a small range as the specific gravities of Strathcona and Raglan do not change abruptly. This new output equation is simply stated as:

$$M_{Total} = M_{SR} + M_{RR} + M_W \tag{5.2.2.1}$$

Moreover, looking at (2.7), the output, the mass flow rate is formulated as the information of the input, the pump speed and the specific gravity of the mixed mass, SG_M. This means the mass flow rate depends on the pump speed and the uncertain characteristic constant. This is certainly not favorable. As in (4.22), SG_M depends on the specific gravities of both Strathcona and Raglan. Hence, as seen in (3.24), the mass flow rate of the output also depends on the two uncertain specific gravities of Strathcona and Raglan. Therefore, (3.24) is not deemed appropriate as the output equation.

On the other hand, the pump speed should be regulated in order to give the required mass flow rate. Since the specific gravity of the mix is changing from time to time due to fluctuations of specific gravity of Strathcona and Raglan, and the pump characteristic constant can change nonlinearly due to different viscosity, the pump speed should be controlled independently using a simple feedback SISO loop. In this way, the output mass flow rate can be insured even with all the uncertainties.

The alternative ideal output is to be related only with states and not involving the specific gravities of Strathcona and Raglan. Nevertheless, after much of the search, it is not possible to find another output, which relates only to the masses of the three states: Strathcona, Raglan and water.

Hence for the sake of best performance, as stated as the goal, a second stabilizing tank is required to mix the density-varied incoming Strathcona slurry with the required water or filter cakes to reach the critical set density point: 64.067%. As when the Strathcona slurry is at the critical density percentage, it satisfies the requirements of water and Strathcona exactly for the final mixing of the Repulper tank. Then only Raglan and the stabilized Strathcona slurry is needed to add in the Repulper tank at the end.

In the second tank, the Strathcona slurry normalizing tank, as there are only two state variables, Strathcona slurry and water, two appropriate output equations are enough to solve for the state information. These two appropriate output equations are easily found as: the solid density and the total mass of the stabilizing tank:

$$f_{m\_Str} = \frac{M_{S\_Str}}{M_{S\_Str} + M_{W\_Str}} \tag{5.2.2.2}$$

$$M_{Total\_Str} = M_{S\_Str} + M_{W\_Str} \tag{5.2.2.3}$$

With the above two output equations, as no uncertain parameters are involved, accurate state information can be obtained. If the incoming Strathcona slurry's density is above 64.067%, there is no need to use the normalized filter cakes input from the filter normalizing tank at all. Hence water is poured in to dilute the incoming Strathcona slurry to bring it to 64.067%. Otherwise, when the incoming Strathcona slurry is below 64.067%, normalized filter cake slurry will be drawn to add into the Strathcona normalizing tank.

Phase III: Repulper Tank

For the last tank, the Repulper tank, as now all the input uncertainties and input parametric variations have already been dealt with, only Raglan is required to add in with the stabilized Strathcona slurry to the tank. It is assumed that the Strathcona slurry then only varies slightly around the critical Strathcona density point, 64.067%. Hence only the amount of Raglan needed to be regulated is to ensure that the final mix out of the Repulper tank has the required Raglan to Strathcona ratio, 0.309. The final solid density out of the mix, 70%, is less sensitive to the errors as the small variation of state masses can only change the total solids density slightly as well. Practically, only a SISO feedforward Raglan controller is needed since the Strathcona slurry's required density should have been regulated sufficiently in the first two tanks. However, it is always safer to consider to have a feedback control of all the inputs and outputs. Since then, still there are three state variables: Strathcona slurry, Raglan and water, three appropriate output equations are needed to make the states observable.

There are two appropriate equations already, (3.4) and (5.2.2.1), the total density equation and the total masses' equation. There is a lack of one appropriate equation.
The only other possible outputs which relates outputs to states is the specific gravity of the solution:

$$SG_M = \frac{(M_{SR} + M_{RR} + M_{WR})}{(M_{SR}/SG_S + M_{RR}/SG_R + M_{WR})} \qquad (5.2.2.4)$$

The specific gravity of the solution mix of the Repulper tank can be obtained by calculating the ratio of the two measurements: the mass flow rate and the volumetric flow rate of the of the output of the Repulper tank:

$$SG_M = \frac{\dot{M}_{Total\_out\_\mathrm{Re}p}}{\dot{V}_{Totol\_out\_\mathrm{Re}p}} \qquad (5.2.2.5)$$

However, actually, (5.2.2.5) is not really a good choice of output. This is because it depends on the uncertain parameters, SG_S and SG_R. On the other hand, no other appropriate outputs can be found. Also, if we use the three output equations,

$$y_{rep} = \begin{bmatrix} \dfrac{M_{SR} + M_{RR}}{M_{SR} + M_{RR} + M_{WR}} \\ M_{SR} + M_{RR} + M_{WR} \\ \dfrac{(M_{SR} + M_{RR} + M_{WR})}{(M_{SR}/SG_S + M_{RR}/SG_R + M_{WR})} \end{bmatrix} \qquad (5.2.2.6)$$

our three state information obtained are so sensitive to any errors. As a result, we can even get negative states if SG_S and SG_R vary. Consequently, we do not have three observable states available.

The normalized Strathcona slurry solution from Phase II just needs Raglan to be added in. Hence, we can add the respective amount of Raglan, calculated with respect to the Raglan to Strathcona ratio of 0.309, into the Repulper tank. Hence, open-loop control is feasible

for controlling the amount of Raglan needed. However, what about if the state masses in the Repulper tank are not in equilibrium? If we do not have feedback control, we cannot correct any errors in the states. But yet, we cannot get the all three correct state information as we mentioned in the last paragraph. Also, without any feedback control, the tank level cannot be well monitored. This is in fact a difficult dilemma.

To resolve this dilemma, we have to recognize the limitations of this system and hence we have to make certain assumption. Let us consider a new variable which represents the sum of Strathcona dry mass and Raglan dry mass. Hence, the Repulper tank would now have two states, the combined dry mass, the sum of Strathcona and Raglan, and water. We can still allow the possibility of having state perturbations in the tank, but we have to have the following assumption:

"The Raglan to Strathcona ration in the Repulper tank is always at 0.3092."

But what happen when the tank is disturbed, can we get back the states in equilibrium so that our output tracking requirements, such as total solid density, are violated? The answer is 'yes'. It is possible that the Repulper tank lacks water (solid density less than 70%), or there is too much water (solid density larger than 70%). But with the above assumption, no matter whether the tank is more concentrated or more dilute, Raglan to Strathcona ratio still remains constant.

Moreover, to maintain this ratio, we need to make sure that the Raglan mass flow rate coming in has to be equal to the required ratio, 0.3092, multiplies with whatever the dry mass flow rate of Strathcona coming into the Repulper tank.

When the tank is too concentrated, it is easy to make it more dilute by adding the corresponding amount of water needed to the tank in order to bring the total solid density back o70%. However, when the solution is too dilute, then we need more total solids to put into the tank. We have to make sure first the solids that we put into the tank has to be composed with the right amount of Strathcona and Raglan. Also, when we add

Strathcona, we inevitably add water into the tank as well. Hence, we have to also make sure also that the final solid density does come to 70%. The detail of the formulation of the solution is addressed in the Chapter 7, section 7.3.

Hence, we have two controls working in the tank. On one hand, we have two SISO open loop controls to control the right amount of Strathcona and Raglan coming into the Repulper tank. This is to ensure that the Raglan to Strathcona ratio maintains at 0.3092. To ensure that the respective pumps works properly, respective mass flow meters can be installed right after the pumps to check if indeed what we calculated is what we get. If not, then the respective pumps can be adjusted accordingly. But actually, we don't really control the mass flow of Strathcona because it is determined previously as the output mass flow rate of Phase II Strathcona normalizing tank:

$$\dot{M}_{S\_rep} = \dot{M}_{mix\_out\_Str} = 27.5019 / f_S \qquad (5.2.2.7)$$

Going back to the Repulper tank, on the other hand, we have a closed loop system to monitor the state changes in the tank and act when necessary to ensure that total solid density in the Repulper tank is being kept at 70%. Also, the closed loop system can monitor the total masses in the tank, and hence indirectly monitor the level of the tank.

If we need to make the solution in the tank more concentrated, we shall pour the slurry from the normalized filter tank, and the corresponding amount of Raglan, altogether into the Repulper tank. To make the solution more dilute is merely to add more water.

How about the mass flow rate out of the Repulper tank? Since the downstream roaster feed tank is a large storage which serves as a sink to average out any fluctuations of the upper stream flow, we can allow the output mass flow rate fluctuate so that the net inflow is zero in the smaller Repulper tank. This means the mass flow rate out of the Repulper tank is equal to the total mass flow rate coming into the tank. This is based on the assumption that the masses coming in are instantaneously being mixed and thus forming

a homogenous solution. Whether this assumption can make sense depends on if our sampling interval, 0.01hour, or 36 seconds is enough to well mix the solution.

Thus, finally, we can resolve the dilemma and with the other two phases, we have full controllability of the nonlinear system and robustness to undertake all uncertainties.

Meanwhile, to conclude this chapter, the whole alternative control three-phase design scheme is illustrated using a state diagram as Figure 5.2.1 in the next page:

Fig. 5.2.1: State flow Diagram for the Alternative Process

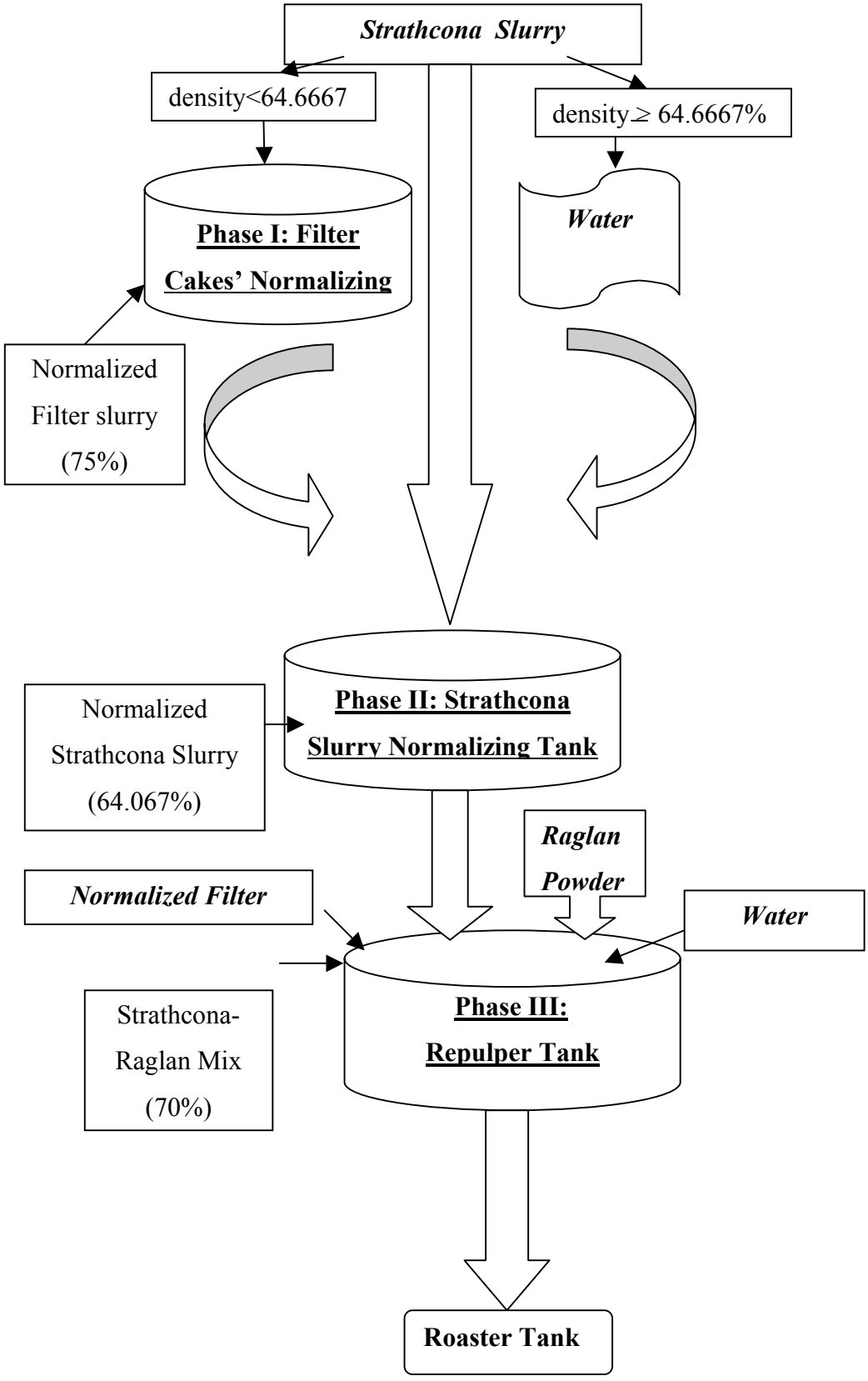

Chapter 6

Nonlinear Analysis, Design & Simulation of Existing Repulper Tank Process

6.1 System Analysis: Repulper Tank ("Rep")

$$
\begin{aligned}
&x_1 = M_{S\,\mathrm{R}}; \qquad x_2 = M_{RR}; \qquad x_3 = M_{WR} \\
&u_1 = \dot{M}_S; \quad u_2 = \dot{M}_R; \quad u_{3a} = \dot{M}_f; \quad u_{3b} = \dot{M}_W \\
&y_1 = f_m; \quad y_2 = M_{Total}; \quad y_3 = SG_M
\end{aligned}
\tag{6.1.1}
$$

In the Repulper tank, we switch control strategies between the two cases:

a) $f_S < 64.067\%$ (6.1.2)

b) $f_S \geq 64.067\%$ (6.1.3)

In case *a)*, whenever the incoming Strathcona slurry is detected to have solids density lower than 64.067%, then we switch to controller one which uses filter cakes to increase the slurry's density, in this case water input is not used. On the other hand, in case *b)*, if the Strathcona slurry density is equal to or greater than 64.067%, then we do not use filter cakes input, but water is used to dilute the slurry instead.
The output equations are the same in the two cases:

$$y_1 = \frac{x_1 + x_2}{x_1 + x_2 + x_3} \tag{6.1.4}$$

$$y_2 = x_1 + x_2 + x_3 \tag{6.1.5}$$

$$y_3 = \frac{(x_1 + x_2 + x_3)}{(x_1 / SG_S + x_2 / SG_R + x_3)} \tag{6.1.6}$$

However, two new outputs are used instead of the two original outputs: the Repulper tank level and the ratio between Raglan and Strathcona. To control the tank level, it is best to measure the level directly. But, there is an advantage of using the total mass in the tank to control the volume in the tank instead of using the tank level. Total mass can be measured more accurately, while tank level is subject to errors caused by the turbulence created by the mixing mechanism. With a suitable pressure measurement, e.g. load cells, it is possible to measure the weight and then the masses of the tank at every instant. Then, the slight changes of the specific gravity of Strathcona (SG_S) or Raglan (SG_R) would not affect our objective of controlling the volume of the mix within a prescribed range in the tank. Even though the specific gravity of SG_S and SG_R might vary, the tank level will stay within the safe level. Another new output is the SG_M specific gravity of the masses. This specific gravity of masses can be obtained by having the ratio of the mass flow rate and the volumetric flow rate.

$$SG_M = \frac{\dot{M}}{\dot{V}} \tag{6.1.7}$$

The mass flow rate can be measured with a Coriolis mass flow meter, while volumetric flow can be measured by magnetic flow meter which is already in use in the plant. In addition, in the original plant, the pump velocity is one of the inputs. However, in this new design, the pump velocity depends on the states information and the desired total mass flow rate, which is a constant parameter. We replace it with its equivalent function which depends on states and some parameters. In this way, a command is issued to the pump each time we compute the new required pump velocity. However, there is one thing we have to check constantly in case the pump deteriorates or fails.

$$\omega_p = \frac{\dot{M}_{m+w} \cdot (x_1 / SG_S + x_2 / SG_R + x_3)}{k_p \cdot (x_1 + x_2 + x_3)} \qquad (6.1.8)$$

$$(k_p = 0.02511 m^3 / h / RPM, \dot{M}_{m+w} = 51.43\, tonnes / h.)$$

In this way, we will give the required pump speed command to the pump each time we compute the new required pump velocity. In order to check constantly the performance of the pump, however, we need to constantly monitor the pump characteristic constant. This constant has an inherent nonlinear proportional relationship with the pump speed and an inversely proportional relationship with the viscosity of the slurry. Since the instantaneous pump characteristic constant can be obtained by the ratio of the instantaneous volumetric flow rate and the input pump speed,

$$k_p(n) = \frac{\dot{V}(n)}{\omega_p(n)}, (n : current sampling\ time) \qquad (6.1.9)$$

this calculated pump characteristic constant value can check with the previous constant. If we set the error threshold to be (+/-) 1% for instance, then the new pump characteristic constant will replace the previous value if the error exceeds the prescribed threshold.

$$if \ \frac{|k_p(n)-k_p(n-1)|}{k_p(n-1)} \geq \delta \qquad (6.1.10)$$
$$\Rightarrow k_p(n) = k_p(n-1)$$

Alternatively, we can use a moving average filter as well. This is because it can filter out the random signal noise by averaging a few samples so that k_p would not be too sensitive to noises. In either way, henceforth, this new pump characteristic constant will be used to calculate the new required pump velocity. Then we can always have three inputs and three states. We now derive the state space equations for the two cases, "f_S <64.067%" and "$f_S \geq$64.067%".

Case a): $f_S < 64.067\%$

$$\dot{x}_1 = f_S \cdot u_1 + f_f \cdot u_{3a} - \frac{\omega_p \cdot k_p \cdot x_1}{(x_1/SG_S + x_2/SG_R + x_3)} \qquad (6.1.11)$$

$$\dot{x}_2 = u_2 - \frac{\omega_p \cdot k_p \cdot x_2}{(x_1/SG_S + x_2/SG_R + x_3)} \qquad (6.1.12)$$

$$\dot{x}_3 = (1-f_S) \cdot u_1 + (1-f_f) \cdot u_{3a} - \frac{\omega_p \cdot k_p \cdot x_3}{(x_1/SG_S + x_2/SG_R + x_3)} \qquad (6.1.13)$$

Case b): $f_S \geq 64.067\%$

$$\dot{x}_1 = f_S \cdot u_1 - \frac{\omega_p \cdot k_p \cdot x_1}{(x_1/SG_S + x_2/SG_R + x_3)} \qquad (6.1.14)$$

$$\dot{x}_2 = u_2 - \frac{\omega_p \cdot k_p \cdot x_2}{(x_1/SG_S + x_2/SG_R + x_3)} \qquad (6.1.15)$$

$$\dot{x}_3 = (1-f_S) \cdot u_1 + u_{3b} - \frac{\omega_p \cdot k_p \cdot x_3}{(x_1/SG_S + x_2/SG_R + x_3)} \qquad (6.1.16)$$

If we substitute (6.1.8) into the state equations above, then we would have:

Case a): $f_S < 64.067\%$

$$\dot{x}_1 = f_S \cdot u_1 + f_f \cdot u_{3a} - \frac{\dot{M}_{m+w} \cdot x_1}{(x_1 + x_2 + x_3)} \tag{6.1.17}$$

$$\dot{x}_2 = u_2 - \frac{\dot{M}_{m+w} \cdot x_2}{(x_1 + x_2 + x_3)} \tag{6.1.18}$$

$$\dot{x}_1 = (1 - f_S) \cdot u_1 + (1 - f_f) \cdot u_{3a} - \frac{\dot{M}_{m+w} \cdot x_3}{(x_1 + x_2 + x_3)} \tag{6.1.19}$$

Case b): $f_S \geq 64.067\%$

$$\dot{x}_1 = f_S \cdot u_1 - \frac{\dot{M}_{m+w} \cdot x_1}{(x_1 + x_2 + x_3)} \tag{6.1.20}$$

$$\dot{x}_2 = u_2 - \frac{\dot{M}_{m+w} \cdot x_2}{(x_1 + x_2 + x_3)} \tag{6.1.21}$$

$$\dot{x}_3 = (1 - f_S) \cdot u_1 + u_{3b} - \frac{\dot{M}_{m+w} \cdot x_3}{(x_1 + x_2 + x_3)} \tag{6.1.22}$$

Then, we rewrite our system, in the standard state-space format, for each of the two cases:

Case a): $f_S < 64.067\%$

$$\begin{bmatrix} \dot{x}_1 \\ \dot{x}_2 \\ \dot{x}_3 \end{bmatrix} = \begin{bmatrix} -\frac{\dot{M}_{m+w} \cdot x_1}{(x_1 + x_2 + x_3)} \\ -\frac{\dot{M}_{m+w} \cdot x_2}{(x_1 + x_2 + x_3)} \\ -\frac{\dot{M}_{m+w} \cdot x_3}{(x_1 + x_2 + x_3)} \end{bmatrix} + \begin{bmatrix} f_S & 0 & f_f \\ 0 & 1 & 0 \\ (1 - f_S) & 0 & (1 - f_f) \end{bmatrix} \begin{bmatrix} u_1 \\ u_2 \\ u_{3a} \end{bmatrix} \tag{6.1.23}$$

$$\begin{bmatrix} y_1 \\ y_2 \\ y_3 \end{bmatrix} = \begin{bmatrix} \frac{x_1 + x_2}{x_1 + x_2 + x_3} \\ x_1 + x_2 + x_3 \\ \frac{(x_1 + x_2 + x_3)}{(x_1 / SG_S + x_2 / SG_R + x_3)} \end{bmatrix}$$

Case b): $f_S \geq 64.067\%$

$$\begin{bmatrix} \dot{x}_1 \\ \dot{x}_2 \\ \dot{x}_3 \end{bmatrix} = \begin{bmatrix} -\dfrac{\dot{M}_{m+w} \cdot x_1}{(x_1 + x_2 + x_3)} \\ -\dfrac{\dot{M}_{m+w} \cdot x_2}{(x_1 + x_2 + x_3)} \\ -\dfrac{\dot{M}_{m+w} \cdot x_3}{(x_1 + x_2 + x_3)} \end{bmatrix} + \begin{bmatrix} f_S & 0 & 0 \\ 0 & 1 & 0 \\ (1 - f_S) & 0 & 1 \end{bmatrix} \begin{bmatrix} u_1 \\ u_2 \\ u_{3b} \end{bmatrix} \tag{6.1.24}$$

$$\begin{bmatrix} y_1 \\ y_2 \\ y_3 \end{bmatrix} = \begin{bmatrix} \dfrac{x_1 + x_2}{x_1 + x_2 + x_3} \\ x_1 + x_2 + x_3 \\ \dfrac{(x_1 + x_2 + x_3)}{(x_1 / SG_S + x_2 / SG_R + x_3)} \end{bmatrix}$$

Since we have intentionally set up to have equal number of states and outputs, we can obtain the states information from the measurable outputs. However, since our output equations are nonlinear, we cannot obtain them directly from matrix manipulation. Solving for the states from the outputs, we have:

$$x_1 = y_1 \cdot y_2 - \frac{y_2 \cdot \left(y_3 - y_1 \cdot y_3 \cdot \left(1 - \dfrac{1}{SG_S} \right) - 1 \right)}{y_3 \cdot \left(\dfrac{1}{SG_S} - \dfrac{1}{SG_R} \right)} \tag{6.1.25}$$

$$x_2 = \frac{y_2 \cdot \left(y_3 - y_1 \cdot y_3 \cdot \left(1 - \dfrac{1}{SG_S} \right) - 1 \right)}{y_3 \cdot \left(\dfrac{1}{SG_S} - \dfrac{1}{SG_R} \right)} \tag{6.1.26}$$

$$x_3 = (1 - y_1) \cdot y_2 \tag{6.1.27}$$

The nominal or desired values for the state variables are:

$$x_1 = 13.39\,\text{tonnes} \tag{6.1.28}$$

$$x_2 = 4.14\,\text{tonnes} \tag{6.1.29}$$

$$x_3 = 7.51\,\text{tonnes} \tag{6.1.30}$$

The corresponding desired output values are:

$$y_1 = 0.70 \tag{6.1.31}$$

$$y_2 = 25.04\ \text{tonnes}, (SG_S = 4.2\,\text{tonnes/m}^3, SG_R = 3.9\,\text{tonnes/m}^3) \tag{6.1.32}$$

$$y_3 = 2.13\,\text{tonnes/m}^3; (SG_S = 4.2\,\text{tonnes/m}^3, SG_R = 3.9\,\text{tonnes/m}^3) \tag{6.1.33}$$

However, one has to note that the desired output values of (6.1.31) and (6.1.32) varies due to the fluctuation of SG_S (4.0 – 4.3 t/m^3) and SG_R, (3.8 – 4.0 t/m^3). Nevertheless, the total masses would vary slightly only and the tank level would still be around 2.4m.

In the search of a nonlinear controller, both input-output linearization and robust sliding control has been considered. The problem with input-output linearization is that it cannot provide a definite guarantee of its robustness to uncertainties. On the other hand, switching control, a much simpler formulation can perform satisfactorily and can handle uncertainties very well, but it requires the g matrix to be invertible.

The detail theoretical treatment and the comparison of the performance and robustness of the two control methods are the major topics of the following sections.

6.2 Input-Output Linearization

6.2.1 Input-Output Linearization Formulation

We shall differentiate output y until we could get a direct dependence between the output *y* and the input, *u*. By definition,

$$\dot{y} = \nabla h(f + gu) = L_f h + L_g h u \qquad (6.2.1.1)$$

Again, there are two conditions to be fulfilled for a multivariable nonlinear system to have relative degree at a point x_0:

i) $Lg_i L_f^k h_j(x) = 0, i = 1,...,m; j = 1,...,p; k = 0,...,\gamma_i - 2$ (6.2.1.2)

ii) The matrix *M(x)*, from (5.1.1.3.7) is non-singular at x_0. (6.2.1.3)

For our system, the difference between case *a)* and case *b*) lies in the matrix of g. However, the gradient of *h* is the same, as below: (6.2.1.1.4):

$$\nabla h = \begin{bmatrix} \dfrac{x_3}{(x_1+x_2+x_3)^2} & \dfrac{x_3}{(x_1+x_2+x_3)^2} & \dfrac{-(x_1+x_2)}{(x_1+x_2+x_3)^2} \\ 1 & 1 & 1 \\ \dfrac{\left\{ x_2 \cdot \left(\dfrac{1}{SG_R} - \dfrac{1}{SG_S} \right) \right\} + x_3 \cdot \left(1 - \dfrac{1}{SG_S} \right)}{\left(\dfrac{x_1}{SG_S} + \dfrac{x_2}{SG_R} + x_3 \right)^2} & \dfrac{\left\{ x_1 \cdot \left(\dfrac{1}{SG_S} - \dfrac{1}{SG_R} \right) \right\} + x_3 \cdot \left(1 - \dfrac{1}{SG_R} \right)}{\left(\dfrac{x_1}{SG_S} + \dfrac{x_2}{SG_R} + x_3 \right)^2} & \dfrac{\left\{ x_1 \cdot \left(\dfrac{1}{SG_S} - 1 \right) \right\} + x_2 \cdot \left(\dfrac{1}{SG_R} - 1 \right)}{\left(\dfrac{x_1}{SG_S} + \dfrac{x_2}{SG_R} + x_3 \right)^2} \end{bmatrix} \quad (6.2.1.4)$$

As expected, the equation above is a 3 by 3 matrix with 3 ones in the middle row. Also, $L_f h$ is the same in both cases:

$$L_f h = \begin{bmatrix} 0 \\ -\dot{M}_{mix\_out\_rep} \\ 0 \end{bmatrix} \quad (6.2.1.5)$$

Since, the g matrix is different for the two cases, $L_g h$ is also different. Hence:

Case a): $f_S < 64.067\%$

(6.2.1.6):

$$L_g h =$$

$$\begin{bmatrix} \dfrac{\{(x_1+x_2)\cdot(f_S-1)+x_3\cdot f_S\}}{(x_1+x_2+x_3)^2} & \dfrac{x_3}{(x_1+x_2+x_3)^2} & \dfrac{\{(x_1+x_2)\cdot(f_S-1)+x_3\cdot f_S\}}{(x_1+x_2+x_3)^2} \\ 1 & 1 & 1 \\ \dfrac{\left\{\begin{array}{l} x_1\cdot(1-f_S)\cdot\left(\dfrac{1}{SG_S}-1\right) \\ +x_2\cdot\left(\dfrac{1}{SG_R}-\dfrac{f_S}{SG_S}+f_S-1\right) \\ +x_3\cdot\left(f_S-\dfrac{f_S}{SG_S}\right) \end{array}\right\}}{\left(\dfrac{x_1}{SG_S}+\dfrac{x_2}{SG_R}+x_3\right)^2} & \dfrac{\left\{\begin{array}{l} x_1\cdot\left(\dfrac{1}{SG_S}-\dfrac{1}{SG_R}\right) \\ +x_3\cdot\left(1-\dfrac{1}{SG_R}\right) \end{array}\right\}}{\left(\dfrac{x_1}{SG_S}+\dfrac{x_2}{SG_R}+x_3\right)^2} & \dfrac{\left\{\begin{array}{l} x_1\cdot(1-f_f)\cdot\left(\dfrac{1}{SG_S}-1\right) \\ +x_2\cdot\left(\dfrac{1}{SG_R}-\dfrac{f_f}{SG_S}+f_f-1\right) \\ +x_3\cdot\left(f_f-\dfrac{f_f}{SG_S}\right) \end{array}\right\}}{\left(\dfrac{x_1}{SG_S}+\dfrac{x_2}{SG_R}+x_3\right)^2} \end{bmatrix}$$

Since no row in (6.2.1.6) contains all zeros, all relative degrees with respect to each output equation is well defined:

$$\gamma_1=1;\gamma_2=1;\gamma_3=1; \qquad (6.2.1.7)$$

Generally the respective relative degrees exists in all x belongs to R^n, except possibly a few rare cases such as when all three state variables are zero. In this case, the first row of the matrix $L_g h$, as in (6.2.1.6) would explode to infinity. Moreover, even though all the state variables are semi-positive definite, there are still possibilities that certain combinations of fractions of SG_S and SG_R may result in having a row all zeros. However,

it is impossible to obtain all the combinations of state variables and the uncertain parameters which result in at least one row having all its entries zeros. Hence, we will accept that (6.2.1.7) does hold in general for most x belonging to R^n. Then the total relative degree is:

$$\gamma = \gamma_1 + \gamma_2 + \gamma_3 = 3; \qquad (6.2.1.8)$$

Hence, our first condition (6.2.1.2) is fulfilled. Also, the relative degree is equal to n. For the second condition, the checking of the singularity of $L_g h$ is not computed analytically due to the complicated structure of the determinant. We use the 'cond' function, with the states in equilibrium, in Matlab to check the singularity of the determinant. If there is a singularity of a matrix, 'cond' function will return an infinity value. If there is no singularity at all, for example, an identity matrix, 'cond' function will return 1. We found that the condition number is high at 936, which means that the determinant of Lgh is quite close to being singular. Now, we would look at the situation of case *b)*.

Case b): $f_S \geq 64.067\%$

(6.2.1.9):

$$L_g h = \begin{bmatrix} \dfrac{\{(x_1+x_2)\cdot(f_S-1)+x_3\cdot f_S\}}{(x_1+x_2+x_3)^2} & \dfrac{x_3}{(x_1+x_2+x_3)^2} & \dfrac{-(x_1+x_2)}{(x_1+x_2+x_3)^2} \\ 1 & 1 & 1 \\ \dfrac{\left\{\begin{array}{l} x_1\cdot(1-f_S)\cdot\left(\dfrac{1}{SG_S}-1\right) \\ +x_2\cdot\left(\dfrac{1}{SG_R}-\dfrac{f_S}{SG_S}+f_S-1\right) \\ +x_3\cdot\left(f_S-\dfrac{f_S}{SG_S}\right) \end{array}\right\}}{\left(\dfrac{x_1}{SG_S}+\dfrac{x_2}{SG_R}+x_3\right)^2} & \dfrac{\left\{\begin{array}{l} x_1\cdot\left(\dfrac{1}{SG_S}-\dfrac{1}{SG_R}\right) \\ +x_3\cdot\left(1-\dfrac{1}{SG_R}\right) \end{array}\right\}}{\left(\dfrac{x_1}{SG_S}+\dfrac{x_2}{SG_R}+x_3\right)^2} & \dfrac{\left\{\begin{array}{l} x_1\cdot\left(\dfrac{1}{SG_S}-1\right)+ \\ x_2\cdot\left(\dfrac{1}{SG_R}-1\right) \end{array}\right\}}{\left(\dfrac{x_1}{SG_S}+\dfrac{x_2}{SG_R}+x_3\right)^2} \end{bmatrix}$$

Similar to case *a)*, the respective relative degrees exist for almost all *x*. The total relative degree is therefore again be three, which is equal to the dimension of the states.
The condition number of case *b)* however is at 756, which is lower than case *a)*. Nevertheless, 756 is still quite high and this implies also that the *Lgh* for case *b)* is quite close to being singular.

After stating *Lgh* for the two cases, since there is no difference between the two cases for the rest of the formulation, only one set of formulation is presented. Henceforth, the rest of the formulation applies to both cases respectively. This is because either case *a)* or case *b)* is regarded as a separate but similar system. The two systems are switched from one to the other depending on the solid density of the incoming Strathcona slurry.

Now, the diffeomorphic transformation of the system is as follows:

$$\begin{aligned}
&\dot{\zeta}_1 = v_1; \\
&\dot{\zeta}_2 = v_2; \\
&\dot{\zeta}_3 = v_3; \\
&\zeta_1 \equiv y_1 = h_1(x); \\
&\zeta_2 \equiv y_2 = h_2(x); \\
&\zeta_3 \equiv y_3 = h_3(x);
\end{aligned} \tag{6.2.1.10}$$

$$\begin{bmatrix} \dot{y}_1 \\ \dot{y}_2 \\ \dot{y}_3 \end{bmatrix} = \begin{bmatrix} L_f h_1 \\ L_f h_2 \\ L_f h_3 \end{bmatrix} + L_g h \cdot \begin{bmatrix} u_1 \\ u_2 \\ u_{3(a,b)} \end{bmatrix} \tag{6.2.1.11}$$

Then the state feedback control law is:

$$u = \begin{bmatrix} u_1 \\ u_2 \\ u_{3(a,b)} \end{bmatrix} = -L_g h^{-1} \cdot \begin{bmatrix} L_f h_1 \\ L_f h_2 \\ L_f h_3 \end{bmatrix} + L_g h^{-1} \cdot \begin{bmatrix} v_1 \\ v_2 \\ v_3 \end{bmatrix} \tag{6.2.1.12}$$

The new defined states then are:

$$\begin{bmatrix} \xi_1 \\ \xi_2 \\ \xi_3 \end{bmatrix} = \begin{bmatrix} y_1 \\ y_2 \\ y_3 \end{bmatrix} \tag{6.2.1.13}$$

It then yields the corresponding linear closed loop system.

$$\begin{bmatrix} \dot{\xi}_1 \\ \dot{\xi}_2 \\ \dot{\xi}_3 \end{bmatrix} = \begin{bmatrix} v_1 \\ v_2 \\ v_3 \end{bmatrix} \tag{6.2.1.14}$$

Since it is controlling the error, the feedback information should be the errors:

$$v = A \cdot d\xi \tag{6.2.1.15}$$

and

$$d\xi \equiv \begin{bmatrix} \xi_1 - \xi_{1des} \\ \xi_2 - \xi_{2des} \\ \xi_3 - \xi_{3des} \end{bmatrix} \tag{6.2.1.16}$$

However, since, (6.2.1.14) is a decoupled linear system, a diagonal matrix with all negative definite entries, which implies that all poles are in the left-half plane, will be able to control the system and achieve the tracking objectives. Hence, we can define a negative definite diagonal matrix, *K*:

$$K = \begin{bmatrix} -k_1 & 0 & 0 \\ 0 & -k_2 & 0 \\ 0 & 0 & -k_3 \end{bmatrix}, \{k_1, k_2, k_3 > 0\} \tag{6.2.1.17}$$

Hence,

$$\begin{aligned} u = \begin{bmatrix} u_1 \\ u_2 \\ u_3 \end{bmatrix} = & -Lgh^{-1} \cdot \begin{bmatrix} L_f h_1 \\ L_f h_2 \\ L_f h_3 \end{bmatrix} \\ & + Lgh^{-1} \cdot \begin{bmatrix} -k_1 & 0 & 0 \\ 0 & -k_2 & 0 \\ 0 & 0 & -k_3 \end{bmatrix} \cdot \begin{bmatrix} \xi_1 - \xi_{1des} \\ \xi_2 - \xi_{2des} \\ \xi_3 - \xi_{3des} \end{bmatrix} \end{aligned} \tag{6.2.1.18}$$

6.2.2 Input-Output Linearization Simulation

Since the *g* matrix of the two cases is different, simulation of the two cases is done respectively. Also, in each case, there are two parts of the simulation. The first part is the performance part with which no uncertainties are given to the system. The second part of

the simulation is with all the uncertainties and to see if the system can still be stable and perform satisfactorily.

Case a) $f_S < 64.067\%$

The simulation parameters of the performance part are as follows:

$$\{f_S = 0.58; f_f = 0.75; SG_S = 4.2t/m^3; SG_R = 3.9t/m^3\} \qquad (6.2.2.1)$$

Since the Strathcona slurry's solid density, f_S is measurable by sensor, hence f_S, is allowed to vary with the range:

$$0.58 \le f_S < 0.6407 \qquad (6.2.2.2)$$

Also, the initial states in the Repulper tank are not in equilibrium. Hence, we can see if the controller can steer the system back to equilibrium. The perturbed states are:

$$\begin{bmatrix} x_1(0) \\ x_2(0) \\ x_3(0) \end{bmatrix} = \begin{bmatrix} x_1^* \cdot 0.9 \\ x_2^* \cdot 1.2 \\ x_3^* \cdot 0.7 \end{bmatrix} = \begin{bmatrix} 13.39 \cdot 0.9 \\ 4.14 \cdot 1.2 \\ 7.51 \cdot 0.7 \end{bmatrix} = \begin{bmatrix} 12.0510 \\ 4.9680 \\ 5.2570 \end{bmatrix} \qquad (6.2.2.3)$$

The K matrix selected is:

$$K_a = \begin{bmatrix} -5 & 0 & 0 \\ 0 & -5 & 0 \\ 0 & 0 & -5 \end{bmatrix} \qquad (6.2.2.4)$$

The simulation results are very encouraging. Mostly all the desired output values are met. Due to the limitations of space, the results are being described rather than shown graphically. The total solids density returns back to 70% from 76% within an hour. Total mass output is also stabilized at 25 tonnes. But, unfortunately, the ratio of Raglan to

Strathcona does not go back to the desired one, 0.309, it settles at 0.2817. This is due to the inability of the system to correct the state errors to the desired accuracy. Nevertheless, it shows that input-output linearization does perform satisfactorily. Unfortunately, even after long time of settling, some of the input values still chatter considerably. Filter cakes' mass flow rates chatter largely from 10 to the maximum limit, 20 tonnes per hour. Strathcona mass flow rate varies as well but not as vigorous. It changes from 25 to 33 tonnes per hour. Meanwhile, Raglan mass flow rate stays at 8 tonnes/hr steadily.

Now we turn to more realistic uncertain situation. Here, most of the conditions are the same as above, except f_f, SG_S and SG_R, These parameters vary with a uniform random distribution but within their uncertainties bounding values which are:

$$0.75 \le f_f < 0.90 \qquad (6.2.2.5)$$

$$4.0 \le SG_S \le 4.3 \qquad (6.2.2.6)$$

$$3.8 \le SG_R \le 4.0 \qquad (6.2.2.7)$$

Moreover, the mass flow rate of the filter cakes varies as:

$$u_{3a\_actual} = u_{3a\_calculated} \cdot (1 \pm 30\%) \qquad (6.2.2.8)$$

Surprisingly, with the same K_a in (6.2.2.4), we are able to stabilize the all the output values with a moving average of about the desired setpoints. Nevertheless, due to the uncertainties, the output values and the input values fluctuates considerably. The output solid density does maintain around about 70% (+/-1%), while the total mass maintains at about 21.7 tonnes (+/-15%), which is lower than the desired setpoint, 25.04 tonnes. The Raglan to Strathcona ratio varies largely from 0.25 to 0.42. These output fluctuations should be deemed as unacceptable in real practice. Also, the input values have vary in a great extent: Strathcona mass flow rate varies from 0 to 60 tonnes/hr.; Raglan mass flow rate varies from 0 to 35 tonnes/hr.; filter cakes mass flow rate vary from 0 to 20 tonnes/hour. Inevitably, the large ranges of input values would wear out the actuators

quickly.

Case b) $f_S \geq 64.067\%$

Same procedures and parameters of simulation as in case *a)* are being used. For the case of no uncertainty, the system is very easy to control. The same K_a matrix, with –5 in diagonal entries, performs as satisfactorily as before. However, in the case of uncertainty, since now, there is no more input uncertainty, the system may behave better than before. In fact, with some tuning, it is found that the matrix:

$$K_b = \begin{bmatrix} -2 & 0 & 0 \\ 0 & -10 & 0 \\ 0 & 0 & -0.5 \end{bmatrix} \qquad (6.2.2.9)$$

can tame the uncertainties very well. The output solid density settles at 70% after two hours with (+/-0.1%) variation. Also, total mass settles almost flat at 25 tonnes in an hour. Unfortunately, the Raglan to Strathcona ratio varies a little bit more, from 0.23 to 0.31, after two hours. The input values vary as well, though to a lesser extent than case *a)*: Strathcona mass flow rate varies from 30 to 50 tonnes/hr.; Raglan mass flow rate varies from 2 to 12 tonnes/hr.; water mass flow rate vary from 0 to 5.5 tonnes/hr.

Case a) and b)

The combination of the two cases is also simulated, with f_S varies from 0.56 to 0.68 randomly with a uniform distribution. The K matrix is switched from K_a to K_b as f_S varies.

First of all we simulate with no uncertainties. When there is no uncertainties, all tracking requirements are met, though with longer settling time, five hours. Otherwise, inputs are smooth, and outputs are smooth as well. No chattering behavior is observed with the output or the inputs when there are no uncertainties. Unfortunately, the Raglan to Strathcona ratio settles flat again at 0.28. It does not go to the desired ratio 0.309.

Secondly, uncertainties are added to the combined system to determine the robust performance. The output solids density acquired fluctuates from 69.5% to 70%. Total mass varies from 20 to 24 tonnes. Raglan to Strathcona Ratio gradually fluctuate less after seven hours. It varies from 0.2 to 0.25. Obviously, the ratio is too low. The input values vary considerably as well. Strathcona mass flow rate varies from 3 to 80 tonnes/h. Raglan mass flow rate varies from 0 to 20 tonnes/h. Water mass flow rate varies from 0 to 8 tonnes/hr. Filter cakes mass flow rate varies from 0 to 20 tonnes/h. Hence, the robustness performance is rather poor when we combine the two cases into one switching system.

This might be due to the fact that we did not use the ratio as one of the output. If we do, we might be able to better track the system. We still need the measurement of SG_M to calculate the states, as the ratio is not measurable. Hence, we separate the operation of obtaining state information from the output measurements, from the outputs that we use to formulate the input-output linearization control system.

After a slight modification of the *h(x)* in the system,

$$\begin{bmatrix} y_1 \\ y_2 \\ y_3 \end{bmatrix} = \begin{bmatrix} \dfrac{x_1 + x_2}{x_1 + x_2 + x_3} \\ x_1 + x_2 + x_3 \\ \dfrac{x_2}{x_1} \end{bmatrix} \qquad (6.2.2.10)$$

and the corresponding changes in the gradient of *h(x)*:

$$\nabla h = \begin{bmatrix} \frac{x_3}{(x_1+x_2+x_3)^2} & \frac{x_3}{(x_1+x_2+x_3)^2} & \frac{-(x_1+x_2)}{(x_1+x_2+x_3)^2} \\ 1 & 1 & 1 \\ \frac{-x_2}{x_1^2} & \frac{1}{x_1} & 0 \end{bmatrix} \qquad (6.2.2.11)$$

The above expression is much simpler than the original one. Also, the determinants of the $L_g h$ of the two cases can be derived as:

$$\det(L_g h_a) = \frac{(x_1+x_2)\cdot(f_f - f_S)}{x_1^2 \cdot (x_1+x_2+x_3)} \qquad (6.2.2.12)$$

$$\det(L_g h_b) = \frac{-(x_1+x_2)}{x_1^2 \cdot (x_1+x_2+x_3)} \qquad (6.2.2.13)$$

For case *a)*, (6.2.2.12) shows that only in the case that the filter cakes' density equals to the Strathcona slurry's density would the determinant be zero. This should not happen under normal circumstances as the maximum f_S, which is at 0.68, is still smaller than the minimum f_f, 0.75. Hence, the diffeomorphism should exist in most cases. On the other hand, for case *b)*, (6.2.2.12) shows that the determinant would only be zero if there is only water in the Repulper tank. However, this could rarely happen. Hence, we can continue with the rest of the design. We use the same K_a and K_b as before in the modified system. Running the simulation again for the combined cases, we found that indeed, the ratio objective is being met. It stabilizes at 0.3099. There are still slight errors, but it is already much better than before. Also, since in the modified system, the uncertain SG_R and SG_S do not come into play in the modified h matrix, the system do not need to handle as much uncertainties. As a result, the control system behaves very robust under this modified system. Let us look at the figure below which shows the three outputs' ratio of its values to their respective setpoints.

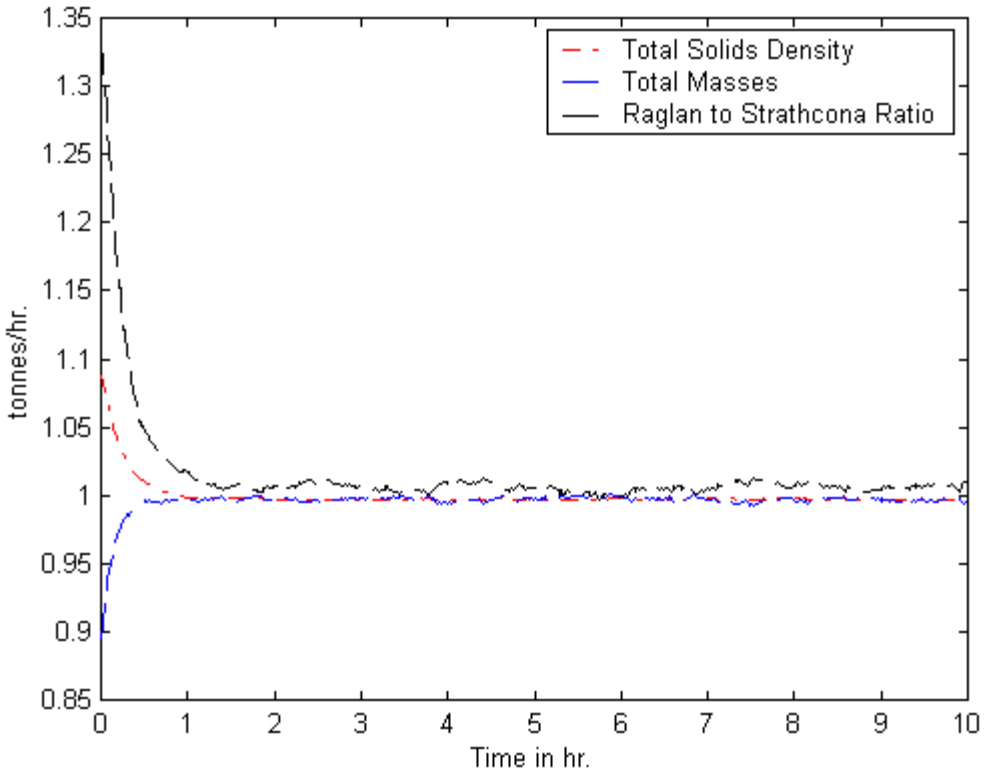

Fig. 6.2.1: Ratio of Outputs Values to their setpoints, (y/y_d), under input-output linearization with uncertain parameters for the existing Repulper tank process.

From Fig. 6.2.1, we can see that as the first two outputs reaches their respective setpoints within an hour. Meanwhile the Raglan to Strathcona ratio fluctuates between 0.3133 to 0.3081. Nevertheless, in most circumstances, this ratio is already accurate enough with respect to the setpoint 0.3092. The errors are only about (+/- 1.3%). Hence, with the modified system, the objective of robust performance is achieved. Hereinafter, we would like to see how the input values vary:

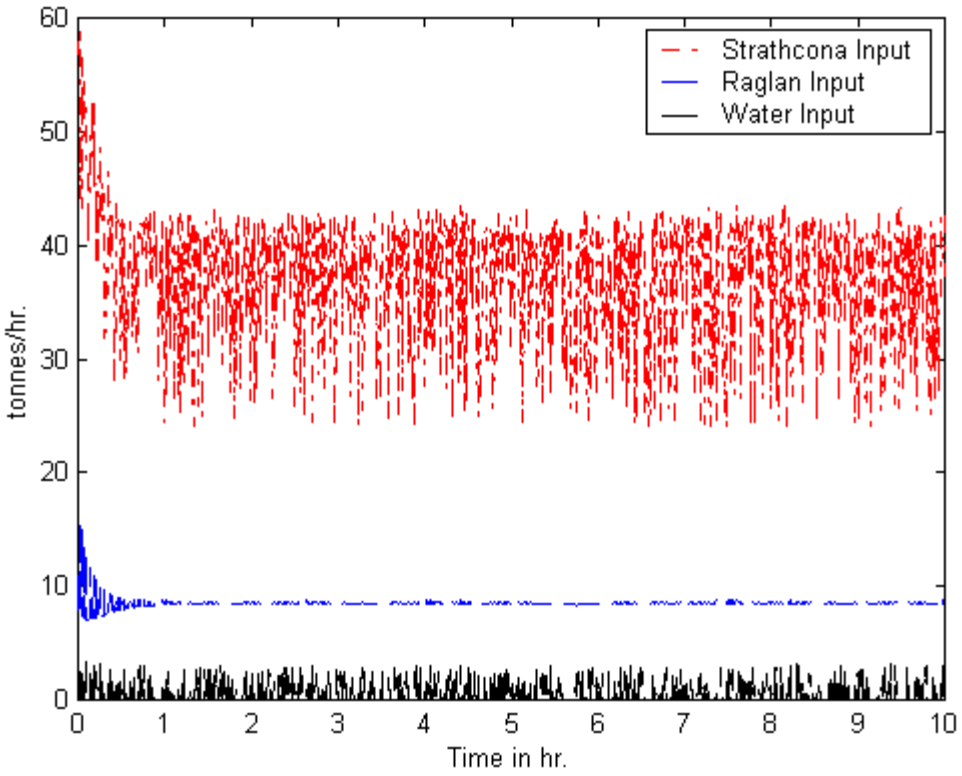

Fig. 6.2.2: Mass Flow Rate Controls commanded under input-output linearization with uncertain parameters for the existing Repulper tank process.

From Fig. 6.2.2, we can see how input controls vary. Strathcona mass flow rate chatters from 25 to 43 tonnes/hour. Raglan mass flow rate only varies slightly, from 8.35 to 8.80 tonnes/hour, after two hours of settling. Water flow rate chatters quite seriously from 0 to 3 tonnes/hour. Filter cakes mass chatters most, it fluctuates from 0 to 20 tonnes/hour.

We know that as the SG_R and SG_S vary, the final specific gravity of total solids, SG_M will also vary. Since, SG_M varies quite a lot, it is important to see how the pump speed varies as well. If the variation is too drastic, then there is a potential problem of delay and the pump can get wear out quickly. The pump speed as we mentioned in the last chapter is open-loop controlled with the simple equation as below,

$$\omega_{p\_rep} = \frac{\dot{M}_{mix\_out\_rep}}{k_{p\_rep} \cdot SG_{M\_rep}} \qquad (6.2.2.14)$$

$$\left(k_{p\_rep} = 0.02511\text{m}^3/(\text{h}\cdot\text{RPM}),\ \dot{M}_{mix\_out\_rep} = 51.43\text{tonnes/hr}\right)$$

Assume that the total desired output mass flow rate and the pump constant does not change, we get the following figure below for the pump speed:

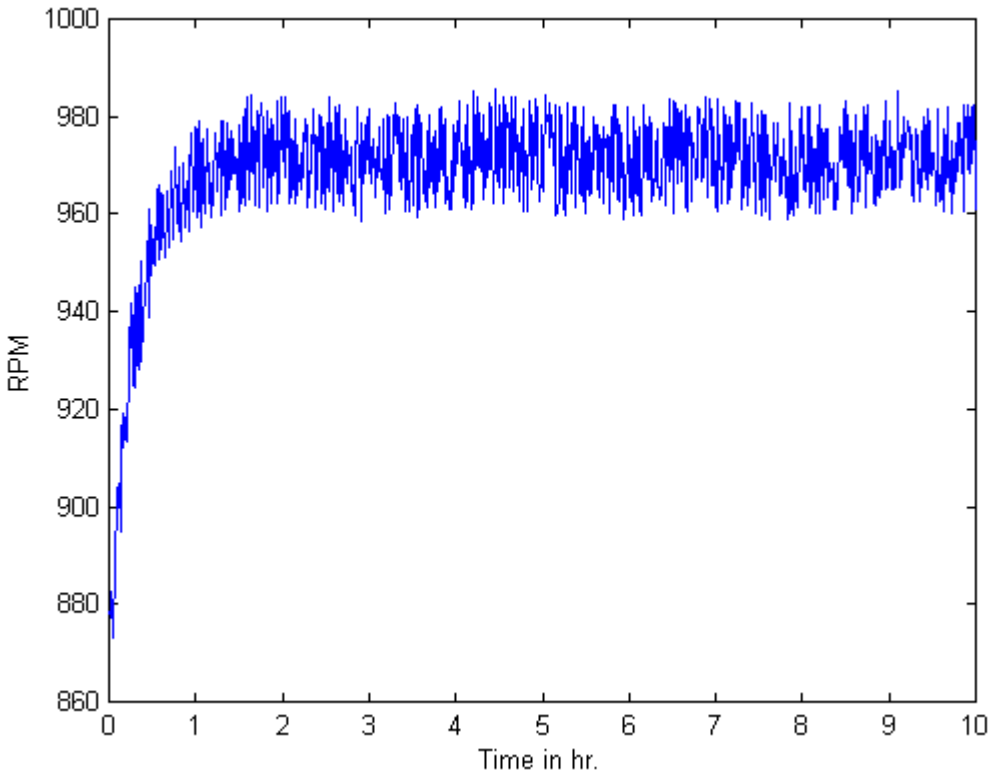

Fig. 6.2.3: Pump Speed Controls commanded under input-output linearization with uncertain parameters for the existing Repulper tank process.

From Fig. 6.2.3, we are pleased to see that that pump speed vary only in a small range, from 960 to 980 RPM. Hence, our modified system with input-output linearization has successfully controlled the system to attain all its desired tracking objectives within a reasonable time, even under the severe input uncertainties of the filter cakes. The drawback however is to inevitably tolerate the chattering of the inputs.

6.2.3 Input-Output Linearization Conclusion

In conclusion, input-output linearization can attain tracking objectives very well if there are no uncertainties. With the right choice of outputs, the output responses are smooth and they can attain the desired setpoints. Unfortunately, the input efforts are inevitably chatter quite severely with or without uncertainties. Nevertheless, the robustness performance can and does exist in input-output linearization but it requires efforts in fine tuning the *K* matrix. Moreover, we can control the rate of the output response easily by varying the magnitudes of *K* correspondingly. Indeed, for input-output linearization, formulation of *K* matrix in a robust context is still a major challenge up to today.

6.3 Switching Control

6.3.1 Switching Control Formulation

The control law formulation is rather simple. As described before in the last chapter, if the *g(x)* matrix is invertible, the control law which can diminish the state errors in the next sampling time is again:

$$u(k+1) = g(x,k)^{-1} \cdot (-dx(k) - f(x,k)) \qquad (6.3.1.1)$$

Hence, for the two cases, the essential criterion is to have an invertible *g* matrix. This means that the determinants of the *g* matrix cannot be zero.
The g matrix for case *a)* is named as g_a and is:

$$g_a = \begin{bmatrix} f_S & 0 & f_f \\ 0 & 1 & 0 \\ (1-f_S) & 0 & (1-f_f) \end{bmatrix} \qquad (6.3.1.2)$$

Its determinant is:

$$\det(g_a) = f_S - f_f \tag{6.3.1.3}$$

From (6.3.1.3), it is clear that under normal circumstance, the determinant would not be zero. This is because there is no intersection region of the two densities' varying ranges:

$$\begin{aligned} 0.56 \le f_S \le 0.68 \\ 0.75 \le f_f \le 0.85 \end{aligned} \tag{6.3.1.4}$$

Hence, g_a is invertible in all normal circumstances.

Next, the g matrix for case *b)* is destined as g_b and is:

$$g_b = \begin{bmatrix} f_S & 0 & 0 \\ 0 & 1 & 0 \\ (1-f_S) & 0 & 1 \end{bmatrix} \tag{6.3.1.5}$$

Its determinant is:

$$\det(g_b) = f_S \tag{6.3.1.6}$$

It is obvious that the determinant of g_b cannot possibly be zero except if the incoming slurry is all water. Hence, we can say that g_b is invertible. Now, we are ready to do the simulation.

6.3.2 Switching Control Simulation

The simulation parameters are the same as in input-output linearization. Again, firstly, performance is determined. Then when we add the uncertainties, we would use the robust

switching control described in the last chapter to try to obtain robust performance. Since, for switching control, the control law is very simple, the combination of the two cases, to form one system which switches between two switching control law is simulated.

The result of the simulation is encouraging as all output tracking objectives are met in about five hours. This time of settling is longer than the input-output linearization. In terms of the behavior of the inputs, Strathcona chatters from 25 to 43 tonnes/hour. Raglan stays flat at the equilibrium input value, 8.5 tonnes/hour after five hours. Water mass flow rate fluctuates between 0 to 3 tonnes/hours. Filter cakes fluctuate from 0 to about 18 tonnes/hour. One has to note that the filter cakes and water mass flow rate are destined to fluctuate largely. This is because of the control which alternates between the two cases.

Next, we are going to test the robustness of switching control. Since robust switching control can apply only to the g matrix which is either in diagonal or triangular format, it is not feasible to apply robust switching control scheme to our system's case *a)*, which contains the input uncertainties. We can however, use the general switching control by approximating the real *g* matrix with the *g* matrix which uses the nominal parameters. As case *b)* does not contain uncertainty, then general switching control can be used to simulate the system with the two cases together. Fortunately, when treated with uncertainties, general switching control does provide stable outputs. However, some of the output errors do not get minimized to the desired values even after ten hours of settling time. Output solid density still hangs at 72.5% at ten hours. It fluctuates from 72 to 73% during the whole course of thirty hours. Though total mass gets stabilized to the desired value after five hours, the Raglan to Strathcona ratio settles at 0.294. In terms of the input variations, Raglan mass flow rate shows a stable 8.5 tonnes/hour after four hours. Water mass flow rate fluctuates from 0 to 2 tonnes/hour. Strathcona mass flow rate again varies from 25 to 43 tonnes/hour. Filter cakes mass flow rate chatters from 0 to its constrained maximum allowable value, 20 tonnes/hour.

Even though switching control cannot provide good robust performance, it has its advantage in providing smooth input values when possible. For example, since Raglan

state equation does not depend on other inputs other than Raglan mass flow rate itself, the optimal Raglan mass flow rate can be computed independently with the other two state equations. Hence, uncertainties in other state equations do not affect its smoothness in providing input values. Apart from the issue of robustness, there is one disadvantage of switching control. Its output response time cannot be controlled easily as in the case of input-output linearization. It may be possible to speed up the response by multiplying the magnitudes of the state errors by some factors, however, this might destabilize the system. Further investigation can be carried out in how to change the rate of the output response by switching control.

It can be interesting also to combine the two types of control for the system. Input-output linearization can be used with case *a)*, while case *b)* can be controlled by general switching control. The results of the hybrid simulation, unfortunately, are not satisfactory at all.

6.4 Conclusion on Control of Existing Process

There are advantages and disadvantages of using either input-output linearization or switching control. Input-output linearization can attain tracking objectives and provide good robust performance through a careful choice of the matrix K. The tuning of K or more general the A matrix can be a tiresome process. There is still no systematic approach of determining the matrix even though the input-output linearization was formulated already 20 years ago. Hence, robustness is not guaranteed by input-output linearization. It is found by empirically tuning the K matrix. Nevertheless, there is no doubt that there is a great potential of developing guaranteed robust control structure for input-output linearization in future. Also, the formulation of input-output linearization is quite tedious and is subject to various constraints, such as the existence of the singularity of $M(x)$. Also, although exact input-output linearization greatly simplifies the formulation process, it is not always possible to have a MIMO system which has the same number of inputs and outputs. However, it is possible to manipulate the system to change the number of outputs or the number of inputs, as we did for the original Repulper tank

process. In general, it is easy to imagine that if the dimension of the states is large, it can greatly increase the difficulty of the formulation. This also means that it requires quite a large computing power should the system is large. Severe chattering behavior for the input values, happens whether the system has uncertainty or not, is also another disadvantage of input-output linearization. As mentioned before, excessive chattering of the input values can eventually wear out the actuators and cause system failure.

Comparatively, switching control, realized by the author through the course of this study, can be formulated much more easily. Since, every control effort is computed in real time, this implies also it requires much less computing power than input-output linearization. The major disadvantage of using switching control is its rather large limitation when robustness is required. To use robust switching control correctly, we need to have the *g* matrix of the nonlinear system to be in either a diagonal or triangular format. This is a rather major limitation so that it can only apply to a rather specific class of nonlinear system. Also, *g* matrix of the inputs is not as easy, if feasible at all, to modify as the *h* matrix of the outputs. If such a g does exist, then, however, robust switching control can guarantee robust performance under parametric bounded uncertainties. This guarantee of robustness does not exist yet in input-output linearization. Another major disadvantage of switching control is its response is rather slow. To increase the rate of the output response would mean a further investigation in switching control in future. Chattering behavior also is being observed in the input values. But if the controlled state is independent of the other ones, it can provide smooth control input commands. For example, in the Raglan state equation, Raglan state changes depends only on the input of Raglan mass flow rate. Since the state error of Raglan does not abruptly changes as in the states of Strathcona and Raglan, smooth control commands are issued to finally bring the state of Raglan from the perturbed state to the equilibrium state, irrespective to other states. This advantage is due to the fact that switching control deals with the state equations independently from each other. Hence, the deterioration of any one state should not affect the other states. For the existing process control structure, it is best to use the modified input-output linearization. It provides superior performance and robustness. It

outperforms switching control. The only drawback is the chattering behavior of the input commands.

It seems perfect now that our nonlinear system can be controlled so well with only one tank. However, in fact, we have neglected an important issue: the availability of the correct state information. Without the correct state information, neither input-output linearization nor switching control can work. As we mentioned in the last chapter, the major obstacle in obtaining the correct state information is the extreme sensitivity of the states obtained from the equations of (6.1.25), (6.1.26) and (6.1.27), to slight errors of SG_R and SG_S. In some cases, these equations can even give negative state values. There are many ways to resolve this problem. The best way is to somehow develop a numerical procedure to desensitize these equations. However, this might lead to unstable system as control efforts would not effect the states as they were commanded to. We cannot find any other reliable and measurable output as we mentioned before. Furthermore, it is too dangerous to generalize the parameters before they come into the tank and those in the tank. SG_R and SG_S in the tank do most likely have different values. The mixing of Strathcona, Raglan and water can potentially change their specific gravities. Therefore, the option of using parameters that are not measured in the tank is not feasible.

There is actually only one option left. This is to go to the alternative process design which has three tanks. In the first two tanks, since there are only two states, only two measurable output, with state variables only, is needed. We do have two reliable output measurements, the solid density and the total mass of a tank. Both of these measurements can be measured instantaneously and accurately. Also, these two output measurements do not depend on the uncertain parameters of either SG_R or SG_S. At the end of the second tank, the Strathcona slurry would have been controlled very well at 64.067%. No water is needed. Hence, actually, in the last phase, only Raglan powder is needed to add into the Repulper tank. Raglan is open-loop controlled. The total mass and the total solids density are controlled closed-loop though to ensure that tank level and total solids density are well tracked to their respective set points. Henceforth, we are going to discuss in details the alternative process control system, the three-phase design.

Chapter 7

Nonlinear Analysis, Design & Simulation of Alternative Process

7.1 Phase I. Filter Cake's Normalizing Tank ("fil")

We are now going to investigate the first phase of the Three Phase system.

7.1.1 System Analysis

$$\begin{aligned} x_{11} &= M_{S\_dry\_fil}; & x_{21} &= M_{W\_fil} \\ u_{11} &= \dot{M}_{f\_wet\_in\_fil}; & u_{21} &= \dot{M}_{W\_in\_fil} \\ y_{11} &= f_{fil}; & y_{21} &= h_{fil} \end{aligned} \qquad (7.1.1.1)$$

After stating the variables for this phase from the last equation, we introduce the following state equations for this phase.

$$\dot{x}_{11} = f_f \cdot u_{11} - \frac{\omega_1 \cdot k_{p1} \cdot x_{11}}{(x_{11}/SG_S + x_{21})} \qquad (7.1.1.2)$$

$$\dot{x}_{21} = (1-f_f)\cdot u_{11} + u_{21} - \frac{\omega_1 \cdot k_{p1} \cdot x_{21}}{(x_{11}/SG_S + x_{21})} \qquad (7.1.1.3)$$

$$y_{11} = \frac{x_{11}}{x_{11}+x_{21}} \qquad (7.1.1.4)$$

$$y_{21} = \frac{4}{\pi \cdot D_{fil}^2}\left(\frac{x_{11}}{SG_S} + x_{21}\right) \qquad (7.1.1.5)$$

We could solve the states using the two output equations (7.1.1.4) and (7.1.1.5). Hence we have indirectly measurable states:

$$x_{11} = \frac{y_{11} \cdot y_{21} \cdot \pi \cdot D_{fil}^2}{4 \cdot \left(1 - y_{11} \cdot \left(1 - \frac{1}{SG_S}\right)\right)} \qquad (7.1.1.6)$$

$$x_{21} = \frac{y_{21} \cdot \pi \cdot D_{fil}^2}{4} - \frac{y_{11} \cdot y_{21} \cdot \pi \cdot D_{fil}^2}{4 \cdot SG_S \cdot \left(1 - y_{11} \cdot \left(1 - \frac{1}{SG_S}\right)\right)} \qquad (7.1.1.7)$$

We would like to have our diluted solid density kept at 75%. For the sake of simplicity of the study, we assume that the dilution tank has the same dimensions of tank as the Repulper tank and hence we would use the same desired tank level, 2.4m. At equilibrium:

$$y_{11}^* = f_{fil}^* = 0.75, y_{21}^* = h_{fil}^* = 2.4\text{m}, \tag{7.1.1.8}$$

Then our equilibrium state variables, the masses in the filter normalizing tank are:

$$\begin{aligned} x_{11}^* &= 20.81843 \text{ tonnes} \\ x_{21}^* &= \ 6.93948 \text{ tonnes} \end{aligned} \tag{7.1.1.9}$$

Since we operate at different equilibrium points according to different conditions of Strathcona slurry, the desired output of the mix mass flow rate would be changed every time the Strathcona slurry density changes. The desired output density of the normalized filter output, on the other hand, would be kept at 75% all the time. We shall look at the input and output equations for the next tank, Strathcona normalizing tank so that we would know how much filter mass flow is needed in the case of the Strathcona slurry density which is below the critical point, 64.067%.

$$\dot{M}_{S\_Total} = f_f \cdot \dot{M}_f + f_S \cdot \dot{M}_S \tag{7.1.1.10}$$

$$\dot{M}_{W\_Total} = (1 - f_f) \cdot \dot{M}_f + (1 - f_S) \cdot \dot{M}_S \tag{7.1.1.11}$$

Solving for the required mass flow rate of the filter cakes and we get:

$$\dot{M}_f = \frac{\{\dot{M}_{W\_Total} - (1 - f_S) \cdot \dot{M}_{S\_Total} / f_S\}}{(1 - f_f / f_S)}$$

$$(where\ \dot{M}_{W\_Total} = 15.4249 \text{ tonnes/h} \qquad \dot{M}_{S\_Total} = 27.5019 \text{ tonnes/h}) \tag{7.1.1.12}$$

The filter cake's mass flow rate into the Strathcona normalizing tank is the output of the mass flow rate of the filter cake's normalizing tank. Moreover, the solid density from the filter cake's normalizing tank's output is the input solid density for the Phase II: Strathcona normalizing tank"

$$\dot{M}_{mix\_out\_fil} = \dot{M}_f = \frac{\{\dot{M}_{W\_Total} - (1-f_S)\cdot \dot{M}_{S\_Total}/f_S\}}{(1-f_{f\_out\_fil}/f_S)} \qquad (7.1.1.13)$$

The basic equation for the required equilibrium pump speed is:

$$\omega_1 = \frac{\dot{M}_{mix\_out\_fil}\cdot(x_{11}/SG_S + x_{21})}{k_{p1}\cdot(x_{11}+x_{21})}, k_{p1} = 0.02511 m^3/(h\cdot RPM) \qquad (7.1.1.14)$$

We substitute (7.1.1.13) into (7.1.1.14) and we would have a direct relationship between the required pump speed and the observable states in the phase I:

$$\omega_1 = \frac{(\dot{M}_{W\_Total} - \frac{(1-f_S)}{f_S}\cdot \dot{M}_{S\_Total})\cdot(x_{11}/SG_S + x_{21})}{k_{p1}\cdot\left(1-f_{f\_out\_fil}/f_S\right)\cdot(x_{11}+x_{21})} \qquad (7.1.1.15)$$

Moreover, our states are available with the two output measurements we have. Then we could make the pump speed be a dependent variable which would depend both the output measurements and the Strathcona slurry solids density:

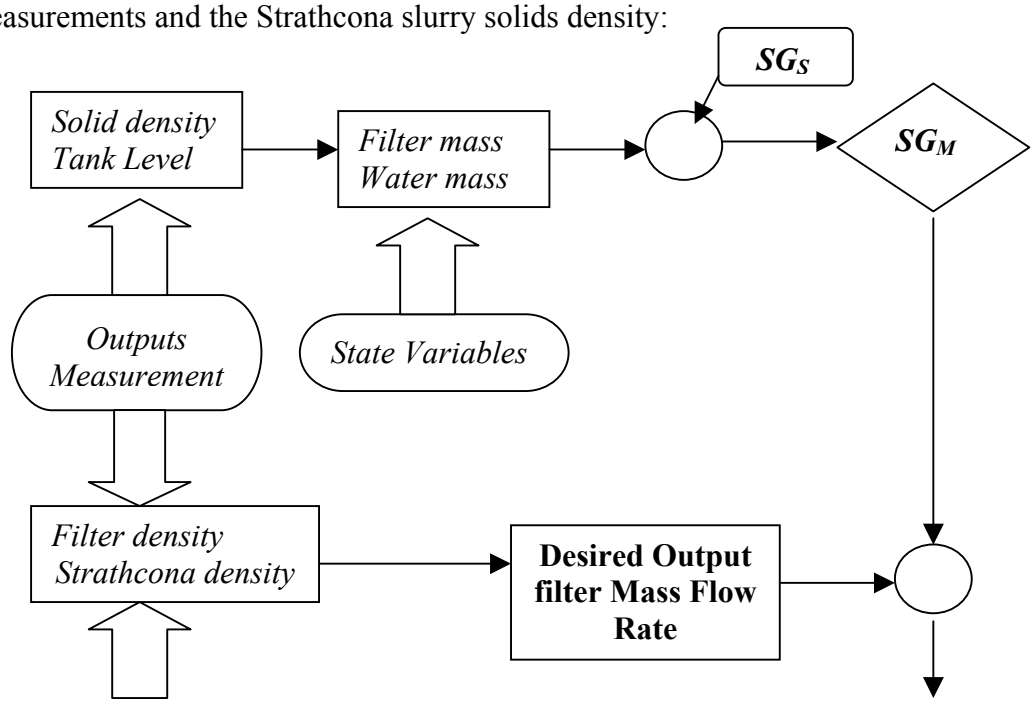

Fig. 7.1.1.1: State flow Diagram for the Pump Speed

Consequently, the pump speed would not be regarded as an input and we could have a system which has 2 states, 2 inputs and 2 outputs. This is important because in our assumption of input-output linearization, we need to have a relative degree which is less than the dimension of the state. This implies that the dimension of states has to be bigger or equal to the dimension of the output. In addition, it is easier for us to have the same dimension of inputs and outputs to carry out MIMO (Multi-Input and Multi-Output) input-output linearization design.

We could then substitute (7.1.1.13) into (7.1.1.2) and (7.1.1.3):

$$\dot{x}_{11} = f_{f\_in} \cdot u_{11} - \frac{x_{11} \cdot (f_S \cdot \dot{M}_{W\_Total} - (1 - f_S) \cdot \dot{M}_{S\_Total})}{(f_S \cdot (x_{11} + x_{21}) - x_{11})} \qquad (7.1.1.16)$$

$$\dot{x}_{21} = (1 - f_{f\_in}) \cdot u_{11} + u_{21} - \frac{x_{21} \cdot (f_S \cdot \dot{M}_{W\_Total} - (1 - f_S) \cdot \dot{M}_{S\_Total})}{(f_S \cdot (x_{11} + x_{21}) - x_{11})} \qquad (7.1.1.17)$$

To rewrite our System Phase I in the format of:

$$\begin{aligned} \dot{x} &= f(x) + g(x)u \\ y &= h(x) \end{aligned} \qquad (7.1.1.18)$$

and the system state space matrix formulation is:

System Phase I:

$$\begin{bmatrix}\dot{x}_{11}\\ \dot{x}_{21}\end{bmatrix}=\begin{bmatrix}-\dfrac{x_{11}\cdot(f_S\cdot\dot{M}_{W\_Total}-(1-f_S)\cdot\dot{M}_{S\_Total})}{(f_S\cdot(x_{11}+x_{21})-x_{11})}\\ -\dfrac{x_{21}\cdot(f_S\cdot\dot{M}_{W\_Total}-(1-f_S)\cdot\dot{M}_{S\_Total})}{(f_S\cdot(x_{11}+x_{21})-x_{11})}\end{bmatrix}+\begin{bmatrix}f_f & 0\\ (1-f_f) & 1\end{bmatrix}\begin{bmatrix}u_1\\ u_2\end{bmatrix} \qquad (7.1.1.19)$$

$$\begin{bmatrix}y_{11}\\ y_{21}\end{bmatrix}=\begin{bmatrix}\dfrac{x_{11}}{x_{11}+x_{21}}\\ \left(\dfrac{4}{\pi D_{dil.}^2}\right)\cdot\left(\dfrac{x_{11}}{SG_S}+x_{21}\right)\end{bmatrix}$$

In the next page, the state plan of Phase I is presented. This plan shows clearly how Phase I is connected with Phase II, and how the variables of Phase I and Phase II relate to each other.

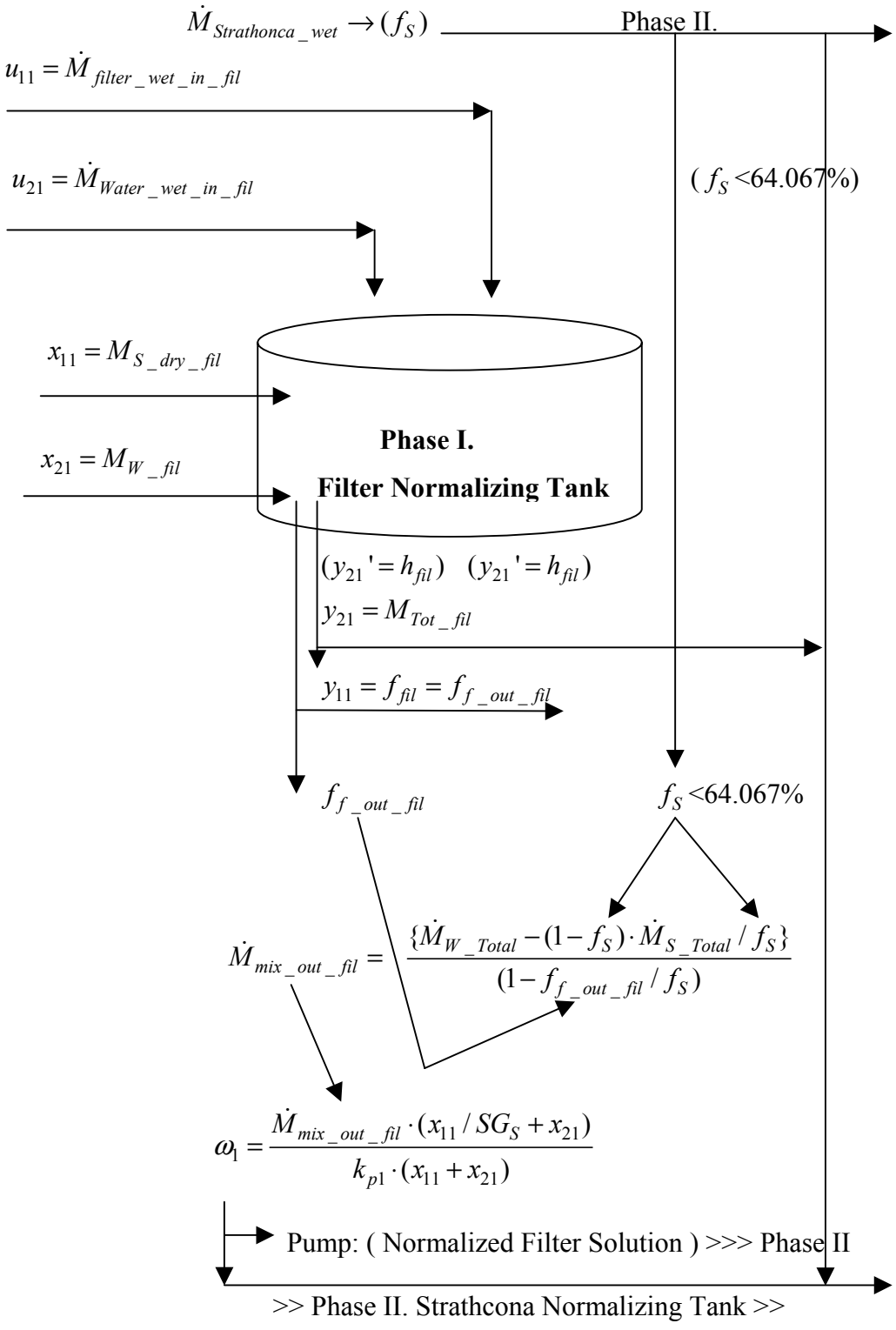

Fig. 7.1.1.2: Phase I System Plan

7.1.2 Input-Output Linearization

7.1.2.1 Input-Output Linearization Formulation

We shall differentiate output *y* until we can get a direct dependence between the output *y* and the input, *u*. By definition,

$$\dot{y} = \nabla h(f + gu) = L_f h + L_g h u \tag{7.1.2.1.1}$$

$$\nabla h = \begin{bmatrix} \frac{\partial h_1}{\partial x_{11}} & \frac{\partial h_1}{\partial x_{21}} \\ \frac{\partial h_2}{\partial x_{11}} & \frac{\partial h_2}{\partial x_{21}} \end{bmatrix} = \begin{bmatrix} \frac{x_{21}}{(x_{11}+x_{21})^2} & \frac{-x_{11}}{(x_{11}+x_{21})^2} \\ \frac{4}{\pi \cdot D_{dil.}^2 \cdot SG_S} & \frac{4}{\pi \cdot D_{dil.}^2} \end{bmatrix} \tag{7.1.2.1.2}$$

$$\begin{aligned} L_f h = & \begin{bmatrix} \frac{x_{21}}{(x_{11}+x_{21})^2} & \frac{-x_{11}}{(x_{11}+x_{21})^2} \\ \frac{4}{\pi \cdot D_{dil.}^2 \cdot SG_S} & \frac{4}{\pi \cdot D_{dil.}^2} \end{bmatrix} \\ & \cdot \begin{bmatrix} -\frac{x_{11} \cdot (f_S \cdot \dot{M}_{W\_Total} - (1-f_S) \cdot \dot{M}_{S\_Total})}{(f_S \cdot (x_{11}+x_{21}) - x_{11})} \\ -\frac{x_{21} \cdot (f_S \cdot \dot{M}_{W\_Total} - (1-f_S) \cdot \dot{M}_{S\_Total})}{(f_S \cdot (x_{11}+x_{21}) - x_{11})} \end{bmatrix} \\ = & \begin{bmatrix} 0 \\ -\frac{4 \cdot (x_{11} + SG_S \cdot x_{21}) \cdot (f_S \cdot \dot{M}_{W\_Total} - (1-f_S) \cdot \dot{M}_{S\_Total})}{\pi \cdot D_{dil.}^2 \cdot SG_S \cdot (f_S \cdot (x_{11}+x_{21}) - x_{11})} \end{bmatrix} \end{aligned} \tag{7.1.2.1.3}$$

$$L_g hu = \begin{bmatrix} \dfrac{x_{21}}{(x_{11}+x_{21})^2} & \dfrac{-x_{11}}{(x_{11}+x_{21})^2} \\ \dfrac{4}{\pi \cdot D_{fil}^2 \cdot SG_S} & \dfrac{4}{\pi \cdot D_{fil}^2} \end{bmatrix} \cdot \begin{bmatrix} f_f & 0 \\ (1-f_f) & 1 \end{bmatrix} \begin{bmatrix} u_1 \\ u_2 \end{bmatrix}$$

$$= \begin{bmatrix} \dfrac{\left(f_{f\_input} \cdot x_{21} - (1-f_{f\_input}) \cdot x_{11}\right)}{(x_{11}+x_{21})^2} & \dfrac{-x_{11}}{(x_{11}+x_{21})^2} \\ \dfrac{4 \cdot (f_{f\_input} - SG_S \cdot (1-f_{f\_input}))}{\pi \cdot D_{fil}^2 \cdot SG_S} & \dfrac{4}{\pi \cdot D_{fil}^2} \end{bmatrix} \begin{bmatrix} u_1 \\ u_2 \end{bmatrix} \qquad (7.1.2.1.4)$$

As stated in [Isidori, 1995], there are two conditions which qualify a multivariable nonlinear system to have relative degree γ at a point x_o:

i) $L_{g_j} L_f^k h_i(x) = 0$ (7.1.2.1.5)

ii) The $L_g h$ matrix is non-singular. (7.1.2.1.6)

Condition (i) is satisfied since both relative degrees of the two outputs are one. However, we have to check if the condition (ii) can be fulfilled and when it can be fulfilled. In order to check if the matrix is singular or not. We check if the determinant of the matrix $L_g h$, is zero or not and if it can be zero, when will it be zero. The determinant of the matrix $L_g h$ is:

$$\det(L_g h) = \left(f_{f\_input} \cdot \left(SG_S \cdot \left(\frac{1}{f_{f\_out}} - 1 \right) + \left(1 + 2 \cdot SG_S\right) \right) - 2 \cdot SG_S \right) \cdot \frac{4 \cdot x_{11}}{\left((x_{11}+x_{21})^2 \cdot \pi \cdot D_{fil}^2 \cdot SG_S \right)} \qquad (7.1.2.1.7)$$

We can see that if the factor equals to zero, which is possible, then our determinant (7.1.2.1.7) would be equal to zero. After appropriate algebraic manipulation, we have the following condition where the determinant would be equal to zero holds:

$$f_{f\_input} = \frac{2 \cdot SG_S}{\left(SG_S \cdot \left(\left(1/f_{f\_out}\right)-1\right)+\left(1+2 \cdot SG_S\right)\right)} \qquad (7.1.2.1.8)$$

f_{f_input} is the filter cake's original solids density coming into the filter normalizing tank.

f_{f_output} is the filter cake's output solids density coming out of the filter normalizing tank.

We can see from (7.1.2.1.8) that as SG_S and the output solid density varies, there is a set where the equality of (7.1.2.1.8) holds. This means when the input solid density which has been known to vary from 75% to 85% equal to the right hand side of (7.1.2.1.8), then our controller would ramp to infinity. We would like to know what ranges of the input filter solid density could cause the problem should the SG_S, the specific gravity of the filter cakes, and the final output solid density varies within its own range. What we found is when SG_S varies from 4.0 to 4.3 tonnes/m^3, and the output solid density varies from 70% to 85%, the input solids density varies from the minimum of 74% to 83%. This result is quite dangerous as we expect the input solid density would fall into this range as well. This means that basically we could not use the nonlinear controller for the Phase I at all.

Is there any way to solve this problem? In [Isidori, 1995], we see that it could be solved by using dynamic extension. But, this is outside the scope of this study. Instead, after careful reformulation, it was found that by choosing an alternative output function, we could achieve a much better result. The idea is to replace the tank level output function with another output which describes the total masses or volume in the filter cake's normalizing tank.

After careful consideration, we would use the total masses of the tank as the second output function. Of course, practically, being able to measure the output is very important. An easy measurement method of the total masses of the tank is provided as follows:

"It could be achieved by using load cells or other weight sensors."

The total equilibrium masses would be set at using the calculated equilibrium masses from (7.1.1.9):

$$x^*_{Total} = x^*_{11+21} = 27.75791 \text{ tonnes} \qquad (7.1.2.1.9)$$

Then by letting SG_S varies from 4.0 to 4.3 tonnes/m^3, and together with (7.1.1.9), substituting them into the original tank level output equation (7.1.1.5), we would be able to see how the tank level varies:

SG_S **(tonnes/m^3)**	**4.0**	**4.1**	**4.2**	**4.3**
Filter Tank Level (m)	*2.48*	*2.45*	*2.42*	*2.40*

Table 7.1.2.1.1 Filter Normalizing Tank Level Changes Variations in SG_S Changes.

From table 7.1.2.1.1, we can see that we do not need to worry about overflow of the tank caused by variations in SG_S. By controlling the total masses in the tank, we indirectly control the tank level within a small boundary of fluctuation. This is much better than losing stability of the process in order to control the tank level absolutely. Even if we could not measure SG_S of the filter cakes directly, with the level tank measurement we have previously, and with the new mass measurement, we would be able to calculate the instantaneous SG_S correspondingly. This instantaneous SG_S information is needed to calculate the respective pump speed required. Hence, we would be able to achieve a very robust system.

Finally, the new output equation is:

$$y_{21} = x_{11} + x_{21} \tag{7.1.2.1.10}$$

The new gradient of *h* function would be:

$$\nabla h = \begin{bmatrix} \frac{\partial h_1}{\partial x_{11}} & \frac{\partial h_1}{\partial x_{21}} \\ \frac{\partial h_2}{\partial x_{11}} & \frac{\partial h_2}{\partial x_{21}} \end{bmatrix} = \begin{bmatrix} \frac{x_{21}}{(x_{11}+x_{21})^2} & \frac{-x_{11}}{(x_{11}+x_{21})^2} \\ 1 & 1 \end{bmatrix} \tag{7.1.2.1.11}$$

With this new output equation, our new $L_f h$ and $L_g h$ are:

$$\begin{aligned} L_f h &= \begin{bmatrix} \frac{x_{21}}{(x_{11}+x_{21})^2} & \frac{-x_{11}}{(x_{11}+x_{21})^2} \\ 1 & 1 \end{bmatrix} \\ &\cdot \begin{bmatrix} -\frac{x_{11}\cdot(f_S\cdot\dot{M}_{W\_Total}-(1-f_S)\cdot\dot{M}_{S\_Total})}{(f_S\cdot(x_{11}+x_{21})-x_{11})} \\ -\frac{x_{21}\cdot(f_S\cdot\dot{M}_{W\_Total}-(1-f_S)\cdot\dot{M}_{S\_Total})}{(f_S\cdot(x_{11}+x_{21})-x_{11})} \end{bmatrix} \\ &= \begin{bmatrix} 0 \\ -\frac{(x_{11}+x_{21})\cdot(f_S\cdot\dot{M}_{W\_Total}-(1-f_S)\cdot\dot{M}_{S\_Total})}{(f_S\cdot(x_{11}+x_{21})-x_{11})} \end{bmatrix} \end{aligned} \tag{7.1.2.1.12}$$

$$\begin{aligned} L_g h u &= \begin{bmatrix} \frac{x_{21}}{(x_{11}+x_{21})^2} & \frac{-x_{11}}{(x_{11}+x_{21})^2} \\ 1 & 1 \end{bmatrix} \cdot \begin{bmatrix} f_f & 0 \\ (1-f_f) & 1 \end{bmatrix} \begin{bmatrix} u_{11} \\ u_{21} \end{bmatrix} \\ &= \begin{bmatrix} \frac{\left(f_f\cdot x_{21}-(1-f_f)\cdot x_{11}\right)}{(x_{11}+x_{21})^2} & \frac{-x_{11}}{(x_{11}+x_{21})^2} \\ 1 & 1 \end{bmatrix} \begin{bmatrix} u_{11} \\ u_{21} \end{bmatrix} \end{aligned} \tag{7.1.2.1.13}$$

The determinant of this $L_g h$ is:

$$\det(L_g h) = \frac{f_f}{(x_{11} + x_{21})} \tag{7.1.2.1.14}$$

The implication of (7.1.2.1.14) is very exciting as it means we have non-singular matrix in almost all situations, except the very non-likely case: the incoming filter cakes have zero solid density. This might happen if water is mistaken as filter cakes input, but way the possibility such a manual error is rare. Hence, we have full confidence to carry on the rest of our design. We then calculate the inverse of the matrix, as it is used later for constructing the controller. It is equal to:

$$\begin{aligned} L_g h^{-1} &= \frac{(x_{11} + x_{21})}{f_f} \begin{bmatrix} 1 & \frac{x_{11}}{(x_{11} + x_{21})^2} \\ -1 & \frac{\left(f_f \cdot (x_{11} + x_{21}) - x_{11}\right)}{(x_{11} + x_{21})^2} \end{bmatrix} \\ &= \begin{bmatrix} \frac{(x_{11} + x_{21})}{f_f} & \frac{x_{11}}{f_f \cdot (x_{11} + x_{21})} \\ -\frac{(x_{11} + x_{21})}{f_f} & \frac{\left(f_f \cdot (x_{11} + x_{21}) - x_{11}\right)}{f_f \cdot (x_{11} + x_{21})} \end{bmatrix} \end{aligned} \tag{7.1.2.1.15}$$

Our modified system has a well-defined relative degree as:

$$\begin{aligned} &\because \gamma_{11} = 1; \gamma_{21} = 1; \\ &\therefore \gamma = \gamma_{11} + \gamma_{21} = 2 = n \end{aligned} \tag{7.1.2.1.16}$$

and

$$\begin{bmatrix} \dot{y}_{11} \\ \dot{y}_{21} \end{bmatrix} = \begin{bmatrix} L_f h_{11} \\ L_f h_{21} \end{bmatrix} + L_g h \begin{bmatrix} u_{11} \\ u_{21} \end{bmatrix} \tag{7.1.2.1.17}$$

Then the state feedback control law is:

$$u = \begin{bmatrix} u_{11} \\ u_{21} \end{bmatrix} = L_g h^{-1} \cdot \begin{bmatrix} L_f h_{11} \\ L_f h_{21} \end{bmatrix} + L_g h^{-1} \cdot \begin{bmatrix} v_{11} \\ v_{21} \end{bmatrix} \qquad (7.1.2.1.18)$$

It then yields the corresponding linear closed loop system.

$$\begin{bmatrix} \dot{y}_{11} \\ \dot{y}_{21} \end{bmatrix} = \begin{bmatrix} v_{11} \\ v_{21} \end{bmatrix} \qquad (7.1.2.1.19)$$

This is the case of "Exact Input-Output Linearization". The diffeomorphic transformation of the system is as follows:

$$\begin{aligned} \dot{\zeta}_{11} &= v_{11}; \\ \dot{\zeta}_{21} &= v_{21}; \\ y_{11} &= \zeta_{11}; \\ y_{21} &= \zeta_{21}; \end{aligned} \qquad (7.1.2.1.20)$$

The inverse change of coordinates is given by:

$$\begin{aligned} x_{11} &= \zeta_{11} \cdot \zeta_{21}; \\ x_{21} &= (1 - \zeta_{11}) \cdot \zeta_{21}; \end{aligned} \qquad (7.1.2.1.21)$$

Since our total relative degree is equal to *n*, the system does not have zero dynamics.

Since our transformed system is linear, pole placement could be used to design the new control *v*. From [Henson & Seborg, 4], the standard stabilization input is:

$$v = -\alpha_1 \cdot \zeta_1 - \alpha_2 \cdot \zeta_2 .... - \alpha_n \cdot \zeta_n \qquad (7.1.2.1.22)$$

However, since the objective is tracking the system from a set point, then:

$$v = -\alpha_1 \cdot (\zeta_1 - \zeta_{1\_desired}) ... - \alpha_n \cdot (\zeta_n - \zeta_{n\_desired}) \qquad (7.1.2.1.23)$$

In the paper by [Sastry & Isidori, 1989], it states that in MIMO system, if the individual output equations' characteristic polynomial of (7.1.2.1.22):

$$p(s) = s^n + \alpha_n \cdot s^{n-1} + ... \alpha_1 = 0 \qquad (7.1.2.1.24)$$

is a Hurwitz polynomial, then the individual control v in (7.1.2.1.23) would result in asymptotic tracking. Also, as the relative degree of each output equation is one, the characteristic polynomial is first order for each output. In addition, since the transformed system (7.1.2.1.20) is decoupled, a diagonal structure is feasible and is preferable due to its simplicity. Henceforth, the corresponding control inputs would become:

$$\begin{aligned} v_{11} &= -\alpha_1 \cdot (\zeta_{11} - 0.75) \\ v_{21} &= -\alpha_2 \cdot (\zeta_{21} - 27.7538) \end{aligned} \qquad (7.1.2.1.25)$$

this means in matrix form:

$$K = \begin{bmatrix} -\alpha_1 & 0 \\ 0 & -\alpha_2 \end{bmatrix} \qquad (7.1.2.1.26)$$

Consequently, in order to have an asymptotically stable controller, we require A to be a Hurwitz matrix. Hence we require both:

$$\alpha_1 > 0 \ \ \& \ \ \alpha_2 > 0 \qquad (7.1.2.1.27)$$

However, although K is then Hurwitz, there are still many choices of the coefficients.
The initial guess of the coefficients of K can start with the system's response rate, in radians per time unit. Assume the system response time is about twenty minutes, then:

$$\omega_S = \frac{2 \cdot \pi}{\left(\frac{20\,\text{min}}{60\,\text{min/h}} \right)} = 6\pi\,\text{rad/h} \approx 18\,\text{rad/h} \qquad (7.1.2.1.28)$$

Hence,

$$K_I = \begin{bmatrix} -18 & 0 \\ 0 & -18 \end{bmatrix} \qquad (7.1.2.1.29)$$

The state feedback control law is then:

$$u = \begin{bmatrix} u_{11} \\ u_{21} \end{bmatrix} = L_g h^{-1} \cdot - \begin{bmatrix} L_f h_{11} \\ L_f h_{21} \end{bmatrix} + L_g h^{-1} \cdot K_I \cdot \begin{bmatrix} \xi_{11} - \xi_{11\_desired} \\ \xi_{21} - \xi_{21\_desired} \end{bmatrix} \qquad (7.1.2.1.30)$$

7.1.2.2 Simulation of Input-Output-Linearization

The initial states in the filter normalizing tank are not in equilibrium. We perturb the states in either direction for (+/-30%). Hence, we can see if the controller can steer the system back to equilibrium. The perturbed initial states are:

$$\begin{bmatrix} x_{11}(0) \\ x_{21}(0) \end{bmatrix} = \begin{bmatrix} x^*_{11} \cdot 0.7 \\ x^*_{21} \cdot 1.3 \end{bmatrix} = \begin{bmatrix} 14.57\,\text{t} \\ 9.02\,\text{t} \end{bmatrix} \qquad (7.1.2.2.1)$$

and

$$\begin{bmatrix} x_{11}(0) \\ x_{21}(0) \end{bmatrix} = \begin{bmatrix} x^*_{11} \cdot 1.3 \\ x^*_{21} \cdot 0.7 \end{bmatrix} = \begin{bmatrix} 27.0586\,\text{t} \\ 4.8576\,\text{t} \end{bmatrix} \qquad (7.1.2.2.2)$$

Initially, we simulate without uncertainty and we fix the filter cakes solid density to be:

$$f_f = 0.75 \qquad (7.1.2.2.3)$$

We use our initial K_I matrix to start with the simulation:

$$K_I = \begin{bmatrix} -18 & 0 \\ 0 & -18 \end{bmatrix} \qquad (7.1.2.2.4)$$

The simulation shows that the magnitude of the K_I is not big enough. After some tuning, it is found that the K_I that can assure tracking is:

$$K_I = \begin{bmatrix} -122 & 0 \\ 0 & -122 \end{bmatrix} \qquad (7.1.2.2.5)$$

With the above (7.1.2.2.5), we can attain tracking within an hour. The time constants corresponding to K_I are about seven minutes.

Now we turn to more realistic uncertain situation. In the filter normalizing tank, the major uncertainties come from the filter cakes incoming solid density and mass flow rate. The variation of the uncertainties is simulated with a uniform random but bounded distribution of the uncertainties. The filter cakes' solid density is bounded with:

$$0.75 \le f_f < 0.90 \qquad (7.1.2.2.6)$$

The mass flow rate of the filter cakes varies as:

$$u_{3a\_actual} = u_{3a\_calculated} \cdot (1 \pm 30\%) \qquad (7.1.2.2.7)$$

Unfortunately, this time the input-output linearization does not tolerate the uncertainties. The uncertainties have caused the matrix of $L_g h^{-1}$ close to singular no matter what gain matrix we use. However, we do need robustness in the Phase I due to the existence of huge input and parametric uncertainties.

7.1.2.3 Conclusion of Input-Output Linearization of Phase I

Consequently, in conclusion, input-output linearization is not feasible for the robust design of Phase I. In fact, this is not surprising, as we stated in chapter six, robustness is not guaranteed in input-output linearization.

Fortunately, this time our g matrix of Phase I is in a lower triangular form. Thus, robust switching control can be employed to design the robust controller.

7.1.3 Robust Switching Control of Phase I

7.1.3.1 Robust Switching Control Formulation

Since, we know sliding control can attain tracking objectives, and our main objective in Phase I is to obtain a robust design, we go directly to simulation of uncertainties. Henceforth, due to the fact that the *g* matrix of Phase I is in a lower triangular form:

$$g = \begin{bmatrix} f_f & 0 \\ (1-f_f) & 1 \end{bmatrix} \qquad (7.1.3.1.1)$$

Robust switching control, stated in chapter five, can be employed to design the robust controller. Before going into simulation, we derive the robust switching control law using the general robust switching equation in (5.1.2.2.1) and (5.1.2.2.2). Applying this equation to our filter tank design, we obtain the following regulation rules:

$$\left.\begin{cases} u_{11} = \dfrac{-dx_{11} - f_{11}}{\underset{\min}{f_{in}} \cdot (1 - k_{ufusk})}; \\ u_{21} = -dx_{21} - f_{21} - (1 - \underset{\max}{f_{in}}) \cdot u_{11} \end{cases}\right\} dx < 0$$

$$\left.\begin{cases} u_{11} = \dfrac{-dx_{11} - f_{11}}{\underset{\max}{f_{in}} \cdot (1 + k_{ufusk})}; \\ u_{21} = -dx_{21} - f_{21} - (1 - \underset{\max}{f_{in}}) \cdot u_{11} \end{cases}\right\} dx > 0 \qquad (7.1.3.1.2)$$

$$(dx = x - x_{des}, 0 < k_{ufusk} \le 1)$$

Note that k_{ufusk} is the variation range for the input uncertainty. With the above control regulation, then we can implement robust control for Phase I.

7.1.3.2 Simulation of Robust Sliding Control of Phase I

The simulation parameters are exactly the same as in input-output linearization. Hence k_{ufusk} is 0.3, or (+/- 30%) of the filter cakes mass flow rate. The simulation results are excellent at the first hand when there is no constraint in inputs. However, after, we constrain the inputs to their respective maximum limits, filter cakes being 17t/h and water being 18t/h, the controller fails and the system becomes unstable. Fortunately, after we increase both maximum limits, the system returns stable again and perform robustly. The lowest maximum limits for the two inputs are found to be 35t/h. This means to double the system's inputs, filter cakes and water. It is feasible to double the amount of filter cakes pouring into the Phase I tank by having two mechanical arm with a centralized control. Water input should also be easily adjusted to adapt to a larger valve which can pump 170USG per minute, or two of the same system's pumps for water with a centralized control. With this adjustment, the following results of the simulation are encouraging:

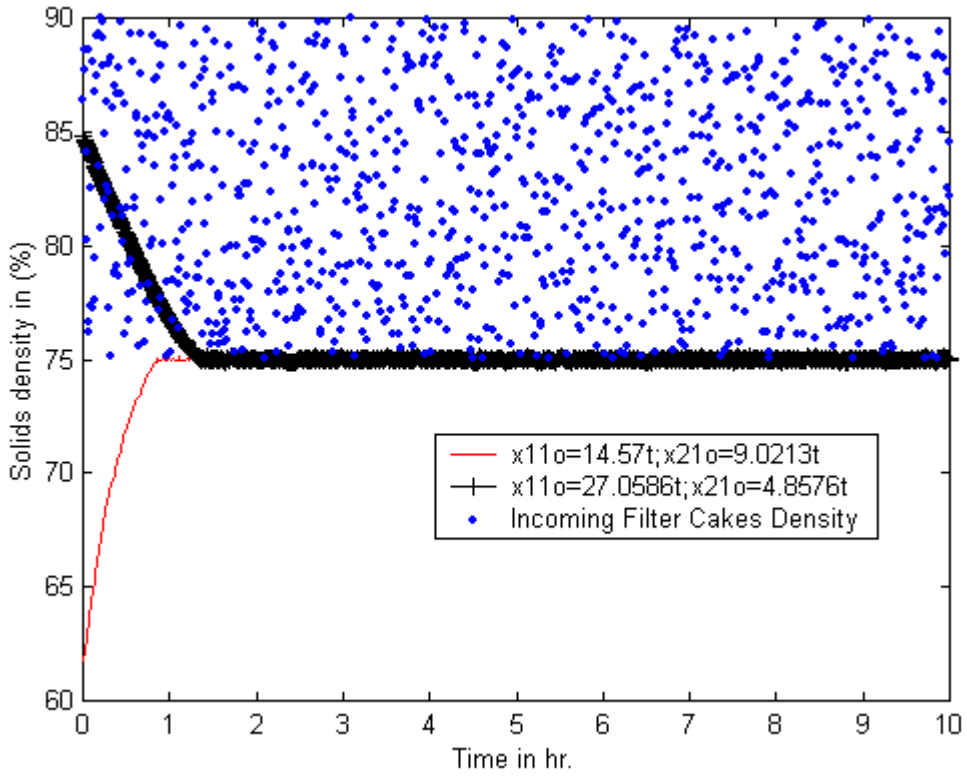

Fig. 7.1.3.2.1: Input Filter Cakes' Density Variation and Output Solid Density Variation of Filter Normalizing Tank regulated with Robust Switching Control.

From the Figure (7.1.3.2.1) above, we see the simulation of two initial cases. The first one with low Strathcona in the tank but high water content in the tank, and vice versa. The solid density of the filter normalizing tank in both cases goes back to the desired setpoint after one and one and half hours respectively. In considering with the highly irregular of the input uncertainty, this performance is very satisfactory.

However, there is an important point to be noticed. If the solid density of the output of the filter normalizing tank is below 64.067%, then the filter cakes solid solution would not be able concentrate the Strathcona solution in the Phase II should the Strathcona slurry's density is below 64.067% also. Hence, this means we should not have the same initial condition as the first condition of the simulation, of which the solid density of the tank is below 64.067%. If we can assure this, then we would not jeopardize our processes downstream. This important issue is also mentioned in the equation (7.1.3.1.3).

Certainly, the more stable and accurate the solid density of the filter cake solution is to the setpoint of 75%, the better it is able to be controlled in the next two phases.

To be more prepared for the next phase, the Strathcona normalizing tank, there should be another storage tank just for the filter cakes' solution which is normalized to 75% already. In this case, Phase II would only draw from the solution which has the right solid density. This way we can control the system very well.

Meanwhile, total mass output is shown next:

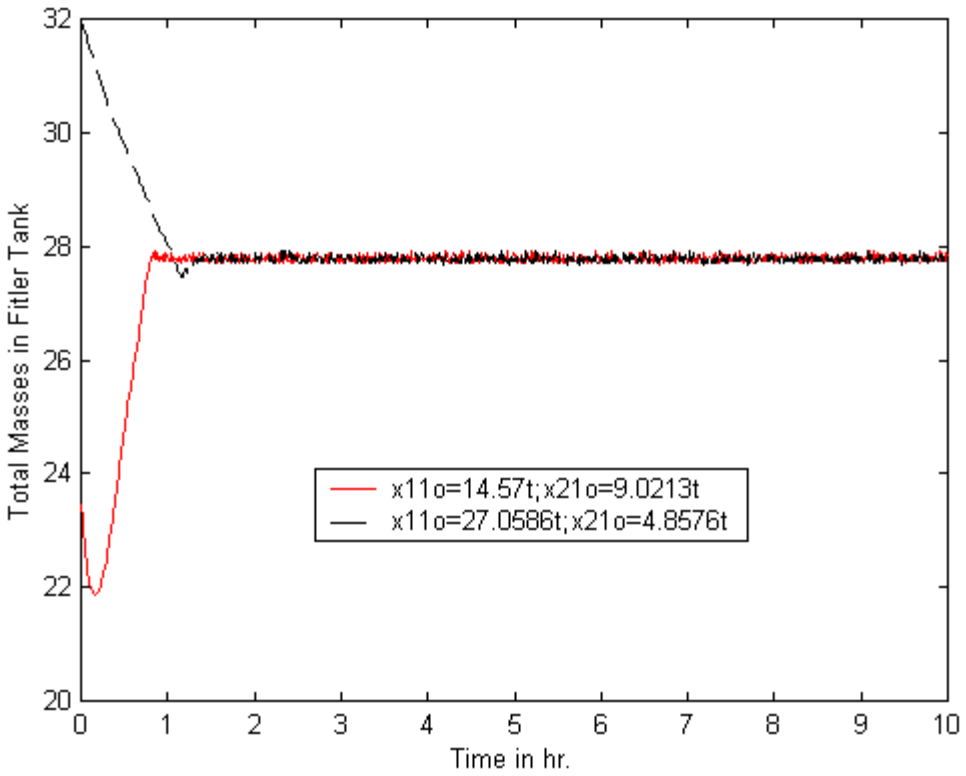

Fig. 7.1.3.2.2: Total Masses of Filter Normalizing Tank with Robust Switching Control.

Similarly, total masses of two initial state conditions are simulated. The results are again very satisfactory. The total mass of the tank in two cases goes back to the desired setpoint in an hour, despite with the uncertainties.

From this result we determine that indeed robust switching control can have robust performance and hence we found the robust nonlinear controller for Phase I.

We should also look at how the input varies. But as we mentioned just before, we have manually constrained the inputs values within the range of their maximum limits. The figure below shows how the inputs of filter cakes and water vary. Chattering inevitably exists in the two inputs. Filter cakes mass flow rate vary from 8 to 35 t/h, while water vary through the whole range, from 0 to 35 t/h. The figure showing the inputs fluctuation is in the next page.

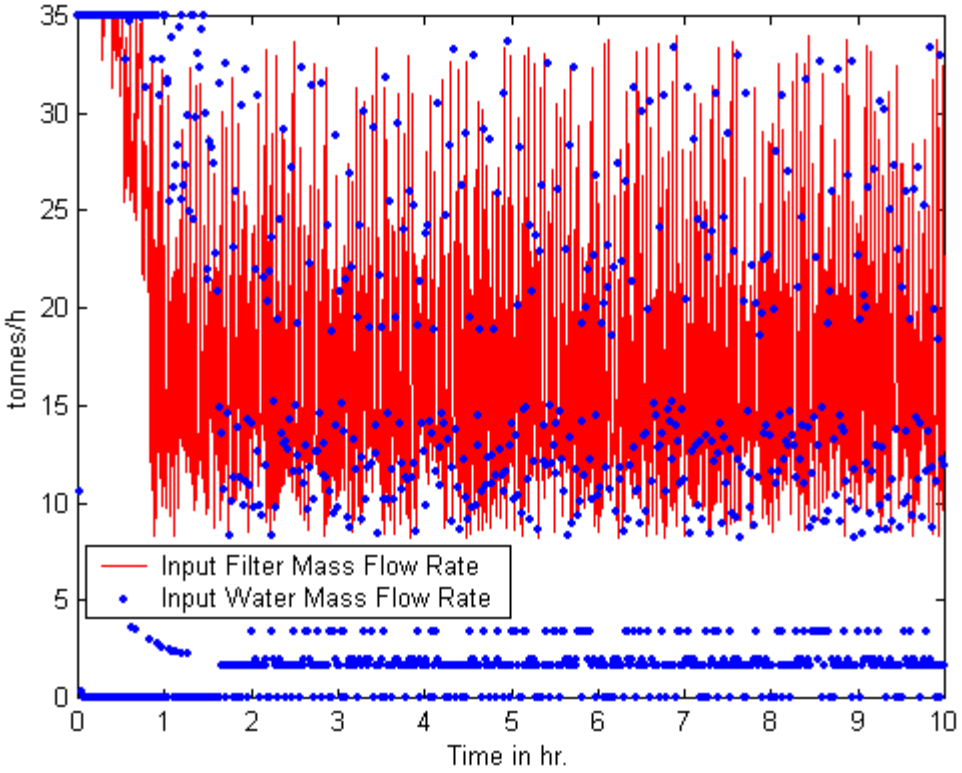

Fig. 7.1.3.2.3: Inputs of Filter Normalizing Tank with Robust Switching Control.

After confirming the stability and performance of our system, the pump speed and the total mass flow rate out of the tank has to be checked. This is because, the mass flow rate of the filter normalizing tank is the input of the Strathcona normalizing tank. As we mentioned in the section 7.1 and the equation (7.1.1.13),

$$\dot{M}_{mix\_out\_fil} = \dot{M}_f = \frac{\{\dot{M}_{W\_Total} - (1 - f_S) \cdot \dot{M}_{S\_Total} / f_S\}}{(1 - f_{f\_out\_fil} / f_S)}$$

the mass flow rate of the filter tank depends on the solid density of the output and the incoming Strathcona slurry density of the Phase II, Strathcona normalizing tank. Remembering that we only need to turn on the filter normalizing tank when the incoming Strathcona slurry's solid density is below 64.067%. Henceforth, the more dilute the incoming Strathcona slurry, the more normalized filter tank solution it needs.

However, there is one important point to be noted. In (7.1.1.3), if the solid density of the output of the filter tank is more dilute than the incoming Strathcona slurry, then the output mass flow rate calculated with (7.1.1.3) becomes negative. Under normal circumstances, this should not happen. But since we perturb the states initially, it is possible that if we perturb the states too much, it would cause the needed mass flow rate negative. By (7.1.1.14),

$$\omega_1 = \frac{\dot{M}_{mix\_out\_fil} \cdot (x_{11} / SG_S + x_{21})}{k_{p1} \cdot (x_{11} + x_{21})}, k_{p1} = 0.02511 \, \mathrm{m}^3/(\mathrm{h} \cdot \mathrm{RPM})$$

a negative total-mass-flow-rate out of the filter tank will give rise to a negative pump speed. Certainly, this situation is disastrous. Hence, to avoid this situation happening, we need to find out what is the maximum limit of perturbation of the states without jeopardizing the stability of the system. This implies that the initial solid density of the solution in the filter tank has to be greater or equal to 64.067%. Hence:

$$0.64067 = \frac{x_{11} \cdot (1 - k)}{\left(x_{11} \cdot (1 - k) + x_{21} \cdot (1 + k)\right)}; k > 0 \qquad (7.1.3.1.3)$$

We found that 'k=0.256'. It means that the maximum percentage we can perturb the initial states according to our formula in (7.1.3.1.3) is 25.6% less for the Strathcona state in the filter tank. To be more prudent, 20% of lower limit perturbation of the Strathcona

state is taken. On the other hand, there is no maximum limit for the Strathcona state in the filter tank. This means that higher solid density of the tank never makes the system unstable. With the adjustment, the mass flow rate is being simulated below:

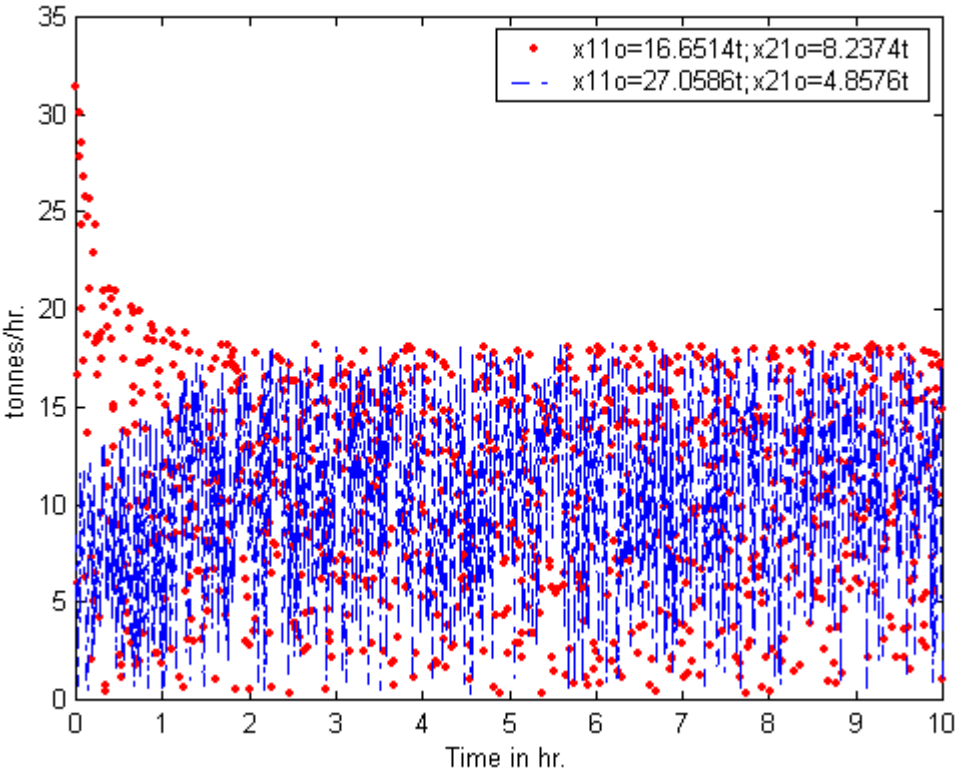

Fig. 7.1.3.2.4: Output Mass Flow Rate of Filter Tank with Robust Switching Control.

In Fig. 7.1.3.2.4, the upper set of the initial states is based on the following equation:

$$x_{11}(0) = x_{11}^{*} \cdot (1-0.2) = 20.8143 \cdot (0.8) = 16.6514 \text{ tonnes}$$
$$x_{21}(0) = x_{21}^{*} \cdot (1+0.3) = 6.93948 \cdot (1.3) = 8.2374 \text{ tonnes} \qquad (7.1.3.1.4)$$

These initial states correspond to the initial solid density of the filter tank of 66.9%.

The lower set of initial conditions are still the same as the other previous simulations, with Strathcona state 30% higher than its equilibrium value, and water state 30% lower

than its equilibrium value. Also, Fig. 7.1.3.2.4 is simulated with following additional parameters randomly varying, along with other parameters stated before:

$$f_S \le 0.64067\,;\ 4.0 \le SG_S \le 4.3\,(\text{tonnes/m}^3) \qquad (7.1.3.1.5)$$

Since SG_S of the solution is equal to SG_M of the output of the filter tank, which is measurable, this is not an uncertain parameter.

The following figure is the pump speed variation which show exactly the same trend as the previous figure on total mass flow rate.

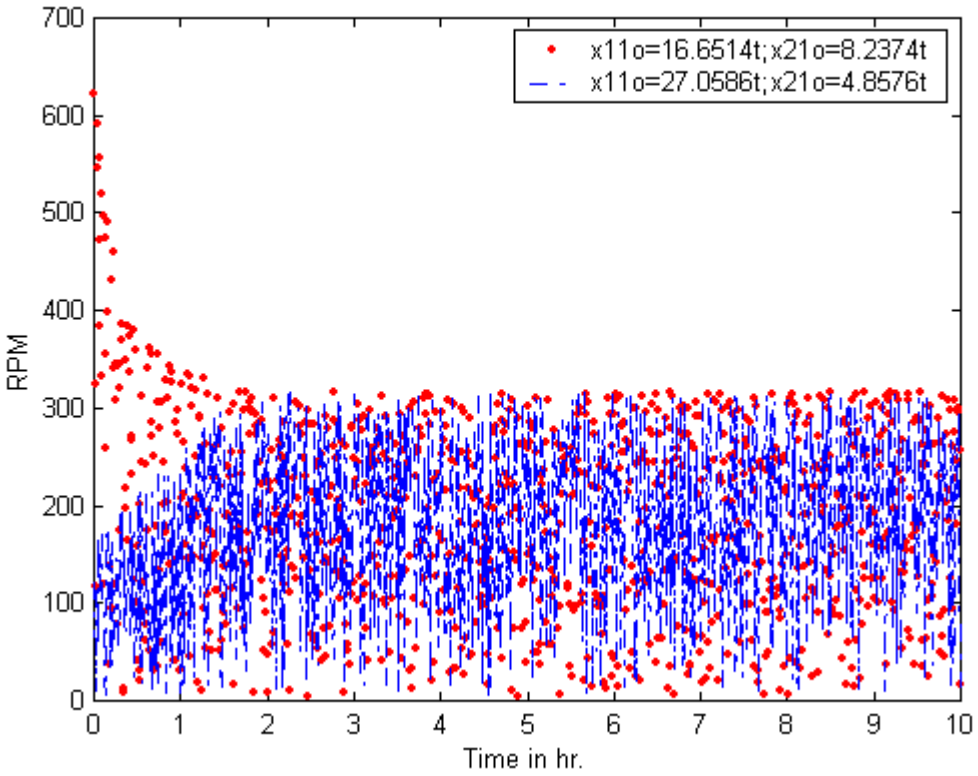

Fig. 7.1.3.2.5: Pump Speed of Filter Tank with Robust Switching Control.

From Fig. 7.1.3.2.4 and Fig. 7.1.3.2.5, it is satisfactory to see that the total mass flow rate, and hence the pump speed vary within the operating range under two different sets of initial conditions and input parametric uncertainties.

7.1.3.3 Conclusion of Robust Sliding Control of Phase I

In conclusion, as seen from the simulation tests, robust switching control performs satisfactorily in all aspects. Although it behaves severely in chattering, it provides a simpler, quicker means of obtaining the desired assured robust tracking performance.

7.1.4 Conclusion of Phase I Design

Unfortunately, input-output linearization cannot provide the required robust performance. Nevertheless, input-output linearization does attain tracking objectives when there is no uncertainty. In order to accommodate a large initial state perturbation (+/-30%), robust switching control has to have higher inputs' saturation limits. This in turn allows the inputs to fluctuate even more. Besides wearing out the actuators, excessive chattering through a large dynamic range can cause severe time delay problems. Control efforts that are calculated in one time instant might only be able to completely realize them after couple more time instants. This delay can cause uncontrollability and hence instability of the system. In general, the actuator's reaction time should be always smaller than the sampling time. In this study, the sampling instants are every 36 seconds. This large time interval between two successive sampling times shall give the actuators ample time to do the corrective control efforts.

For further studies, it would be interesting to study how to obtain the K matrix analytically, which can ensure robustness and performance. This may cause recent efforts in trying to utilize both input-output linearization and H_2/H_∞, to design a nonlinear robust controller. Besides robustness, systematic way of treating inputs and states constraints in input-output linearization is challenging as well. For switching control, boundary layer could also be introduced to eliminate chattering. Then the actuators would not wear out as quickly.

In this Phase I study, robust switching control, has proved to be very effective and is feasible to provide satisfactory tracking for system with bounded linear parametric uncertainties and systems with de-coupled or diagonal input structure in the state equations. Hence, robust switching control is determined to be the robust controller for this phase.

Next we are going to look into Phase II design.

7.2 Phase II. Strathcona Normalizing Tank ("Str"):

For the Phase II system, we again have a switching situation. We switch from case *a)*, Strathcona slurry solid density below 64.067% and case *b)* Strathcona slurry solid density equal to or above 64.067%. Again, state formulation is treated firstly.

7.2.1 State Space System Formulation

$$\begin{aligned} &x_{12} = M_{S\_dry\_Str}; && x_{22} = M_{W\_Str} \\ &u_{12} = \dot{M}_{Str.\_wet\_in\_Str}; && u_{22a} = \dot{M}_{f\_wet\_in\_Str}; \quad u_{22b} = \dot{M}_{W\_in\_Str} \\ &y_{12} = f_{Str}; && y_{22} = M_{Tot\_Str} \end{aligned} \qquad (7.2.1.1)$$

In the Strathcona normalizing tank, we utilize switching control between the two cases:

a) $f_S < 64.067\%$ (7.2.1.2)

b) $f_S \geq 64.067\%$ (7.2.1.3)

In case *a)*, whenever the incoming Strathcona slurry has detected having the solids density lower than 64.067%, then it would switch to controller *a)* which uses filter cakes to increase the slurry's density, as in this case water input is not appropriate. On the other

hand, in case b), if the Strathcona slurry density is equal to or greater than 64.067%, then we will not use filter cakes input, but we will use water to dilute the slurry instead.
Even though the state equations differ in these two cases, the output equations are the same:

$$y_{12} = \frac{x_{12}}{x_{12} + x_{22}} \tag{7.2.1.4}$$

$$y_{22} = x_{12} + x_{22} \tag{7.2.1.5}$$

Similarly, the pump speed will be controlled separately by an independent SISO switching controller. The pump speed for the Strathcona normalizing tank's equation is:

$$\omega_2 = \frac{\dot{M}_{mix\_out\_Str} \cdot (x_{12} / SG_S + x_{22})}{k_{p2} \cdot (x_{12} + x_{22})} \tag{7.2.1.6}$$
$$(k_{p2} = 0.02511 \mathrm{m}^3/(\mathrm{h} \cdot \mathrm{RPM})$$

The mass flow rate of the pump gets updated as well. This is because the output of the Strathcona normalizing tank is to fill the Repulper tank. The system requires the output give all the necessary Strathcona, i.e. 27.5019 tonnes/h regardless of the density. Hence,

$$\dot{M}_{mix\_out\_Str} = \dot{M}_{S\_Total} / f_{S\_out\_Str} = \frac{\dot{M}_{S\_Total}}{\left(\frac{x_{12}}{x_{12} + x_{22}}\right)}$$
$$= \frac{\dot{M}_{S\_Total} \cdot (x_{12} + x_{22})}{x_{12}} \tag{7.2.1.7}$$
$$(\dot{M}_{S\_Total} = 27.5019)$$

The above equation, (7.2.1.7), guarantees that the Repulper tank always has the necessary Strathcona input for the following Repulper tank. This is because if there is not enough water, there is water input for the Repulper tank as well. Hence, for determining the amount of Strathcona mix mass flow rate flowing into the Repulper tank, it is better to be

short of water than the dry mass Strathcona. Also it is important to realize that (7.2.1.7) depends on the every changing Strathcona solid density, in the Strathcona normalizing tank. Hence, as f_S, the solids density of Strathcona, varies, the amount of mix flow rate out of the Strathcona normalizing tank varies also accordingly. Henceforth, as can be seen the relationship of (7.2.1.6) and (7.2.1.7), the pump speed varies too, but to a larger extent as the pump speed also depends on SG_M, which varies as well.

Lastly, in order to calculate the pump speed in (7.2.1.6), we still need the parameter SG_S. Fortunately, since we can measure SG_M, as SG_S is a parameter of SG_M, then, SG_S can be calculated from the equation:

$$SG_S = \frac{SG_M \cdot x_{12}}{\left(x_{12} - SG_M \cdot x_{22}\right)} \qquad (7.2.1.8)$$

The above equation is derived from:

$$SG_M = \frac{x_{12}}{\left(x_{12} / SG_S + x_{22}\right)} \qquad (7.2.1.9)$$

Hence, then, the pump speed can be calculated with no ambiguity. In addition, since the pump speed is anticipated to vary to a certain extent, it is safer to check the validity of the pump characteristic constant using the equation (6.1.9), derived in section 6.1 Henceforth, the validated pump characteristic constant will be used to calculate the required pump velocity.

Thus, in either case, the system has two inputs, two states and two outputs. Each of the two cases will be dealt with subsequently.

Case a): $f_S < 64.067\%$

$$\dot{x}_{12} = f_S \cdot u_{12} + f_f \cdot u_{22a} - \frac{\dot{M}_{mix\_out\_Str} \cdot x_{12}}{(x_{12} + x_{22})} \tag{7.2.1.10}$$

$$\dot{x}_{22} = (1 - f_S) \cdot u_{12} + (1 - f_f) \cdot u_{22a} - \frac{\dot{M}_{mix\_out\_Str} \cdot x_{22}}{(x_{12} + x_{22})} \tag{7.2.1.11}$$

Case b): $f_S \geq 64.067\%$

$$\dot{x}_{12} = f_S \cdot u_{12} - \frac{\dot{M}_{mix\_out\_Str} \cdot x_{12}}{(x_{12} + x_{22})} \tag{7.2.1.12}$$

$$\dot{x}_{22} = (1 - f_S) \cdot u_{12} + u_{22b} - \frac{\dot{M}_{mix\_out\_Str} \cdot x_{22}}{(x_{12} + x_{22})} \tag{7.2.1.13}$$

Then if we substitute (7.2.1.6) and (7.2.1.7) into the state equations above, then we have:

Case a): $f_S < 64.067\%$

$$\dot{x}_{12} = f_S \cdot u_{12} + f_f \cdot u_{22a} - \dot{M}_{S\_Total} \tag{7.2.1.14}$$

$$\dot{x}_{22} = (1 - f_S) \cdot u_{12} + (1 - f_f) \cdot u_{22a} - \frac{\dot{M}_{S\_Total} \cdot x_{22}}{x_{12}} \tag{7.2.1.15}$$

Case b): $f_S \geq 64.067\%$

$$\dot{x}_{12} = f_S \cdot u_{12} - \dot{M}_{S\_Total} \tag{7.2.1.16}$$

$$\dot{x}_{22} = (1 - f_S) \cdot u_{12} + u_{22b} - \frac{\dot{M}_{S\_Total} \cdot x_{22}}{x_{12}} \tag{7.2.1.17}$$

Then, let us rewrite our system in the standard state-space format, for each of the two cases:

Case a): $f_S < 64.067\%$

$$\begin{bmatrix} \dot{x}_{12} \\ \dot{x}_{22} \end{bmatrix} = \begin{bmatrix} -\dot{M}_{S\_Total} \\ -\dfrac{\dot{M}_{S\_Total} \cdot x_{22}}{x_{12}} \end{bmatrix} + \begin{bmatrix} f_S & f_f \\ 1-f_S & 1-f_f \end{bmatrix} \begin{bmatrix} u_{12} \\ u_{22a} \end{bmatrix}$$
$$\begin{bmatrix} y_{12} \\ y_{22} \end{bmatrix} = \begin{bmatrix} \dfrac{x_{12}}{x_{12}+x_{22}} \\ x_{12}+x_{22} \end{bmatrix} \qquad (7.2.1.18)$$

Case b): $f_S \geq 64.067\%$

$$\begin{bmatrix} \dot{x}_{12} \\ \dot{x}_{22} \end{bmatrix} = \begin{bmatrix} -\dot{M}_{S\_Total} \\ -\dfrac{\dot{M}_{S\_Total} \cdot x_{22}}{x_{12}} \end{bmatrix} + \begin{bmatrix} f_S & 0 \\ 1-f_S & 1 \end{bmatrix} \begin{bmatrix} u_{12} \\ u_{22b} \end{bmatrix}$$
$$\begin{bmatrix} y_{12} \\ y_{22} \end{bmatrix} = \begin{bmatrix} \dfrac{x_{12}}{x_{12}+x_{22}} \\ x_{12}+x_{22} \end{bmatrix} \qquad (7.2.1.19)$$

Since we have intentionally set up to have equal number of states and outputs, we can obtain the states information from the measurable outputs. However, since our output equations are nonlinear, we cannot obtain them straightly from matrix manipulation. Solving for the states from the outputs, we have:

$$x_{12} = y_{12} \cdot y_{22} \qquad (7.2.1.20)$$

$$x_{22} = (1-y_{12}) \cdot y_{22} \qquad (7.2.1.21)$$

The nominal or desired values for the state variables are:

$$x_{12} = 14.74521 \text{ tonnes} \qquad (7.2.1.22)$$

$$x_{22} = 8.27020 \text{ tonnes} \qquad (7.2.1.23)$$

The corresponding desired output values in equilibrium are:

$$y_{12} = 0.64067 \text{ tonnes} \qquad (7.2.1.24)$$

$$y_{22} = 23.01541 \text{ tonnes} \qquad (7.2.1.25)$$

(7.2.1.24) and (7.2.1.25), along with the nominal values of SG_S (4.2 t/m^3), will give the nominal height of the Strathcona normalizing tank to be exactly 2.40 meters. However, as we already mentioned in sections before, since SG_S varies within its range (4.0 – 4.3 t/m^3) randomly, the level of the tank varies accordingly as well. In the search of the nonlinear controllers, both input-output linearization and robust switching control have been considered. Although the parameter SG_S varies unpredictably, from (7.2.1.8) we can obtain this parameter accurately. Therefore, in Phase II, in either cases of *a)* or *b)*, the model of the system, "the Strathcona normalizing tank", can be considered exact. Henceforth, input-output linearization can be employed as well as general switching control. It is interesting to study the effect of combining the two methods. Hence, for case *a)*, input-output linearization is chosen to be the method of nonlinear control. Then, for case *b)*, general switching control can be used instead. Formulation is addressed next.

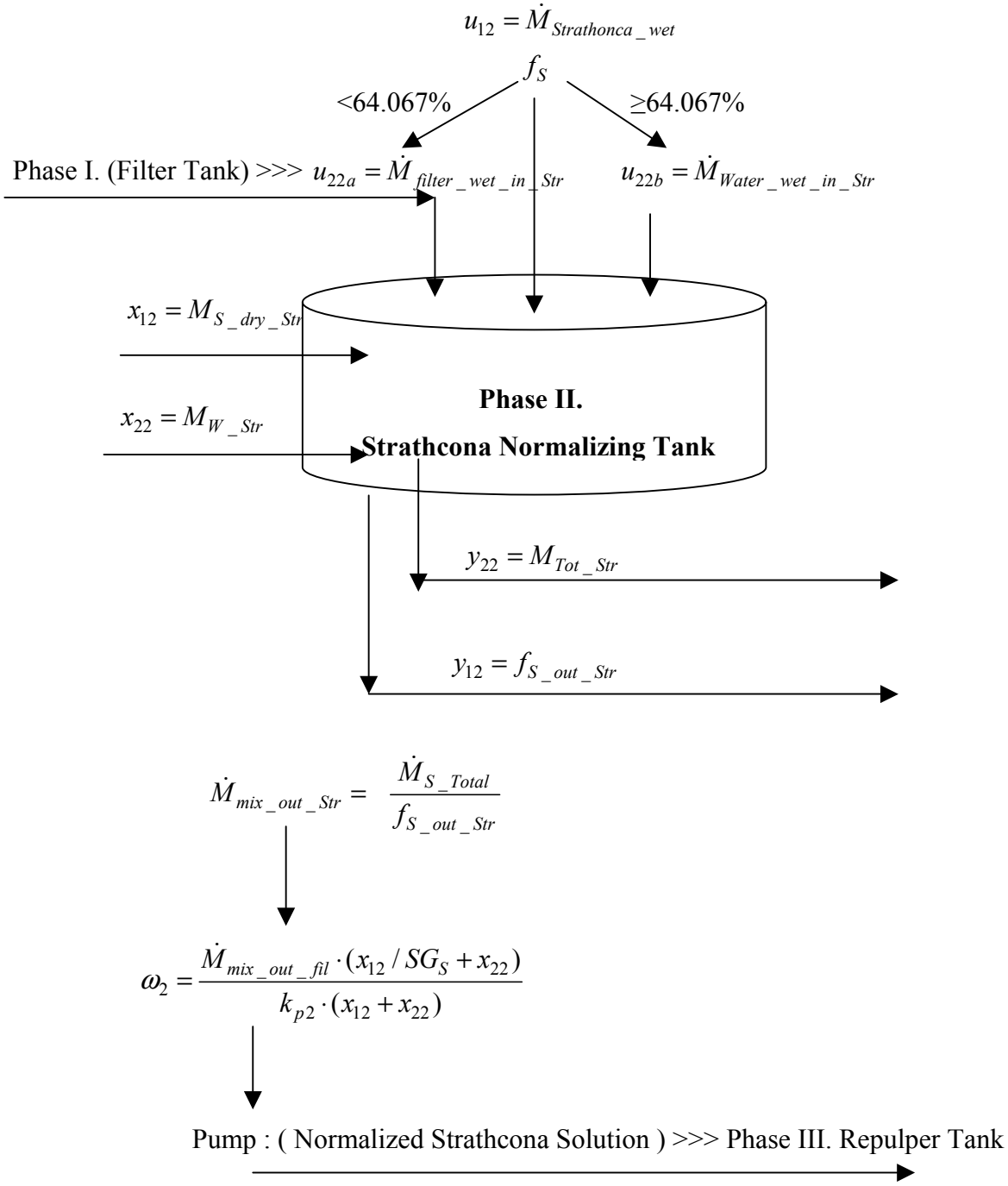

Fig. 7.2.1.1: Phase II System Plan

7.2.2 Control Law Formulation and Simulation:

Case a): $f_S < 64.067\%$

As the usual procedure for input-output linearization, we shall differentiate outputs *y* until there is a direct dependence relationship between the outputs *y* and the inputs, *u*.

Hence, then by definition,

$$\dot{y} = \nabla h(f + gu) = L_f h + L_g hu \tag{7.2.2.1}$$

$$\nabla h = \begin{bmatrix} \frac{\partial h_1}{\partial x_{11}} & \frac{\partial h_1}{\partial x_{21}} \\ \frac{\partial h_2}{\partial x_{11}} & \frac{\partial h_2}{\partial x_{21}} \end{bmatrix} = \begin{bmatrix} \frac{x_{22}}{(x_{12}+x_{22})^2} & \frac{-x_{12}}{(x_{12}+x_{22})^2} \\ 1 & 1 \end{bmatrix} \tag{7.2.2.2}$$

$$\begin{aligned} L_f h &= \begin{bmatrix} \frac{x_{22}}{(x_{12}+x_{22})^2} & \frac{-x_{12}}{(x_{12}+x_{22})^2} \\ 1 & 1 \end{bmatrix} \cdot \begin{bmatrix} -\frac{\dot{M}_{mix\_out\_str} \cdot x_{12}}{(x_{12}+x_{22})} \\ -\frac{\dot{M}_{mix\_out\_str} \cdot x_{22}}{(x_{12}+x_{22})} \end{bmatrix} \\ &= \begin{bmatrix} 0 \\ -\dot{M}_{mix\_out\_str} \end{bmatrix} \end{aligned} \tag{7.2.2.3}$$

$$\begin{aligned} L_g hu &= \begin{bmatrix} \frac{x_{22}}{(x_{12}+x_{22})^2} & \frac{-x_{12}}{(x_{12}+x_{22})^2} \\ 1 & 1 \end{bmatrix} \cdot \begin{bmatrix} f_S & f_f \\ (1-f_S) & (1-f_f) \end{bmatrix} \cdot \begin{bmatrix} u_{12} \\ u_{22a} \end{bmatrix} \\ &= \begin{bmatrix} \frac{\left(f_S \cdot x_{22} - (1-f_S) \cdot x_{12}\right)}{(x_{12}+x_{22})^2} & \frac{\left(f_f \cdot x_{22} - (1-f_f) \cdot x_{12}\right)}{(x_{12}+x_{22})^2} \\ 1 & 1 \end{bmatrix} \begin{bmatrix} u_{12} \\ u_{22a} \end{bmatrix} \end{aligned} \tag{7.2.2.4}$$

Again, there are two conditions to be fulfilled for a multivariable nonlinear system to have relative degree at a point x_0:

i) $Lg_i L_f^k h_j(x) = 0, i = 1,...,m; j = 1,...,p; k = 0,...,\gamma_i - 2$ (7.2.2.5)

ii) The matrix $M(x)$, from (5.1.1.3.7) is non-singular at x_0. (7.2.2.6)

We have fulfilled condition one (7.2.2.5) with ease since both relative degrees of the two outputs are one. However, we have to check if the condition two can be fulfilled and when it can be fulfilled. In order to check if the matrix is singular or not, compute the determinant of the matrix $L_g h$:

$$\det(L_g h) = \frac{f_S - f_f}{(x_{11} + x_{21})} \tag{7.2.2.7}$$

The implication of (7.2.2.7) means that the determinant can be zero if and only if the incoming Strathcona slurry's solid density is equal to the filter cakes' solid density. Fortunately, the filter cakes' density has been normalized to 75%, and the nominal maximum solid density of the incoming Strathcona slurry does not exceed 70%. Hence, in most general cases, using input-output linearization is feasible. But certainly, for the safety check, it is important to stay alert to check if there is any incoming Strathcona slurry which has a solid density close to 75%. Nevertheless, in general, the conditions of (7.2.2.5) and (7.2.2.6) are satisfied and the rest of the design procedures can carry on.

When checking the relative degree, as can be seen (7.2.2.4), the relative degree is:

$$\begin{aligned} &\gamma_1 = 1; \gamma_2 = 1; \\ &\gamma = \gamma_1 + \gamma_2 = n = 2; \end{aligned} \tag{7.2.2.8}$$

As our total relative degree is equal to n, there is no zero dynamics.

The new output equations are:

$$\begin{bmatrix} \dot{y}_{12} \\ \dot{y}_{22} \end{bmatrix} = \begin{bmatrix} L_f h_{12} \\ L_f h_{22} \end{bmatrix} + L_g h \begin{bmatrix} u_{12} \\ u_{22a} \end{bmatrix} \tag{7.2.2.9}$$

Then the state feedback control law becomes:

$$u = \begin{bmatrix} u_{12} \\ u_{22a} \end{bmatrix} = L_g h^{-1} \cdot \begin{bmatrix} L_f h_{12} \\ L_f h_{22} \end{bmatrix} + L_g h^{-1} \cdot \begin{bmatrix} v_{12} \\ v_{22} \end{bmatrix} \tag{7.2.2.10}$$

It then yields the corresponding linear closed-loop system.

$$\begin{bmatrix} \dot{y}_{11} \\ \dot{y}_{21} \end{bmatrix} = \begin{bmatrix} v_{12} \\ v_{22} \end{bmatrix} \tag{7.2.2.11}$$

The diffeomorphic transformation of the system is as follows:

$$\begin{aligned} \dot{\zeta}_{12} &= v_{12}; \\ \dot{\zeta}_{22} &= v_{22}; \\ y_{12} &= \zeta_{12}; \\ y_{22} &= \zeta_{22}; \end{aligned} \tag{7.2.2.12}$$

The inverse change of coordinates is given by:

$$\begin{aligned} x_{12} &= \zeta_{12} \cdot \zeta_{22}; \\ x_{22} &= (1 - \zeta_{12}) \cdot \zeta_{22}; \end{aligned} \tag{7.2.2.13}$$

The new control law has the similar state pole placement structure:

$$v = A \cdot d\xi \tag{7.2.2.14}$$

where,

$$A = \begin{bmatrix} -a_{12} & -a_{22} \\ -a_{32} & -a_{42} \end{bmatrix} \tag{7.2.2.15}$$

Since we have a decoupled structure in (7.2.2.14), we can use a diagonal structure for (7.2.2.15), which is simpler and hence easier to tune:

$$K_{II} = \begin{bmatrix} -a_{12} & 0 \\ 0 & -a_{42} \end{bmatrix} \tag{7.2.2.16}$$

$$d\xi = \begin{bmatrix} \xi_{12} - \xi_{12\_des} \\ \xi_{22} - \xi_{22\_des} \end{bmatrix} \tag{7.2.2.17}$$

Our modified control law is:

$$u = \begin{bmatrix} u_{11} \\ u_{21} \end{bmatrix} = L_g h^{-1} \cdot \left(- \begin{bmatrix} L_f^{\gamma_{11}} h_{11} \\ L_f^{\gamma_{21}} h_{21} \end{bmatrix} \right) + L_g h^{-1} \cdot K_{II} \cdot \begin{bmatrix} \xi_{12} - \xi_{12\_desired} \\ \xi_{22} - \xi_{22\_desired} \end{bmatrix} \tag{7.2.2.18}$$

The choice of K_{II} in Phase II is much easier as the controller does not need to handle uncertainties any more as in Phase I. As usual, the coefficients of K_{II} are required to be all negative definite. Concluding from Phase I, there is no systematic way or 'rule' of choosing the negative coefficients. Hence, from numerous empirical testing of different combinations of the coefficients, the K_{II} that is found to have the best performance is:

$$K_{II} = \begin{bmatrix} -630 & 0 \\ 0 & -630 \end{bmatrix} \tag{7.2.2.19}$$

Hence, the control formulation of case *a)* is finished. Initial testing and simulation has shown that the control laws work very well. Therefore, only the combined simulations of case *a)* and case *b)* is going to be shown at the end of the formulation of case *b)*.

Case b): $f_S \geq 64.067\%$

The general switching control law for case *b)* is simple but effective:

$$u(k+1) = g(x,k)^{-1} \cdot (-dx(k) - f(x,k)) \qquad (7.2.2.20)$$

where,

$$dx = \begin{bmatrix} dx_{12} \\ dx_{22} \end{bmatrix} = \begin{bmatrix} x_{12} - x_{12\_des} \\ x_{22} - x_{22\_des} \end{bmatrix} \qquad (7.2.2.21)$$

But as shown in (7.2.2.20), we do need to check if *g* is invertible or not. The *g* matrix for case *b)* is:

$$\begin{bmatrix} f_S & 0 \\ 1-f_S & 1 \end{bmatrix} \qquad (7.2.2.22)$$

Hence, we calculate the determinant of *g* as:

$$\det(g) = f_S \qquad (7.2.2.23)$$

As we see from (7.2.2.23), if the incoming Strathcona slurry is not being misplaced with water, the determinant of *g* could rarely be zero. Hence, we can proceed to use our general switching control law, (7.2.2.20).

Finally, as the control formulations have just finished, the simulation results are going to be shown in the following subsection. One remark is that, again, it is obvious that general switching control, when is feasible to use, is much simpler and easier to formulate than input-output linearization.

7.2.3 Simulation Results & Discussion

The initial states in the Strathcona normalizing tank are not in equilibrium. We perturb the states in either direction for (+/-30%). Hence, we can see if the controller can steer the system back to equilibrium. The perturbed initial states are:

$$\begin{bmatrix} x_{12}(0) \\ x_{22}(0) \end{bmatrix} = \begin{bmatrix} x^*_{12} \cdot 0.7 \\ x^*_{22} \cdot 1.3 \end{bmatrix} = \begin{bmatrix} 14.74521 \cdot (0.7) \\ 8.2702 \cdot (1.3) \end{bmatrix} = \begin{bmatrix} 10.3216\ \text{t} \\ 10.7536\ \text{t} \end{bmatrix} \qquad (7.2.3.1)$$

$$\begin{bmatrix} x_{12}(0) \\ x_{22}(0) \end{bmatrix} = \begin{bmatrix} x^*_{12} \cdot 1.3 \\ x^*_{22} \cdot 0.7 \end{bmatrix} = \begin{bmatrix} 19.1688 \cdot (1.3) \\ 5.7891 \cdot (0.7) \end{bmatrix} = \begin{bmatrix} 24.9194\ \text{t} \\ 4.5237\ \text{t} \end{bmatrix} \qquad (7.2.3.2)$$

Since we simulate both case *a)* and case *b)* together, the incoming Strathcona slurry solid density varies randomly for the whole range:

$$0.56 \le f_S \le 0.68 \qquad (7.2.3.3)$$

The incoming normalized filter cakes solid density, from Phase I, is simulated with random variation,

$$0.60 \le f_f \le 0.85 \qquad (7.2.3.4)$$

for a large range, the same variations as simulated in the output solid density of Phase I, filter normalizing tank.

In reality, SG_S can be calculated from the measurable SG_M with (7.2.1.8). Meanwhile, its variation is simulated at the same randomly varied range as the other simulations:

$$4.0 \le SG_S \le 4.3 \qquad (7.2.3.5)$$

We use our K_{II} matrix for the case *a)* of the simulation:

$$K_{II} = \begin{bmatrix} -630 & 0 \\ 0 & -630 \end{bmatrix} \qquad (7.2.3.6)$$

With (7.2.3.6), we can attain tracking within one-and-half hour. The corresponding time constants to K_{II} are about six minutes.

In the next page, the output solid density of the Strathcona normalizing tank is being shown. It shows how the output solid density of the two initial conditions come back to the desired setpoint, 64.067% from their respective perturbation.

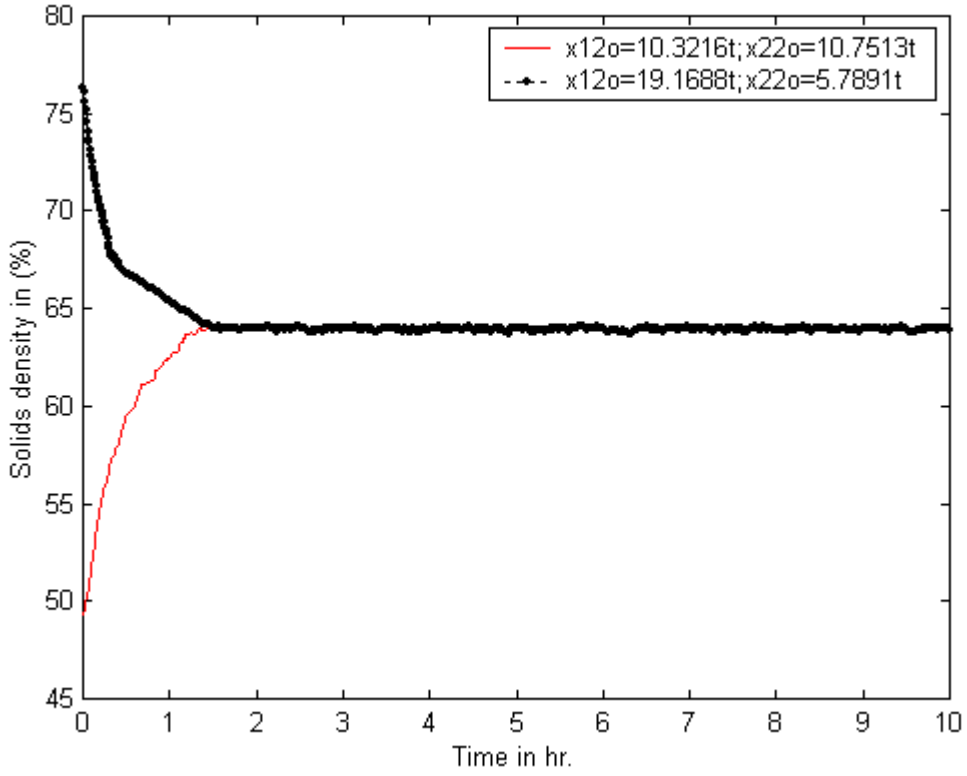

Fig. 7.2.3.1: Output Solid densities of two initial state conditions for Phase II, Strathcona normalizing tank

As can be seen in Fig. 7.2.3.1, with the switching between input-output linearization and sliding control, Strathcona slurry's density is being normalized to the range of 64.4% to 63.6%, even with large initial state perturbations. Output solid density keeps on fluctuating within this small range. Nevertheless, it is accurate enough in most circumstances. Hence, the control laws are very successful. Next, the total masses are going to be shown.

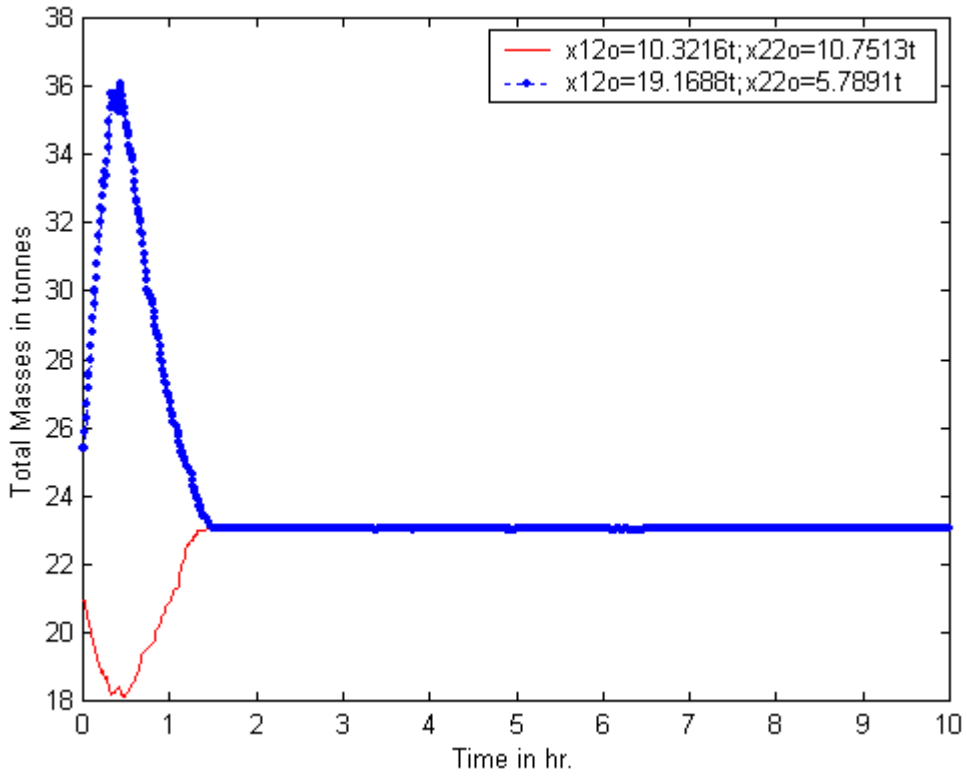

Fig. 7.2.3.2: Total Masses of two initial state conditions for Phase II, Strathcona normalizing tank.

From Fig. 7.2.3.2, the total mass of the tank does go back to the desired setpoint in about 80 minutes, with both initial conditions. However, with the second initial condition, the total mass has a peak at about 30 minutes after the simulation starts. This surge in total mass, 35.7640 tonnes, corresponds to the height of the Strathcona tank at 3.6m. Since, our tank's height is 3m, this means we will have overflow. Hence, to prevent this probable event happening, then the height of the Strathcona normalizing tank should be, with an addition of 20% safety factor, at 4.3m. With this new dimension for the tank, the tank can comfortably handle (+/-30%) perturbations in state masses.

Next, after seeing the success of the tracking, it is also important to see how the pump speed varies.

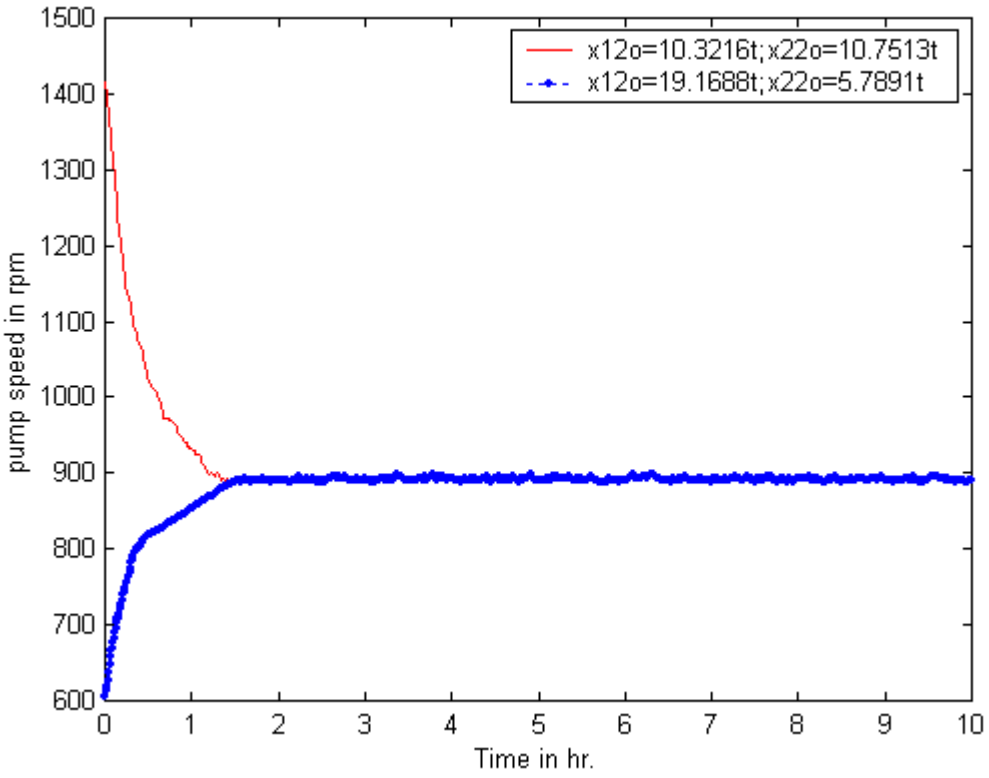

Fig. 7.2.3.3: The output mix flow pump speed of Strathcona normalizing tank.

In Fig. 7.2.3.3, it is satisfactory to see the pump speed goes back to 900rpm and stays there, after it comes back from two initial conditions' perturbations. However, there is a slight problem. The pump speed for the case of the first initial condition starts with a really high rpm. However, if we are going to simulate the vigorous perturbation, this means we need to provide a pump for the Strathcona normalizing tank which can operate as high as 1400 rpm. This is a typical issue of robust performance and cost. Nevertheless, after the peak at the beginning, the pump speed goes down smoothly. Hence, at least, the pump does not suffer from chattering.

Since the mass flow rate out the Strathcona has a direct relationship as in (7.2.1.6) with the pump speed, it varies exactly the way as the pump speed. The maximum mass flow rate is 57 tonnes/h and the minimum mass flow rate is 35 tonnes/hr. After 80 minutes, the mass flow goes to the desired setpoint, 42.95 tonnes/h, and stays there.

Now, how about the inputs of Strathcona slurry, filter cakes and water? Are they chattering a lot? To answer these questions, let us look at the following figures:

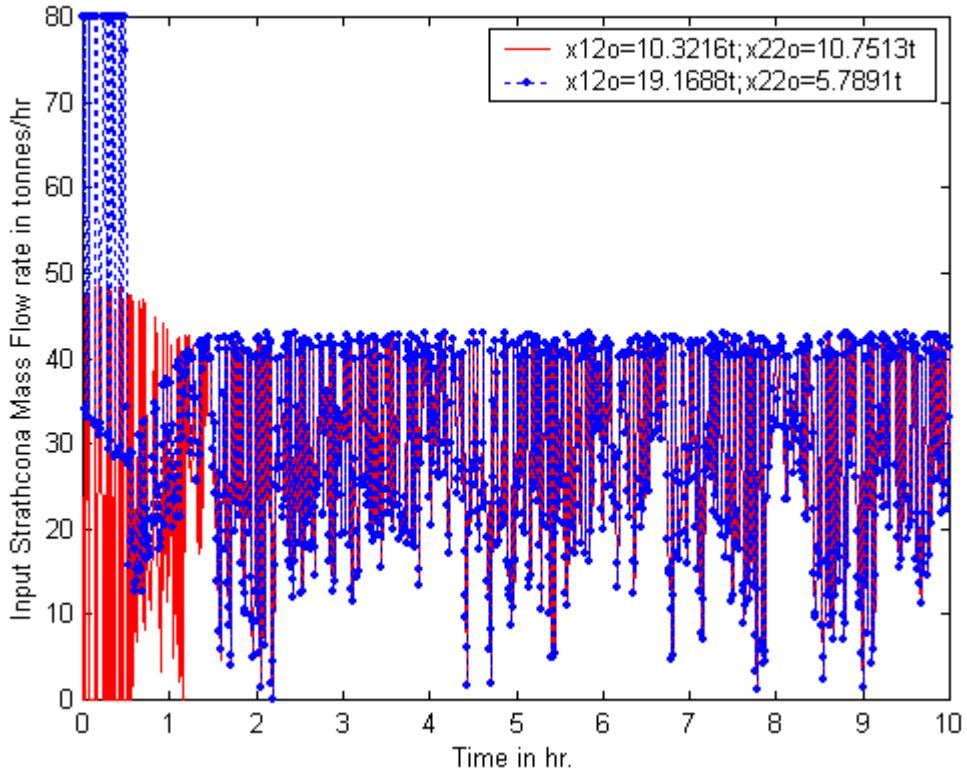

Fig. 7.2.3.4: Input Strathcona Mass flow rate of Strathcona normalizing tank.

From Fig. 7.2.3.4, indeed, the Strathcona slurry input chatters a lot but mostly within the range from 0 to 45 tonnes/h, except the first half-hour for the second initial condition, where there are more Strathcona masses in the tank. This explains why there is a surge of total masse for the tank. Nevertheless, since then the input stays at below 45 tonnes/h. Unfortunately, due to the fact that the incoming filter cakes' density and Strathcona slurry's solid density vary considerably, this chattering behavior is inevitable.

In the case of filter cakes' input, since we have manually constrained the maximum mass flow rate of filter cakes to be at 20 tonnes/h. The input of filter cakes does show that it fluctuates from 0 to 20 tonnes/h all way through. Nevertheless, the water input mass flow rate varies differently:

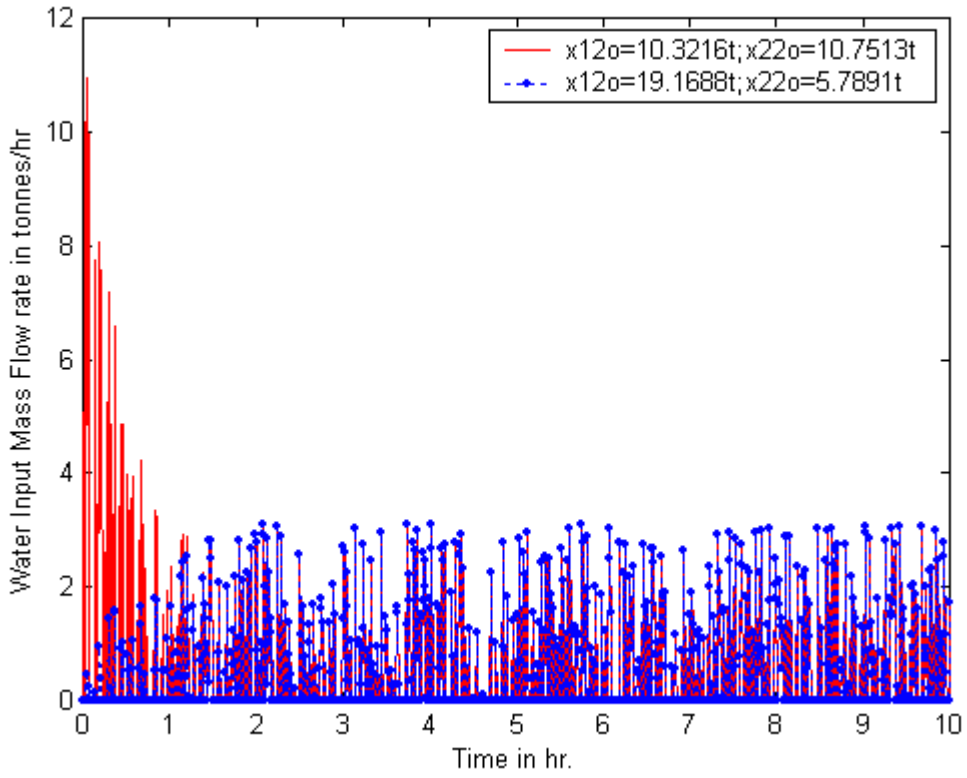

Fig. 7.2.3.5: Input Strathcona Mass flow rate of Strathcona normalizing tank.

From Fig. 7.2.3.5, water does not fluctuate as much. Except for the first 2 hours for the initial condition, water input mass flow rate stays below 3 tonnes/h. Hence, this fluctuation is deemed acceptable.

From the five graphs which have just shown, it is very encouraging that the hybrid of input-output linearization and switching control system performs satisfactorily. Also, chattering does not seem to be a very serious problem, except for the case of Strathcona slurry input and filter cakes input. Also, pump speed of output flow rate does not chatter. Hence, we have had improvements from the conventional control system, where every control input chatters to a certain degree. However, this is an issue to be aware of. What happens if both case *a)* and case *b)* are run with either input-output linearization or general switching control.

From the simulation results which are not shown here, if the incoming filter cakes density is too low, then general switching control does not perform very well. However, when the filter cakes density does not deviate too much from 75%, it can track the system very well and the final output solid density can be controlled at the desired setpoint 64.067 very accurately and do not fluctuate. On the other hand, input-output linearization though can push the output solid density around the setpoint, it cannot settle down right at the setpoint, 64.067%. It keeps on fluctuating within a small range, from 63.6% to 64.4%, no matter how large the magnitude of the K_{II} matrix is. Hence, if accuracy is needed, then general switching control should be used for the whole Phase II. Meanwhile, at the beginning if the incoming filter cakes density varies too much, input-output linearization can stabilize the system and attain tracking objectives approximately. Further manipulation can be considered as having input-output linearization to run first when the incoming filter cakes density deviates too much. Then when the deviation of filter cakes density becomes small, we can turn on general switching control for fine-tuning.

7.2.4 Conclusion of Phase II Design

In this Phase II design, it is encouraging to see the fruit of spending efforts in normalizing the filter cakes' density first in the previous "Filter Normalizing Tank". Without the Phase I process, it is not possible to reach the very best result of the present phase. Now, the only process left is to add Raglan and mix them thoroughly. But as Raglan powder input is not an uncertain parameter as the filter cakes' input, the final Repulper tank becomes a very simple and easy system to control.

7.3 Phase III Repulper Tank ("Rep")

In Chapter 6, we see that the existing process system controller would not work if the states were not available. We have also mentioned that the major obstacle for obtaining correct state information is due to the uncertain parameters of SG_S and SG_R. Now, in this Repulper tank, are we going to have the same kind of setting as in the conventional

control system? If this is the case, then inevitably, we are still having the same problem, we cannot get the correct state information to perform closed-loop control.

But without closed-loop control, we sacrifice stability. Henceforth, we design the controller which is a mix of open loop controller and closed-loop control. In this way, the tracking objectives of regulating Raglan and Strathcona ratio and total solid density are met, while the level of the tank can be well controlled, indirectly by feeding back the output measurement of total mass in the tank. Now, let us look at the formulation of this Phase III.

7.3.1 Phase III State Space Formulation

$$
\begin{aligned}
&x_{13} = M_{S+R\_rep}; && x_{23} = M_{W\_rep} \\
&u_{13} = \dot{M}_{S\_wet\_in\_rep;} && u_{23} = \dot{M}_{f\_in\_rep} \\
&u_{33} = \dot{M}_{R\_in\_rep}; && u_{43} = \dot{M}_{W\_in\_rep} \\
&u_{53} = \omega_{p3}; && y_{13} = f_{rep} \\
&y_{23} = M_{Total}; && y_{33} = SG_M
\end{aligned}
\qquad (7.3.1.1)
$$

In order to control the above problem precisely, we shall again treat this problem in two cases. The first case is when the total solids density is less than or equal to 70%, and the second case is when the solid density is greater than 70%.

Case a) $f_{rep} \leq 70\%$

In this case, we need filter cakes input, and the corresponding Raglan to increase the concentration back to 70%. The filter cakes slurry comes from the filter normalized tank. As the mass flow rate of Raglan is a dependent variable on the mass flow rate of the filter cakes, we shall determine the mass flow rate of the filter cakes first:

$$f_{rep\_desired}(70\%) = \frac{x_{13} + \Delta x_{13}}{\left(x_{13} + \Delta x_{13} + x_{23} + \Delta x_{23}\right)} \tag{7.3.1.2}$$

$$\Delta x_{13} = \dot{M}_{f\_in\_rep} \cdot f_f \cdot (1+R) \tag{7.3.1.3}$$

$$\Delta x_{23} = \dot{M}_{f\_in\_rep} \cdot \left(1 - f_f\right) \tag{7.3.1.4}$$

Then by putting (7.3.1.3) and (7.3.1.4) into (7.3.1.2), we get:

$$f_{rep\_desired} = \frac{x_{13} + \dot{M}_f \cdot f_f \cdot \left(1+R\right)}{\left(x_{13} + x_{23} + \dot{M}_f \cdot \left(1 + f_f \cdot R\right)\right)} \tag{7.3.1.5}$$

$$u_{23} = \dot{M}_f = \frac{\left(x_{13} + x_{23}\right) \cdot f_{rep\_des} - x_{13}}{\left(f_f \cdot \left(1+R\right) - f_{rep\_des} \cdot \left(1 + f_f \cdot R\right)\right)} \tag{7.3.1.6}$$

Henceforth, since, we try to match all incoming Strathcona, whether it comes from filter cakes' normalizing tank or Strathcona normalizing tank, with the corresponding Raglan, we formulate the open loop Raglan control equation input to be:

$$u_{33} = \left(u_{13} \cdot f_{S\_in\_rep} + u_{23} \cdot f_{f\_in\_rep}\right) \cdot R; \qquad R = 0.3092 \tag{7.3.1.7}$$

But note that, from Phase II,

$$u_{13} = \dot{M}_{mix\_out\_Str} \tag{7.3.1.8}$$

Hence, we do not control the input of the Strathcona slurry coming from the Strathcona normalizing tank's output. If the tank's state is in equilibrium, we want the output mass flow rate being equal to the sum of the input flow rates. However, when the tank' total mass is perturbed, then we want also the to adjust the mass flow rates accordingly so that

the tank can return back to its original total mass. Hence, the output mass flow rates shall depend also on the error of the total mass. If we set to correct the output error in an hour:

$$\dot{M}_{mix\_out\_rep} = \left(\sum_{i=1:4} u_i \right) + \left(+ M_{Tot\_rep} - M^*_{Tot\_rep} \right) / h \qquad (7.3.1.9)$$

Also, to relate the output mass flow rate with the pump,

$$\dot{M}_{mix\_out\_rep} = \omega_3 \cdot k_{p3} \cdot SG_M \qquad (7.3.1.10)$$

Then, when we put (7.3.1.6) into (7.3.1.7), then we can equate the pump speed with,

$$\omega_3 = \frac{\left(\sum_{i=1:4} u_{i3} \right) + \left(+ M_{Tot\_rep} - M^*_{Tot\_rep} \right)}{k_{p3} \cdot SG_M} \qquad (7.3.1.11)$$

The above equation is a general one which can apply to both cases. In this case *a)*, as there is no water input, u_{43} is zero. Here, since, we try to avoid the issue of SG_S and SG_R, SG_M becomes a measurable parameter, as we mentioned in the earlier chapters:

$$SG_M = \frac{\dot{M}_{rep}}{\dot{V}_{rep}} \qquad (7.3.1.12)$$

Pump speed and the mass flow rate of the filter cakes are being SISO closed-loop controlled. Henceforth the tank's total solid density and total mass go back to equilibrium points when they deviate. We formulate the system in a state space format so that our states, input and outputs can propagate. Hence, (7.3.1.13)

$$\begin{bmatrix} \dot{x}_{13} \\ \dot{x}_{23} \end{bmatrix} =$$

$$\begin{bmatrix} f_{S\_in\_rep} & f_{f\_in\_rep} & R \cdot \begin{pmatrix} u_{13} \cdot f_{S\_in\_rep} \\ +u_{23} \cdot f_{f\_in\_rep} \end{pmatrix} & 0 & \begin{pmatrix} -k_p \cdot SG_M \\ \cdot \dfrac{x_{13}}{x_{13}+x_{23}} \end{pmatrix} \\ \begin{pmatrix} 1- \\ f_{S\_in\_rep} \end{pmatrix} & \begin{pmatrix} 1- \\ f_{f\_in\_rep} \end{pmatrix} & 0 & 0 & \begin{pmatrix} -k_p \cdot SG_M \\ \cdot \dfrac{x_{23}}{x_{13}+x_{23}} \end{pmatrix} \end{bmatrix} \begin{bmatrix} u_{13} \\ u_{23} \\ u_{33} \\ u_{43} \\ u_{53} \end{bmatrix}$$

$$\begin{bmatrix} y_{13} \\ y_{23} \end{bmatrix} = \begin{bmatrix} \dfrac{x_{13}}{x_{13}+x_{23}} \\ x_{13}+x_{23} \end{bmatrix}$$

Case b): $f_S > 70\%$

In case *b)*, the situation gets simpler since we only need water to add into it.

$$f_{rep\_desired}(70\%) = \frac{x_{13}}{\left(x_{13}+x_{23}+\Delta x_{23}\right)} \tag{7.3.1.14}$$

$$u_{43} = \Delta x_{23} = \frac{\left(x_{13} - f_{rep\_des} \cdot \left(x_{13}+x_{23}\right)\right)}{f_{rep\_des}} \tag{7.3.1.15}$$

This time, the open loop Raglan control equation becomes:

$$u_{33} = R \cdot u_{13} \cdot f_{S\_in\_rep} \tag{7.3.1.16}$$

Again we have the non-controlled incoming Strathcona slurry. For the pump speed, we use the equation we derive previously in (7.3.1.11). The difference is that this time, there is no filer cakes' input, u_{23} is zero, but instead there is water input u_{43}.

Finally, we have managed to manipulate this dilemma well. We have formulated one open loop control, the Raglan mass flow rate, and two independent nonlinear closed-loop controls. Again, we form a state space equation as well for case *b)*:

$$\begin{bmatrix} \dot{x}_{13} \\ \dot{x}_{23} \end{bmatrix} =$$

$$\begin{bmatrix} f_{S\_in\_rep} & 0 & \begin{pmatrix} R \cdot u_{13} \\ \cdot f_{S\_in\_rep} \end{pmatrix} & 0 & -k_p \cdot SG_M \cdot \dfrac{x_1}{x_1 + x_2} \\ \begin{pmatrix} 1- \\ f_{S\_in\_rep} \end{pmatrix} & 0 & 0 & 1 & -k_p \cdot SG_M \cdot \dfrac{x_2}{x_1 + x_2} \end{bmatrix} \begin{bmatrix} u_{13} \\ u_{23} \\ u_{33} \\ u_{43} \\ u_{53} \end{bmatrix} \qquad (7.3.1.17)$$

$$\begin{bmatrix} y_{13} \\ y_{23} \end{bmatrix} = \begin{bmatrix} \dfrac{x_{13}}{x_{13} + x_{23}} \\ x_{13} + x_{23} \end{bmatrix}$$

In the next page, we are going to look at the system plan of this phase, Phase III.

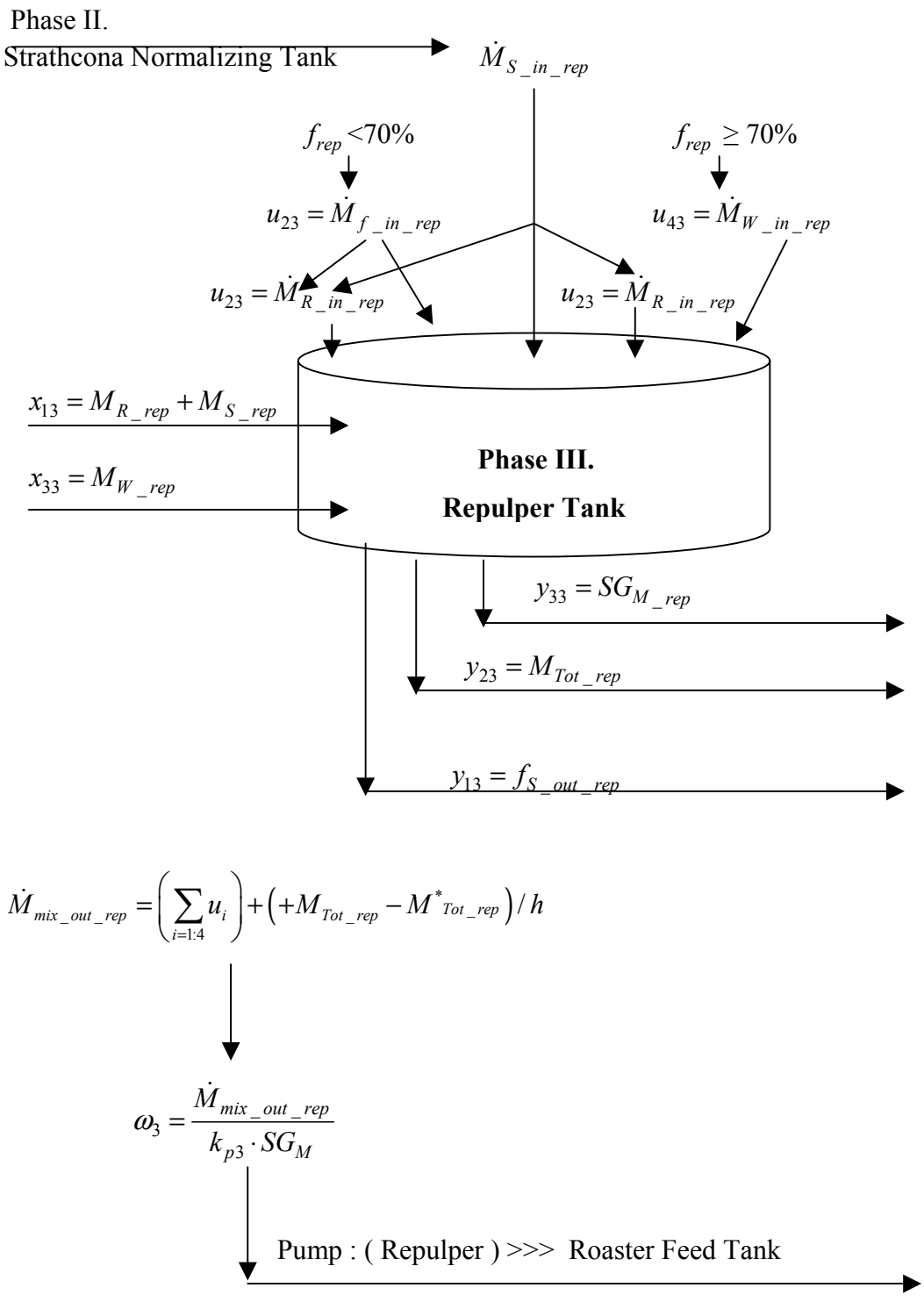

Fig. 7.3.1.1: Phase III System Plan

7.3.2 Simulation

First of all since we get the output from Phase II, which becomes the Strathcona slurry input for this phase, we simulate in Phase II with uniformly random varying parameters:

$$0.6 \le f_{f\_in\_Str} \le 0.9 \qquad (7.3.2.1)$$

Also, the Strathcona slurry coming into Phase II has a solid density variation of:

$$0.56 \le f_{S\_in\_Str} \le 0.69 \qquad (7.3.2.2)$$

Also, the initial states in the Strathcona normalizing tank are not in equilibrium. We perturb the states in either direction for (+/-30%), the same as we did in Section 7.2. The perturbed initial states are:

$$\begin{bmatrix} x_{12}(0) \\ x_{22}(0) \end{bmatrix} = \begin{bmatrix} x^*_{12} \cdot 0.7 \\ x^*_{22} \cdot 1.3 \end{bmatrix} = \begin{bmatrix} 14.7452 \cdot (0.7) \\ 8.2702 \cdot (1.3) \end{bmatrix} = \begin{bmatrix} 10.3216\ \text{t} \\ 10.7513\ \text{t} \end{bmatrix} \qquad (7.3.2.3)$$

$$\begin{bmatrix} x_{12}(0) \\ x_{22}(0) \end{bmatrix} = \begin{bmatrix} x^*_{12} \cdot 1.3 \\ x^*_{22} \cdot 0.7 \end{bmatrix} = \begin{bmatrix} 14.7452 \cdot (1.3) \\ 8.2702 \cdot (0.7) \end{bmatrix} = \begin{bmatrix} 19.1688\ \text{t} \\ 5.7891\ \text{t} \end{bmatrix} \qquad (7.3.2.4)$$

The other parameters are also random varying:

$$4.0 \le SG_S \le 4.3 \qquad (7.3.2.5)$$

$$3.8 \le SG_R \le 4.0 \qquad (7.3.2.6)$$

For the simulation in Phase II, we decided to use general switching control for the whole process. This is because although a hybrid of input-output linearization does work, as demonstrated in section 7.2, the outputs do not chatter in a small range. Hence, it is found that it is better to use general switching control for both case *a)* and case *b)* in Phase II.

Also, the initial states in the Repulper tank are not in equilibrium. We perturb the states in either direction for (+/-30%), the same as we did in section for Phase II. The perturbed initial states are:

$$\begin{bmatrix} x_{13}(0) \\ x_{23}(0) \end{bmatrix} = \begin{bmatrix} x^*_{13} \cdot 0.7 \\ x^*_{23} \cdot 1.3 \end{bmatrix} = \begin{bmatrix} 17.53 \cdot (0.70) \\ 7.51 \cdot (1.30) \end{bmatrix} = \begin{bmatrix} 12.27\ \text{t} \\ 9.76\ \text{t} \end{bmatrix} \qquad (7.3.2.7)$$

$$\begin{bmatrix} x_{13}(0) \\ x_{23}(0) \end{bmatrix} = \begin{bmatrix} x^*_{13} \cdot 1.3 \\ x^*_{23} \cdot 0.7 \end{bmatrix} = \begin{bmatrix} 17.53 \cdot (1.30) \\ 7.51 \cdot (0.70) \end{bmatrix} = \begin{bmatrix} 22.79\ \text{t} \\ 5.26\ \text{t} \end{bmatrix} \qquad (7.3.2.8)$$

Finally, the simulation for Phase III runs simultaneously with Phase II. The simulation graph for the density output of Phase II is shown first:

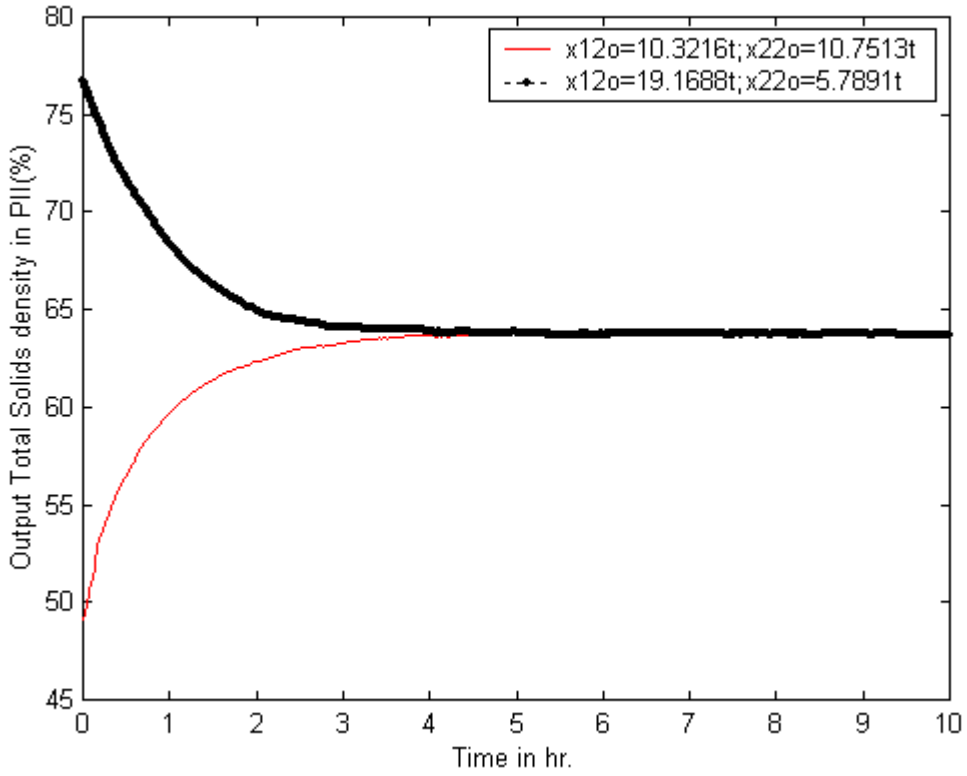

Fig. 7.3.2.1: Output solid density using switching control for Strathcona density for Phase II for the two initial state conditions.

From Fig. 7.3.2.1, we can see that the output solid density converge of the two initial conditions converge very slowly to the desired setpoint, 64.067%. But remembering that we are simulating with the large perturbations of initial states, (+/-30%) in Phase II. Hence, in reality, the situation should be much better as we try to simulate the worst cases.

Also, seeing that the output solid density only goes close to about 64% after about 4 hours for the two initial conditions. Now, let us look at how the output solid density of Phase III varies for the two initial conditions in Phase II.

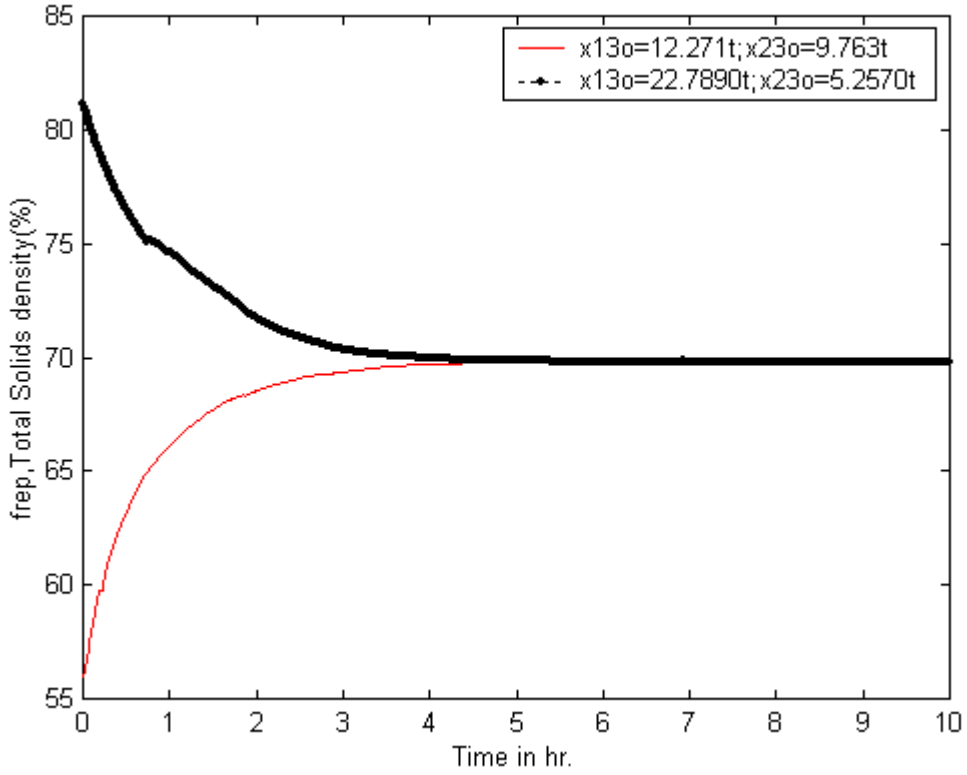

Fig. 7.3.2.2: Output solid density using switching control for Strathcona density for Phase III for the two initial state conditions.

Indeed, from Fig. 7.3.2.2, the results are very satisfactory. With the vigorous simulations in both Phase II and Phase III simultaneously, it is surprising that the solid density do go back to 70% after only four and half hours. Even though it seems that the simulation

results are not very satisfactory in terms of the speed of the response, it in fact represents the worst-case scenario. In real practice, where these worst cases rarely happen, the performance rate should be much faster. Also, the total solids density is not as a sensitive parameter as the Raglan to Strathcona ratio.

Hence, to make sure that the Raglan to Strathcona ratio always being controlled very well. The mass flow rate of Raglan is always equal to the ratio multiplying whatever amount of dry mass of Strathcona coming in, as explained in (7.3.1.2). In this way, the Raglan to Strathcona ratio always stays at the ratio. Hence, there is no need to show its simulation result.

How about Raglan powder, which is going into the Repulper tank? Does it vary a lot? The answer is no. In fact, although it does fluctuate, taking the worst cases of both initial conditions, the range of the fluctuation is from 8.4967t to 8.4992t. Of course, they start to pump whenever they 'see' Strathcona slurry 'start' to pump as well respectively for the two initial conditions. Since the results do not show any peculiarities than we expected, it is not shown here.

Next, we are going to see how the pump perform in the two initial state conditions. Especially we want to see if our feedback equation for the pump speed, (7.3.1.11) works satisfactorily.

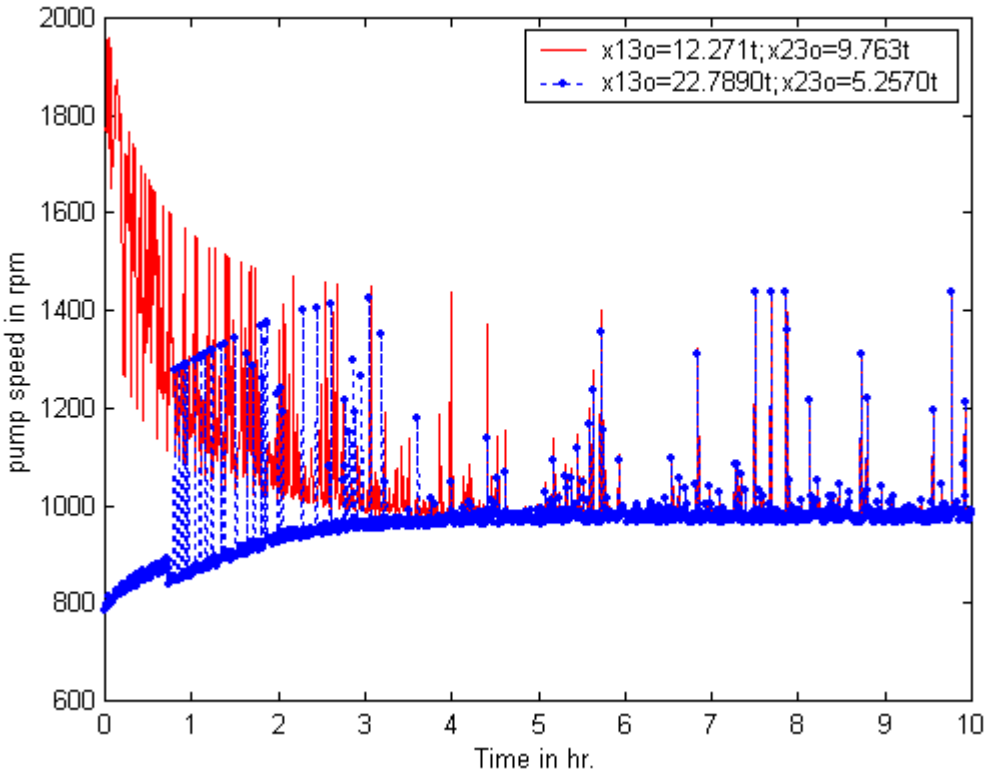

Fig. 7.3.2.3: Pump Speed of Phase III using switching control for the two initial state conditions.

Unfortunately, we see that the pump speed fluctuates to a great range. It maximizes at almost 2000rpm. Is this normal? By looking at the graph carefully, we see that it is the first initial condition that shoots up the pump speed. In the first initial condition, our solid density is very low, only 55%. Since large quantities of filter cakes and Raglan has to pump into the tank to raise up the solid density, the pump has to turn on larger values in order to pump out all the extra loading out of the tank. We can constrain our pump speed. However, if we do that we would risk of overflowing our tank.

We have tried to simulate the situation with constrained pump speed at the maximum of 1200rpm. Without showing the figures, the result is that there is a surge of total mass up to 45 tonnes in the tank after 3 hours. Although, eventually, it does come down to the setpoint, but our tank's maximum capacity is only at about 31 tonnes. Hence, we would have a large overflow and thus a disaster to avoid. Hence, if we are going to demand the

robustness of the system, we have to install a pump which has high rpm, e.g. 2000rpm. Again, note that the simulation here is done for the worst case. So a pump with 2000rpm should be very adequate to meet most of the sudden surges or emergencies.

Inevitably, since we are simulating with such a huge variation of the parameters, the pump chatters. But this seems to be a reality that cannot be gotten rid of.

Let us see how the output mass flow vary for the two initial state conditions:

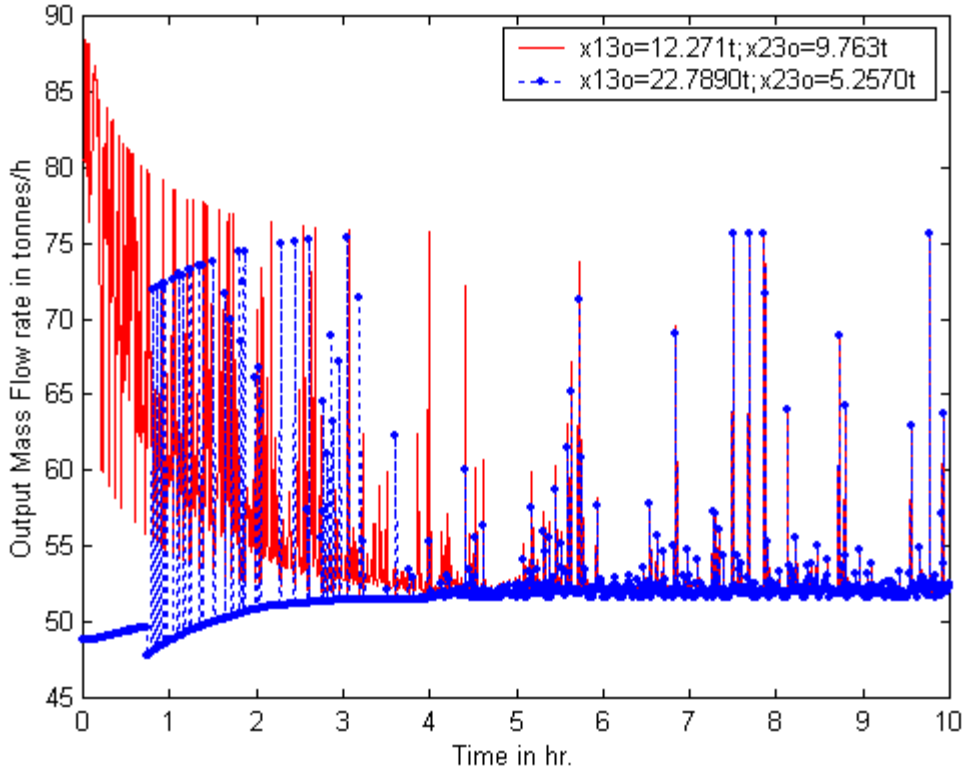

Fig. 7.3.2.4: Output Mass Flow Rate of Phase III using switching control for the two initial state conditions.

Fig. 7.3.2.4 though does not show any new insights, it does show that the mass flow rates of the two initial state conditions, go towards the nominal mass flow rate, 51.43t/h, but with occasional large peaks. Our worst-case scenario again causes these peaks where all the parameters vary to their maximum. Fortunately, that the next process after the

Repulper tank is the roaster tank, which acts like a sink for this process. Hence, the fluctuation of its input, output from Repulper tank, should be tolerable.

How about the various input mass flow rates? Are they chattering a lot? For the filter cakes, the answer is yes. The filter cakes have chattered considerably, meanwhile, water mass flow rate does not chatter at all. It starts with 4.5 tonnes for the second initial condition, which is too concentrated, and then it gradually decreases to 2 tonnes with a nice slope. But Raglan mass flow rate does fluctuate quite vigorously from 8.5 tonnes/h to 13 tonnes/h. Nevertheless, their variation seems acceptable.

7.3.3 Conclusion of Phase III Design

From the various figures in section 7.3, we see that Phase III closed-loop performance is still satisfactory. It is however a bit slow for the outputs to go back to their designated operating point, but this is an inevitable cost of simulating in the worst cases. With the successful simulations of Phase II and Phase III together, we can assure confidently the stability, smoothness and the performance of the overall system.

7.4 Conclusion of Alternative Three-Phase Process

As seen from the various figures in this chapter, the results have validated the design of this three-phase modified alternative control design. This design though complicated and the initial equipment costs are much higher than the original one Repulper tank system, has a much better performance.

In fact, in reality, since the states, obtained from the three output equations of the existing process control system, are subject to huge errors, any controller which uses only the Repulper tank will probably fail. This is because, without the correct state information, no controller can work properly.

The alternative design can also manage to perform satisfactorily even under all large simulated uncertainties of the system. This means it can attain robust performance.

In conclusion, we are satisfied with the performance of the alternative control system. However, it is difficult to accept that the states of the conventional control system are basically unobservable. Hence, we have avoided using three state variables through the implementation of Phase I, filter normalizing tank, and Phase II, Strathcona normalizing tank. At last, we compose a hybrid system which have an open-loop control component for Raglan mass flow rate, and yet we have closed loop control for the pump speed and the mass flow rate of the filter cakes and water. Hence, any perturbations in the Repulper tank can get corrected promptly. Although the total design efforts are tremendous, the award is a new totally controllable system.

7.5 Conclusion of Nonlinear Control Design

In Chapter 6, we try to use nonlinear control methods to control the actual one tank process, the Repulper tank. Input-output linearization and switching control are used to try to control the original Repulper tank. Due to the incapability of applying robust switching control, only input-output linearization is feasible. Fortunately, we have found a K matrix which has very good robust performance and can undertake most of the uncertainties.

However, even with the sophisticated nonlinear control techniques, we still need to have the correct state information. If we rely on only a one-tank system, we may not have reliable state information. This is due to the fact that the states obtained from the output equations are subject to huge errors. This means we cannot use feedback to control the system when it has three states, Strathcona, Raglan and water. But we cannot use just open-loop controller either. This is due to the disturbance of the input uncertainties of the filter cakes.

Consequently, a new design concept was proposed and the result is the three-phase alternative control design. Phase I is destined to normalize the incoming filter cakes. The success of the installation of Phase I has eliminated the uncertainties of the mass flow rate and the density of the incoming filter cakes. Indeed, the success of the normalizing of filter cakes lays the final success of the whole alternative control design.

Subsequently, the output of the filter cakes' normalizing tank provides filter cakes slurry at a well-controlled solid density set point: 75%. Hence, now filter cakes solution is ready to use whenever it needs to. The button which tell the "filter normalizing tank" to pump slurry out is determined by the process in Phase II. As in case *a)*, when the incoming Strathcona slurry's solid density is below the critical percentage, 64.067%, the filter cakes' normalizing tank will then be commanded to pump the required mass flow rate of filter cakes' solution into the Phase II tank, the "Strathcona normalizing tank". On the other hand, in case *b)*, if the incoming Strathcona slurry has solid density above or the critical point, water is added to dilute the solution. The aim is to normalize the incoming Strathcona slurry to be at the critical point, 64.067%. The control results of Phase II have complied with the design requirements. The pump speed of the tank is determined by assuring that there is enough Strathcona going into the next tank, the Repulper tank, at any instant. As a result, the mass flow rate varies slightly.

After two phases of normalizing, filter cakes slurry has been normalized to having solid density of 75% and Strathcona slurry is normalized to have solid density at 64.067%.
Now, basically, only Raglan is needed to add into the Repulper tank along with the normalized Strathcona slurry from Phase II.

In Phase III, we need to solve the dilemma of closed-loop stability and the unavailability of state information. Firstly, we have one open loop control which varies least, the Raglan powder mass flow rate. But we need to have state information if we want to create closed-loop control. Hence, we create a new state model with two states. We put together the two dry masses, Strathcona and Raglan to form one state variable and the other one naturally is water. Since these two new states can be readily obtained from the

output measurements of total solids density and total mass, then we have full state information for this new model. Hence, the pump speed and the mass flow rates of the filter cakes, from the filter normalizing tank, and the mass flow rate of water, are all being controlled nonlinearly with feedback information from the states. But this new model has to be based on the assumption that the initial ratio of two components of dry masses in the tank is obliged with the desired Raglan to Strathcona ratio of 0.3092. If we can make this assumption true, then with our equations, the following dry masses coming into the tank would also follow the ratio and hence, the desired ratio objective can be kept. We can still perturb the state masses, but the relative ratio of the two dry masses is still being kept at 0.3092. Under this assumption, all the tracking objectives would be met. This hybrid system is feasible because we know that the dry Raglan powder mass flow rate is well controlled. Hence, it can be controlled in an open-loop way, and with a mass flow rate measurement after the pump, which pumps the Raglan powder, we can also ensure that the pump works properly. Henceforth, with the Raglan to Strathcona ratio being well kept, we can have closed-loop-controlled inputs of filter cakes and water to offset any disturbance in total solids density in the tank. In addition, the closed-loop-controlled pump can correct any deviations of the total mass of in the tank, and hence maintain a steady tank level.

Hence, all the difficult issues of the original Repulper tank are solved completely and satisfactorily with the Three-Phase alternative process system. Even though the Three-Phase alternative control design seems to be clumsy, it fulfils the output tracking objectives, while undertaking all the uncertainties.

In conclusion, the alternative control system, the “Three-Phase” design, with the essential tools of various nonlinear control tools, has demonstrated the effectiveness and the performance of using nonlinear control methods to deal with systems which are subject to parameter variation and model uncertainties.

After seeing that the success of dealing with uncertain system with nonlinear control, it is interesting to see that if linear MIMO control techniques can solve an uncertain system as well. Hence, in the next chapter, two different linear MIMO control methods are employed to tackle the actual one tank process.

Chapter 8

Linear MIMO Control

8.1 Introduction

All linear MIMO control techniques are based on a linearized system. Especially, mostly we deal with the *A, B, C, D* matrices of the linear system only. Our linear system, *Z*, is a perturbed model of *P* at the set of operating points. The *A, B, C, D* matrices of our linearized system are, stating them again as of (4.38), (4.39), (4.40), (4.41):

$$A = \begin{bmatrix} -1.4972 & 0.5997 & 2.3389 \\ 0.1732 & -1.8687 & 0.7232 \\ 0.3123 & 0.3364 & -0.7423 \end{bmatrix} \qquad (4.38)$$

$$B = \begin{bmatrix} 0.6500 & 0.8000 & 0 & 0 & -0.0286 \\ 0 & 0 & 1.0000 & 0 & -0.0088 \\ 0.3500 & 0.2000 & 0 & 1.0000 & -0.0088 \end{bmatrix} \quad (4.39)$$

$$C = \begin{bmatrix} 0.0120 & 0.0120 & -0.0280 \\ 1.0000 & 1.0000 & 1.0000 \\ 0.0419 & 0.8386 & -0.096 \\ 1.0127 & 0.9326 & -2.3198 \end{bmatrix} \quad (4.40)$$

$$D = \begin{bmatrix} 0 & 0 & 0 & 0 & 0 \\ 0 & 0 & 0 & 0 & 0 \\ 0 & 0 & 0 & 0 & 0 \\ 0 & 0 & 0 & 0 & 0.0535 \end{bmatrix} \quad (4.41)$$

Then our linear system can be formed as (4.37) in state space convention:

$$Z = \begin{bmatrix} A & B \\ C & D \end{bmatrix} \quad (4.37)$$

After obtaining the linearized system, *Z*, then it is possible to carry out different linear optimal MIMO control. In designing the MIMO linear controllers, there are two very different but yet intrinsically related directions. The first one is design in the time domain and the second one is design in frequency domain.

The design in time domain mainly involves with formulating the controller with the feedback of the states. The state information is used to determine the deviation of the states from the state equilibrium values. The state deviations are used, as a feedback, by the controller to provide the corresponding control actions to achieve tracking.

For systems which cannot measure the state information directly, the availability of the state information depends on the measurements and the derivation of the outputs. In our

system, since there are three states only, it is necessary to have at least three output equations, which contain only the states, to solve for the state values at every instant. Fortunately, in our system, there are three output equations which contain the three states. However, as pointed out in Chapter 5, it is then necessary to ensure that the three output measurements can invariably deduce the states. The only problem is that the solution of the states in terms of the outputs is very sensitive to errors in specific gravities.

8.2 State Feedback with Pole Placement

If the states are available, then the control law can minimize the state errors with a certain K gain matrix. If we design this gain matrix well, we can force the system to have the poles that we want. Hence, we can force the system to have faster response by having more negative poles. Pole placement is hence a method to help us design the gain matrix K so that we can have the poles we want in A.

8.2.1 Pole Placement State Feedback Formulation

The basic theory of pole placement is not stated here. Rather, the general pole placement procedure is provided here, from [Bélanger, 1995].

1. Calculate the determinant and the adjoint of (sI-A).
2. Then compute the desired closed loop polynomial.
3. Now, apply the following equation:

$$p_c(s) = \det(sI - A) + k^T \cdot Adj(sI - A) \cdot B \qquad (8.2.1.1)$$

   to generate linear equations for the gain components and solve for the gain.

4. Calculate the dc steady state in terms of the desired output.
5. Then obtain the control law:

$$u = u^* - k^T \cdot (x - x^*) \tag{8.2.1.2}$$

The desired poles are determined to be at (-120, -120, -120). Then with Matlab command "place", we obtain the desired *k*. We go directly to test if pole placement can have any robustness. Hence, the simulation parameters are the same as in Chapter 6:

8.2.2 Simulation

After we obtain the *k* controller, we put it in the nonlinear system for simulation. Firstly, the initial states in the Repulper tank are not in equilibrium. Hence, we can see if the controller can steer the system back to equilibrium. The perturbed states are:

$$\begin{bmatrix} x_1(0) \\ x_2(0) \\ x_3(0) \end{bmatrix} = \begin{bmatrix} x_1^* \cdot 0.9 \\ x_1^* \cdot 1.2 \\ x_1^* \cdot 0.7 \end{bmatrix} = \begin{bmatrix} 13.39 \cdot 0.9 \\ 4.14 \cdot 1.2 \\ 7.51 \cdot 0.7 \end{bmatrix} = \begin{bmatrix} 12.0510\,\mathrm{t} \\ 4.9680\,\mathrm{t} \\ 5.2570\,\mathrm{t} \end{bmatrix} \tag{8.2.2.1}$$

and the rest of the parameters are varying randomly as before:

$$0.58 \le f_S < 0.69 \tag{8.2.2.2}$$

$$0.75 \le f_f < 0.90 \tag{8.2.2.3}$$

$$4.0 \le SG_S \le 4.3 \tag{8.2.2.4}$$

$$3.8 \le SG_R \le 4.0 \tag{8.2.2.5}$$

Moreover, the mass flow rate of the filter cakes varies randomly as well:

$$u_{3\_actual} = u_{3\_calculated} \cdot (1 \pm 30\%) \tag{8.2.2.6}$$

The simulation results are very encouraging. Mostly all the desired output values are met. The total solid density returns back to about 70% from 75% within 20 minutes:

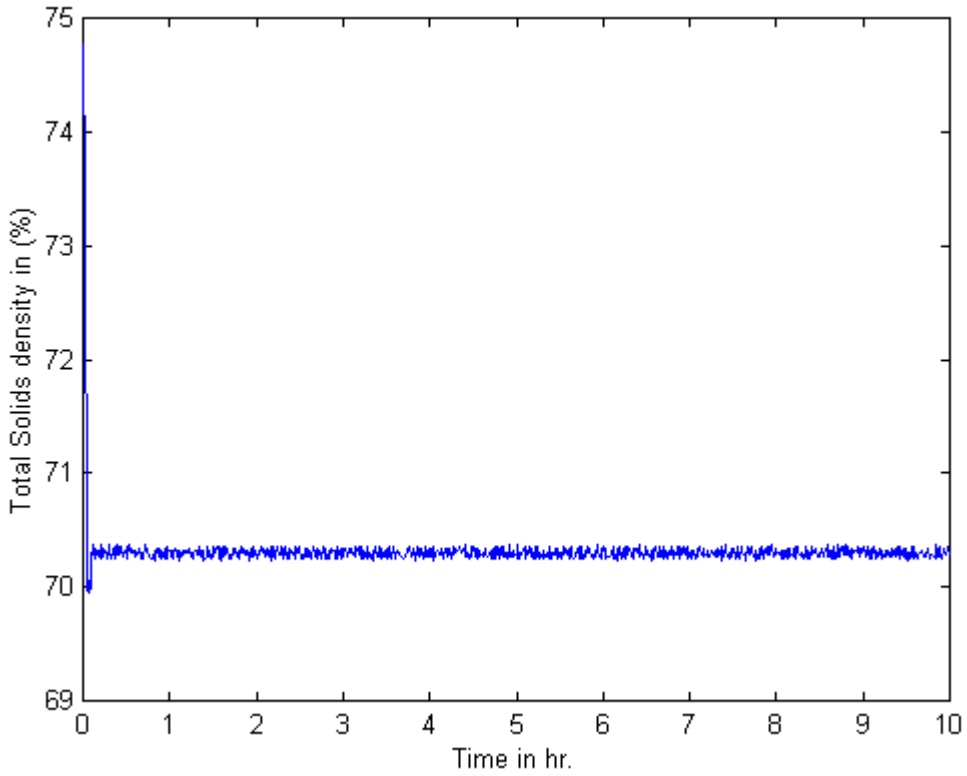

Fig. 8.2.2.1: Total solid density of existing Repulper tank process which is controlled with pole placement state feedback.

From Fig. 8.2.2.1, we can see that total solid density returns back to the desired setpoint within 20 minutes, with a small deviation though. Total mass of the tank is being looked at next.

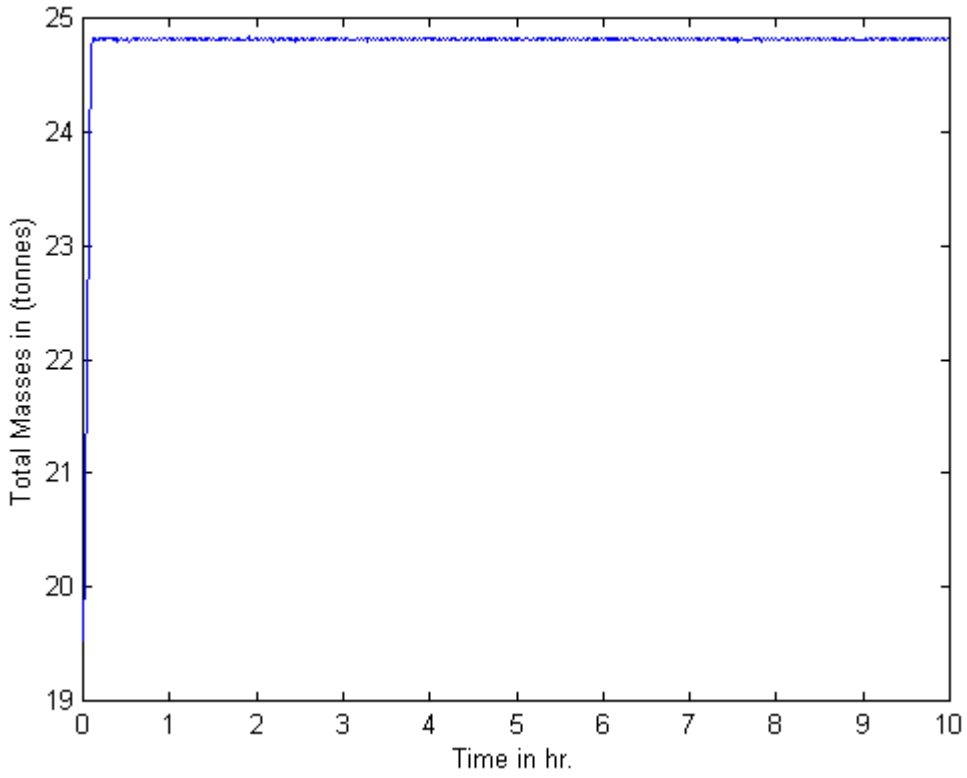

Fig. 8.2.2.2: Total Mass of existing Repulper tank process which is controlled with pole placement state feedback.

The total mass has returned back to its setpoint in 20 minutes as well. From Fig 8.2.2.1 and Fig. 8.2.2.2, we see that indeed state feedback pole placement though seems simple but can work very satisfactorily even under uncertainties.

The total mass flow rate, in the next figure, Fig. 8.2.2.3, though fluctuates but certainly not very much. Hence, it is acceptable considering the uncertainties it is being subject to.

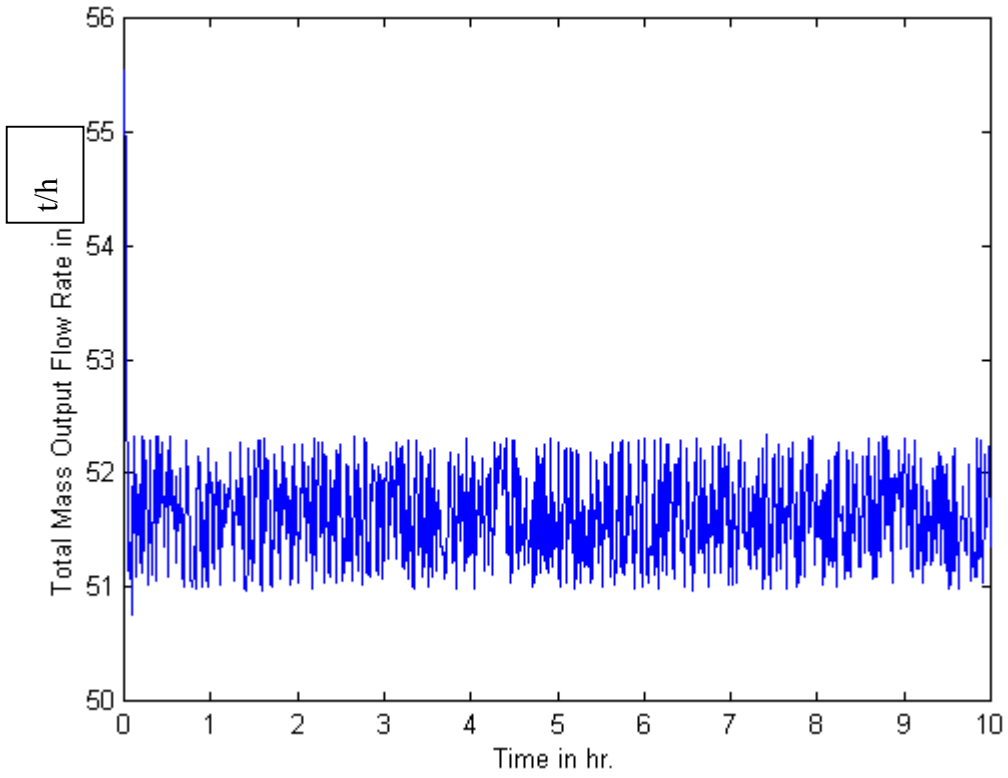

Fig. 8.2.2.3: Total Mass Output Flow Rate of existing Repulper tank process which is controlled with pole placement state feedback.

After seeing the total mass output flow rate does stabilize within an acceptable range, the pump speed in the next figure, Fig. 8.2.2.4, surprisingly can control the system without much variation at all. This situation is hardly ever seen in any other control schemes in this study.

After seeing that the pump speed does not vary much at all, it is then interesting to see if other control efforts chatter. Fortunately, from Fig. 8.2.2.5, all input mass flow rates fluctuate to a much less extent comparing to the system controlled nonlinearly as shown in Chapter 6. Strathcona varies around 35 tonnes/h, while water varies the most, from 10 to 19 tonnes/h. The exogenous filter cakes mass flow rate and Raglan mass flow rate are both stabilized at about 10 tonnes/h.

Lastly, in the last figure, Fig. 8.2.2.6, it is surprising to see that the Raglan to Strathcona

ratio gets stabilized at 0.311 after much less than an hour.

Hence, from Fig. 8.2.2.1 to Fig. 8.2.2.6, all regulation requirements are met and the inputs mass flow rates does not fluctuate seriously.

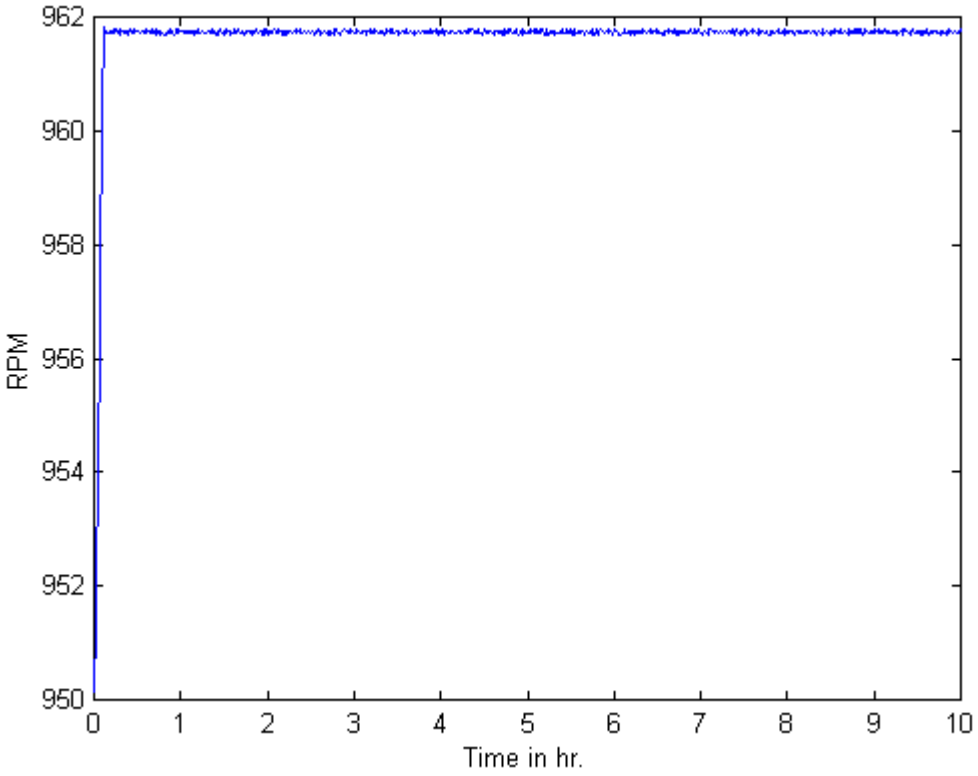

Fig. 8.2.2.4: Pump Speed of existing Repulper tank process which is controlled with pole placement state feedback.

8.2.3 Pole Placement Conclusion

It is very encouraging to see that even with simple state feedback pole placement, we can achieve excellent regulation objectives, and we do not have the same problems as we have in nonlinear control where the inputs tend to always chatter quite seriously. In fact, by comparison, it is a much better control method than the input-output linearization nonlinear control system we developed in chapter 6. This success is due to the fact that it

controls the state errors directly; a similar idea as the author realized as nonlinear switching control.

Unfortunately, our system cannot be controlled by state feedback, as the states err considerably when they depend on the output equations which are so sensitive to slight errors in SG_S and SG_R.

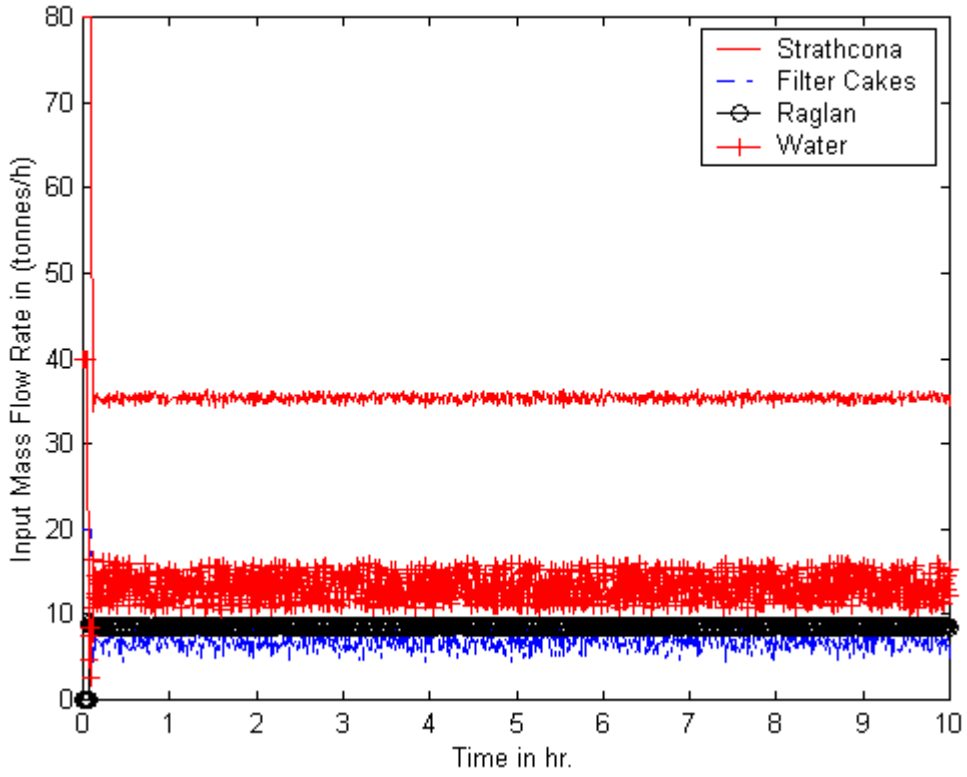

Fig. 8.2.2.5: Input Mass Flow Rate of existing Repulper tank process which is controlled with pole placement state feedback.

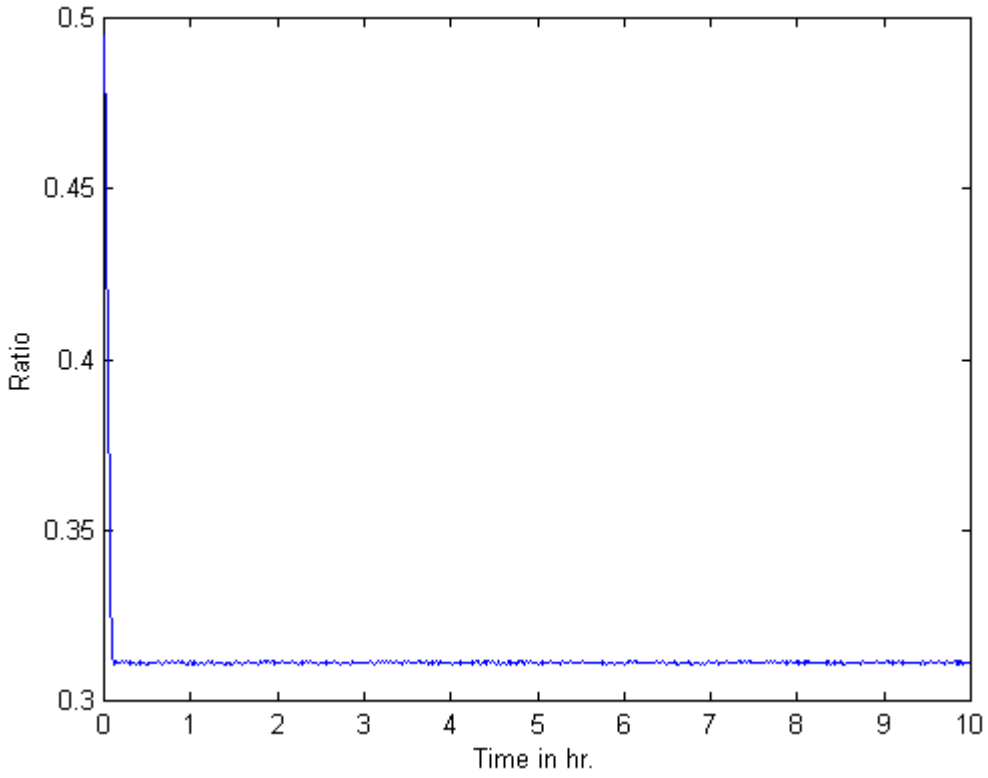

Fig. 8.2.2.6: Raglan to Strathcona Ratio of existing Repulper tank process which is controlled with pole placement state feedback.

Hence, in the next section, we are trying to see if the H_2 optimal control can resolve our problems of state availability.

8.3 H_2 Optimal Control

We have seen earlier that pole placement state feedback is able to control our nonlinear system with very good robust performance. But it assumes the availability of the states. However, as we mentioned in other chapters, this is not quite correct, as the states obtained from the measured outputs are subject to unacceptably large errors. Hence, for H_2 optimal controller, we want to see if this method can really overcome the difficulty of obtaining state information correctly.

But before we are able to formulate our nonlinear system in "H_2 Optimal Control", we need to go through the basic theory.

8.3.1 Theory of H_2 Optimal Control

Now we are going into "H_2 Optimal Control". First of all, we need to define a few terms, from [Boulet, 2001]:

L_2 Norm: The L_2 norm of a signal $x(t)$ is the square root of its total energy over $-\infty<t<\infty$ and is defined as:

$$\| x \|_2 = \left(\int_{-\infty}^{\infty} | x(t) |^2 \right)^{1/2} \qquad (8.3.1.1)$$

A large signal would have a large L_2 norm. Hence, it is a measure of the size of a signal.

L_2 Space: The set of all finite energy signals are called the space, L_2:

$$L_2 := \{ x : \| x \|_2 < +\infty \} \qquad (8.3.1.2)$$

L_2 System Norm: The L_2 system norm is a measure of the size of a system and can be defined as:

$$\| H \|_2 = \left(\frac{1}{2\pi} \int_{-\infty}^{\infty} trace\{ H(j\omega)^* H(j\omega) \} d\omega \right)^{1/2} \qquad (8.3.1.3)$$

By Parseval's theorem, (8.3.1.3) can be written in time domain as:

$$\| H \|_2 = \left(\frac{1}{2\pi} \int_{-\infty}^{\infty} trace\{h(t)^* h(t)\} dt \right)^{1/2} \qquad (8.3.1.4)$$

***H_2* Space:** The *H_2* space is the space of all stable causal systems with finite *L_2* norm:

$$H_2 := \{H\ causal, stable : \| H \|_2 < +\infty\} \qquad (8.3.1.5)$$

Now we need a way to compute the *H_2* system norm. First suppose *H(s)* is stable and strictly proper and we have a state space realization of *H(s)* as *(A,B,C,0)*. Define the

Controllability Grammian matrix:

$$L := \int_0^{\infty} e^{At} \cdot B \cdot B^T \cdot e^{A^T t} dt \qquad (8.3.1.6)$$

As *L* satisfies the *Lyapunov* equation:

$$A \cdot L + L \cdot A^T + B \cdot B^T = 0 \qquad (8.3.1.7)$$

Then a formula to compute the *H_2* system norm is:

$$\| H \|_2 = \left[trace(CLC^T) \right]^{1/2} \qquad (8.3.1.8)$$

Hence, as stated in [Boulet, 2001], *H_2* optimal control theory is a theory to design a finite-dimensional "LTI", controller that minimizes the *H_2* norm of the close loop system. Now we shall look at the general block diagram of a feedback control system:

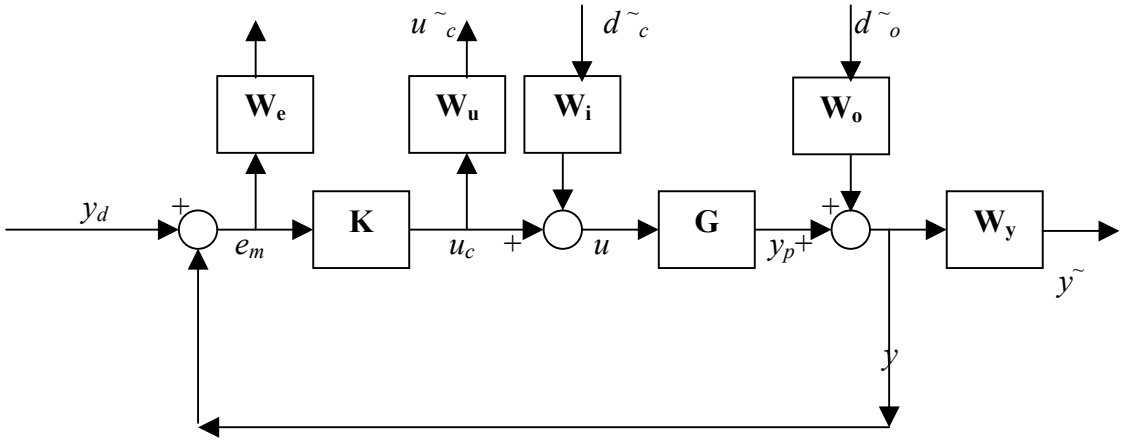

Fig. 8.3.1.1: Typical Feedback Control Diagram

The weighting functions, in Fig. 8.3.1.1, W_x are added for different reasons as stated in [Boulet, 2001]:

a) To enforce closed-loop performance specifications.
b) To represent the frequency contents of disturbances and noises.
c) To normalize signals with different units in an optimal control setting.

Looking at Fig. 8.3.1.1, there is the controller, **K** and the plant **G** in the diagram. It is essential to use appropriate weighting functions so that we can utilize the optimal control theory. An important step in the controller design process is to select reasonable weighting functions, W_i, W_e, W_y, W_u, W_y, Each of these weighting functions can either constrain or filter the corresponding signal. Hence we could use these weighting functions to shape the response and performance we plan to. To simplify our design process, we carry some simplifications. We try to consider the regulator problem where the effect of the output disturbance, $d\tilde{}_o$, on the weighted output, $y\tilde{}$, must be minimized. We can recast the system as a linear fractional transformation (LFT) as follows:

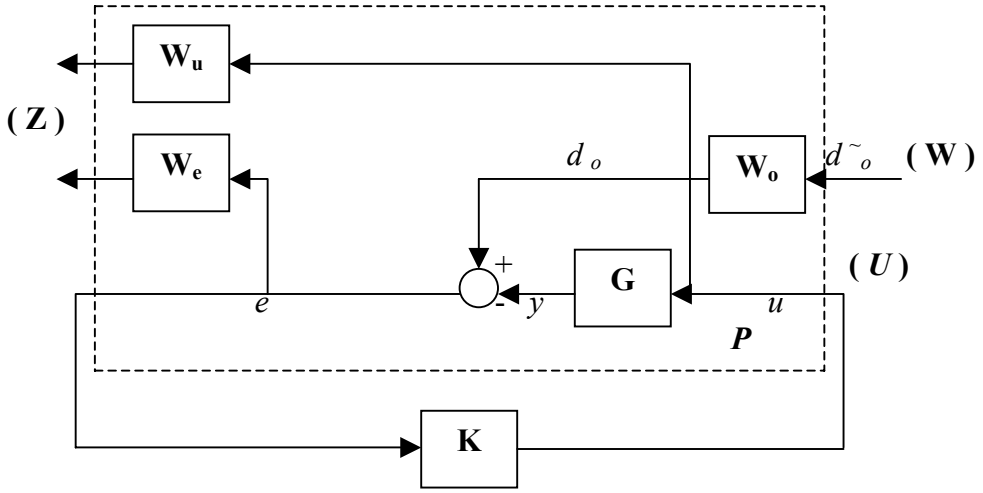

Fig. 8.3.1.2: Typical H_2 optimal Control Design

Usually, people represent Fig. 8.3.1.2 in a simpler (LFT) form:

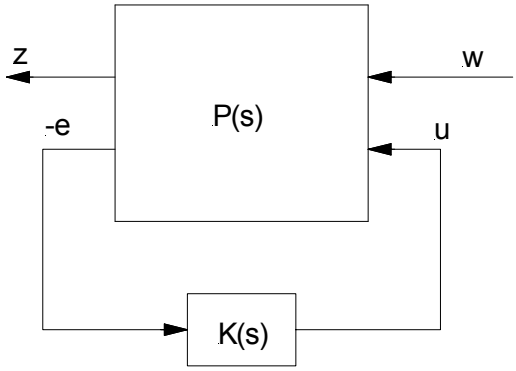

Fig. 8.3.1.3: Standard LFT diagram for H_2 optimal control design.

The P stated in both Fig. 8.3.1.2 Fig. 8.3.1.3 is the generalized plant and is defined as below:

$$P(s) := \begin{bmatrix} P_{11}(s) & P_{12}(s) \\ P_{21}(s) & P_{22}(s) \end{bmatrix} \tag{8.3.1.9}$$

$$
\begin{aligned}
P_{11}(s) &= 0 \\
P_{12}(s) &= \begin{bmatrix} W_u \\ W_e G \end{bmatrix} \\
P_{21}(s) &= W_o \\
P_{22}(s) &= -G
\end{aligned}
\tag{8.3.1.10}
$$

It is important to realize that the weighting function $W_u(s)$ can be used to constrain the control signal while $W_e(s)$ is used to reduce the sensitivity at low frequencies, and $W_o(s)$ is used to model the power spectral density or energy density spectrum of the output disturbance.

Then the design problem is to find the controller K which:

$$
\min_{K \in S} \quad \left\| T_{zw} \right\|_2 \tag{8.3.1.11}
$$

where S is the set of all satisfying controllers and

$$
\begin{aligned}
T_{zw}(s) &= F_L[P(s), K(s)] \\
&= P_{11}(s) + P_{12}(s) \cdot K(s) \cdot [I - P_{22}(s) \cdot K(s)]^{-1} \cdot P_{21}(s)
\end{aligned}
\tag{8.3.1.12}
$$

is the closed-loop transfer matrix from the exogenous input w to the output z. This is a minimization problem that involves calculating the optimal controller K, such that the transfer matrix, T_{zw}, is stabilized and its H_2 norm is minimized.

Now suppose that a stable state-space realization of the generalized plant, $P(s)$, is given by:

$$
P(s) = \left[\begin{array}{c|cc} A & B_1 & B_2 \\ \hline C_1 & 0 & D_{12} \\ C_2 & D_{21} & 0 \end{array}\right] \tag{8.3.1.13}
$$

The above (8.3.1.13) is a convention which represent (8.3.1.9) in another way where

$$P_{11}(s) \coloneqq \begin{bmatrix} A & B_1 \\ C_1 & 0 \end{bmatrix} \tag{8.3.1.14}$$

$$P_{12}(s) \coloneqq \begin{bmatrix} A & B_2 \\ C_1 & D_{12} \end{bmatrix} \tag{8.3.1.15}$$

$$P_{21}(s) \coloneqq \begin{bmatrix} A & B_1 \\ C_2 & D_{21} \end{bmatrix} \tag{8.3.1.16}$$

$$P_{22}(s) \coloneqq \begin{bmatrix} A & B_2 \\ C_2 & 0 \end{bmatrix} \tag{8.3.1.17}$$

Note that in order for P_{11}(s) and P_{22}(s) to be belong to H_2 space, it requires that both matrices to be strictly proper which in turn implies that D_{11}(s) and D_{22}(s) has to be zero. This in turn implies that all output equations of the original plant system, G, should not depend on any inputs.

First, we define two shorthand notations:

$$R_1 = D_{12}^* D_{12} \; ; R_2 = D_{21}^* D_{21} \tag{8.3.1.18}$$

Now, we are going to define two Hamiltonian matrices (the definition of Hamiltonian matrices would not be dealt here, but reader can easily find the information in any standard robust control textbook):

$$H_2 \coloneqq \begin{bmatrix} A - B_2 R_1^{-1} D_{12}^* C_1 & -B_2 R_1^{-1} B_2^* \\ -C_1^* \left(I - D_{12} R_1^{-1} D_{12}^* \right) C_1 & -\left(A - B_2 R_1^{-1} D_{12}^* C_1 \right)^* \end{bmatrix} \tag{8.3.1.19}$$

$$J_2 := \begin{bmatrix} \left(A - B_1 D_{21}^* R_2^{-1} C_2\right)^* & -C_2^* R_2^{-1} C_2^* \\ -B_1\left(I - D_{21}^* R_2^{-1} D_{21}^*\right) B_1^* & -\left(A - B_1 D_{21}^* R_2^{-1} C_2\right) \end{bmatrix} \qquad (8.3.1.20)$$

Note that (8.3.1.15) concerns about state feedback, while (8.3.1.16) is an observer which tries to observe the states from the outputs. Hence, the standard H_2 optimal controller contains on one hand a state feedback "LQ" regulator, and on the other hand contains a Kalman filter, which tries to minimize the estimation errors of the states.

Now, let us define *Ric* which is a function associating a Riccati equation to a Hamiltonian matrix:

$$Ric : R^{2n\times 2n} \rightarrow R^{n\times n} \qquad (8.3.1.21)$$

Now,

$$H_2, J_2 \in dom(Ric) \qquad (8.3.1.22)$$

and

$$X_2 := Ric(H_2) \geq 0 \ ; \ Y_2 := Ric(J_2) \geq 0 \qquad (8.3.1.23)$$

Now, we need two more definitions:

Definition I: The pair (*A,B*) is said to be 'stabilizable' if there exists a state feedback gain matrix *K* such that '*A+BK*' is stable.

Definition II: The pair (*A,C*) is said to be 'detectable' if there exists an observer gain matrix *L* such that '*A+LC*' is stable.

Next, we need the following assumptions before we can compute the optimal controller:

A1: The pair (A,B_1) is stabilizable and the pair (A,C_1) is detectable (8.3.1.24)

A2: The pair (A,B_2) is stabilizable and the pair (A,C_2) is detectable (8.3.1.25)

A3: $R_1, R_2 > 0$ (8.3.1.26)

A4: $\begin{bmatrix} A - j\omega I & B_2 \\ C_1 & D_{12} \end{bmatrix}$ has full column rank for all frequencies (ω). (8.3.1.27)

A5: $\begin{bmatrix} A - j\omega I & B_1 \\ C_2 & D_{21} \end{bmatrix}$ has full row rank for all frequencies (ω). (8.3.1.28)

Now, finally, we can have the unique H_2 optimal controller which minimizes $||T_{ZW}||_2$:

$$K_{opt} = \begin{bmatrix} \hat{A}_2 & -L_2 \\ F_2 & 0 \end{bmatrix} \tag{8.3.1.29}$$

$$L_2 := -\left(Y_2 C_2^* + B_1 D_{21}^*\right) R_2^{-1} \tag{8.3.1.30}$$

$$F_2 := -R_1^{-1}\left(B_2^* X_2 + D_{12}^* C_1\right) \tag{8.3.1.31}$$

$$\hat{A}_2 = A + B_2 F_2 + L_2 C_2 \tag{8.3.1.32}$$

The above formulation is the H_2 optimal controller which assumes that the states are not observable directly, but can only be estimated from the outputs. For our system, this seems to be the case.

However, when the states are available directly, i.e. full state feedback, then this becomes a standard 'LQ' problem. However, in this study, we are not going to dwell into this approach, as we know that our states are not available in fact.

8.3.2 Control Formulation

Our original system has four output equations, but since, we have to satisfy the structure of (8.3.1.13), we cannot use the fourth output equation which contain the input of the pump speed. Hence, we removed the fourth output equation to leave our system to have three states, five inputs and three outputs. The practical implication of this modification is that the outputs equations only depend on the states rather than any inputs which is an essential criteria to have a stable H_2 controller. Now, our generalized plant is similar to Fig. 8.3.1.2. Our weighting functions are defined as follows:

$$W_o = \begin{bmatrix} 1 & 0 & 0 \\ 0 & 1 & 0 \\ 0 & 0 & 1 \end{bmatrix} \tag{8.3.2.1}$$

and, it accepts w as:

$$\tilde{d}_o = y_{des} = \begin{bmatrix} 0.7000 \\ 25.0400 \\ 2.1293 \end{bmatrix} \tag{8.3.2.2}$$

$$W_{u_i} = \frac{0.002s + 0.012}{0.01s + 1}; i = 1,...,5 \tag{8.3.2.3}$$

and

$$W_{u_i} = \begin{bmatrix} W_{u_1} & 0 & 0 & 0 & 0 \\ 0 & W_{u_2} & 0 & 0 & 0 \\ 0 & 0 & W_{u_3} & 0 & 0 \\ 0 & 0 & 0 & W_{u_4} & 0 \\ 0 & 0 & 0 & 0 & W_{u_5} \end{bmatrix} \qquad (8.3.2.4)$$

Also, since we have five inputs, hence, we have five diagonal terms in (8.3.2.4).

Also, we found that for the first input, the gain sets to 100, for Wu_1 can push the performance for the output solid density to be very close to 70%.

For the weighting function of the error, after numerous testing, we found:

$$W_{e_i} = \frac{740}{0.5s+1}; i = 1,2,3 \qquad (8.3.2.5)$$

and

$$W_e = \begin{bmatrix} W_{e_1} & 0 & 0 \\ 0 & W_{e_2} & 0 \\ 0 & 0 & W_{e_3} \end{bmatrix} \qquad (8.3.2.6)$$

Note that in (8.3.2.5), the '0.5s' in the denominator refers to the suppression of the errors during the response time of the system, half an hour, or 0.5 hour. The gain is 760 so as to ensure that:

$$|W_{e_i}^{-1}(j\omega)|; i = 1,2,3 \qquad (8.3.2.7)$$

can be smaller and errors can be decreased. Let us go to the modified state space system:

$$\begin{bmatrix}\dot{x}_1\\ \dot{x}_2\\ \dot{x}_3\end{bmatrix}=\begin{bmatrix}-1.4972 & 0.5997 & 2.3389\\ 0.1732 & -1.8687 & 0.7232\\ 0.3123 & 0.3364 & -0.7423\end{bmatrix}\begin{bmatrix}x_1\\ x_2\\ x_3\end{bmatrix}$$

$$+\begin{bmatrix}0.6500 & 0.8000 & 0 & 0 & -0.0286\\ 0 & 0 & 1.0000 & 0 & -0.0088\\ 0.3500 & 0.2000 & 0 & 1.0000 & -0.0088\end{bmatrix}\begin{bmatrix}u_1\\ u_2\\ u_3\\ u_4\\ u_5\end{bmatrix}$$

$$\begin{bmatrix}y_1\\ y_2\\ y_3\end{bmatrix}=\begin{bmatrix}0.0120 & 0.0120 & -0.0280\\ 1.0000 & 1.0000 & 1.0000\\ 0.0419 & 0.8386 & -0.0960\end{bmatrix}\begin{bmatrix}x_1\\ x_2\\ x_3\end{bmatrix}$$

$$+\begin{bmatrix}0 & 0 & 0 & 0 & 0\\ 0 & 0 & 0 & 0 & 0\\ 0 & 0 & 0 & 0 & 0\end{bmatrix}\begin{bmatrix}u_1\\ u_2\\ u_3\\ u_4\\ u_5\end{bmatrix} \qquad (8.3.2.8)$$

Now, we are ready to compute the controller with Matlab command "h2syn".

8.3.3 Simulation Results

With our H_2 optimal control, we manage to find the controller that has minimized the system norm:

$$\min_{K\in S} \ \left\|T_{zw}\right\|_2 = 697.3 \qquad (8.3.3.1)$$

Our simulation parameters are exactly the same as in the pole placement method, as in (8.2.2.1) to (8.2.2.6). We intentionally put uncertainties into the simulation, the same as with the pole placement as stated in (8.2.2.1) to (8.2.2.6), so that we can see if H_2 optimal control has any robustness or not.

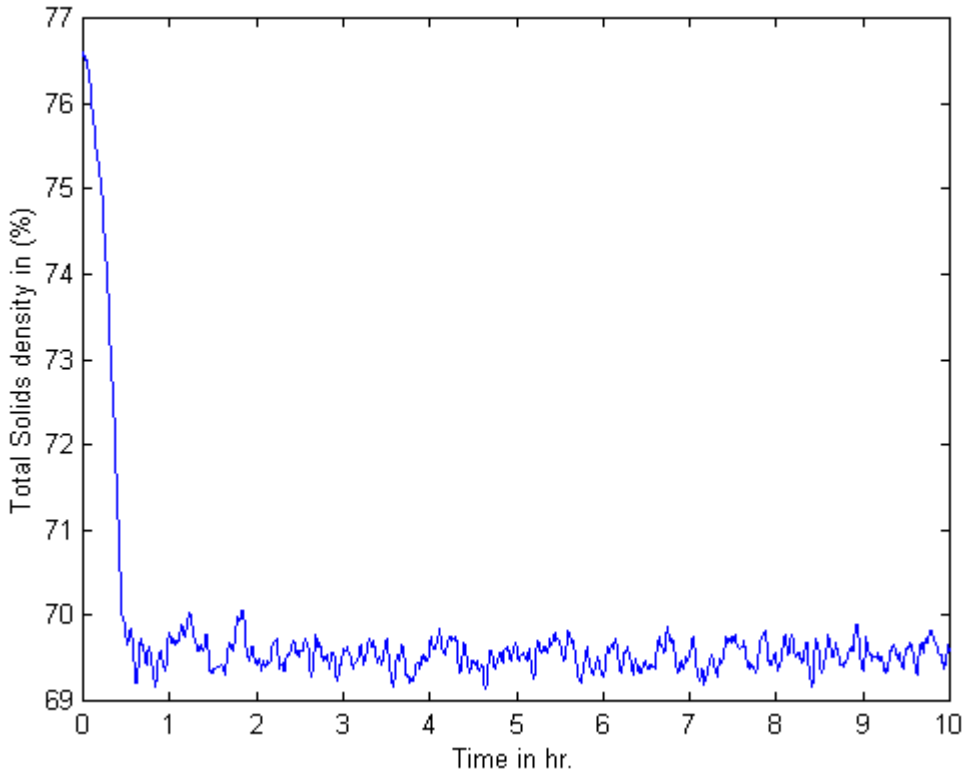

Fig. 8.3.3.1: Total solids density of existing Repulper tank process which is controlled with H_2 optimal control.

It is encouraging to see that even we simulate the system with all the uncertainties, the solid density can stabilize around the setpoint,70%. Next, we are going to look at the total mass of the tank.

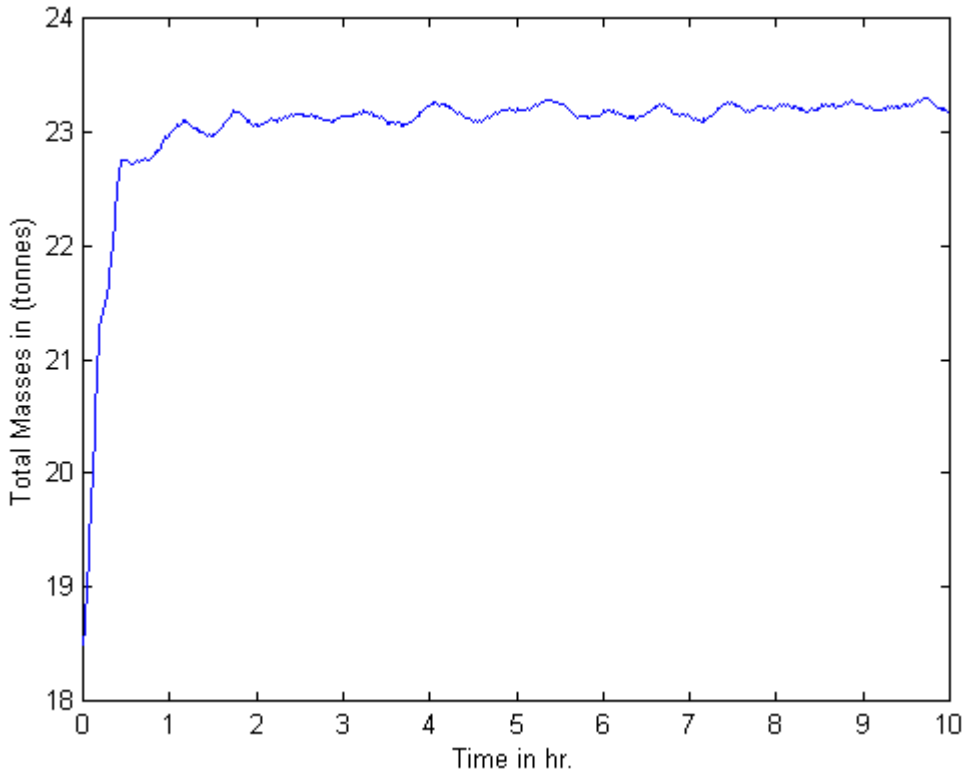

Fig. 8.3.3.2: Total mass of existing Repulper tank process which is controlled with H_2 optimal control.

Total masses of the tank seems to stabilize as well, but it does not really go back to the set point, 25.04 tonnes. However, in order to see exactly how the state errors are being controlled, we are going to look at the state errors next.

From Fig. 8.3.3.3, it seems that there is some problem. We see that the Strathcona and Raglan state errors keep on diverging. In fact, even after numerous simulations and changing the respective gains of different weighting functions, the state errors do not converge. Hence, even though the solid density seems correct, it is probable that the Raglan to Strathcona ratio errs a lot. To see if this is true, we are going to look at the Raglan to Strathcona ratio figure next.

Unfortunately, Fig. 8.3.3.4 really confirms our previous proposition. The Raglan to Strathcona ratio rises to almost one. This means we have almost exactly the same amount

of Raglan and Strathcona. This explains very well as in Fig. 8.3.3.3, the Raglan mass keeps on increasing while the Strathcona mass keeps on decreasing. Since, controlling the ratio is one of the most important objectives of this study, henceforth; we cannot accept the design by "H_2 optimal control". The cause of the divergence of the state errors needs to be investigated further. However, since this would involve the dissecting of more fundamental and in depth theory on H_2 optimal control, hence it is not the scope of this study. Nevertheless, this is certainly an interesting problem to dwell into further as it could potentially give important insights.

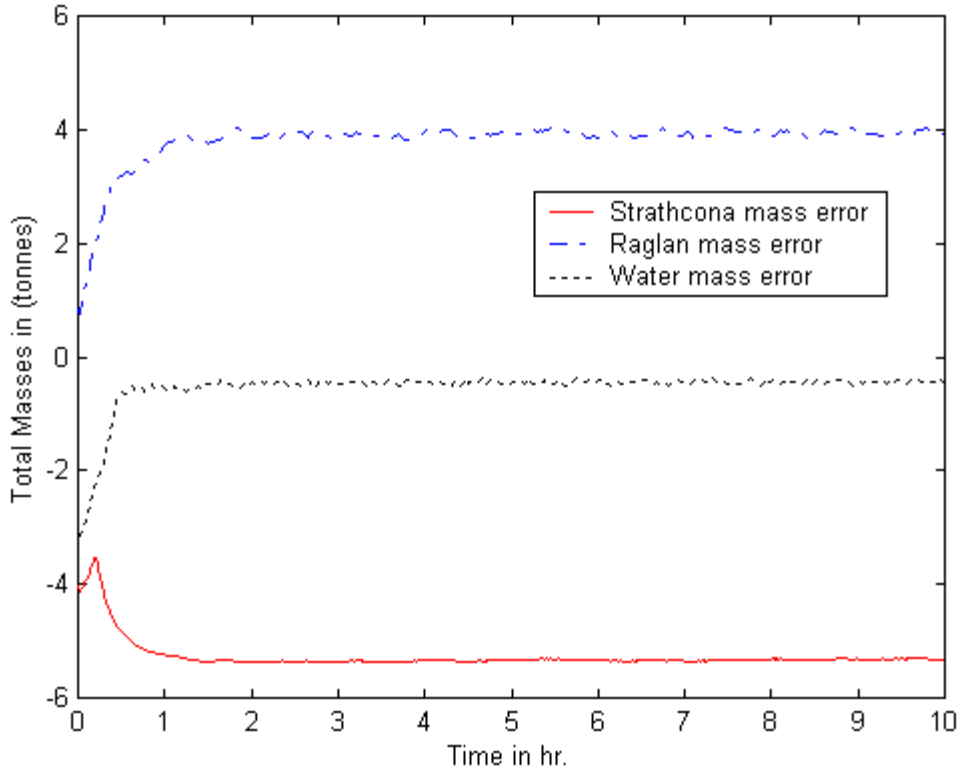

Fig. 8.3.3.3: State Errors of existing Repulper tank process which is controlled with H_2 optimal control.

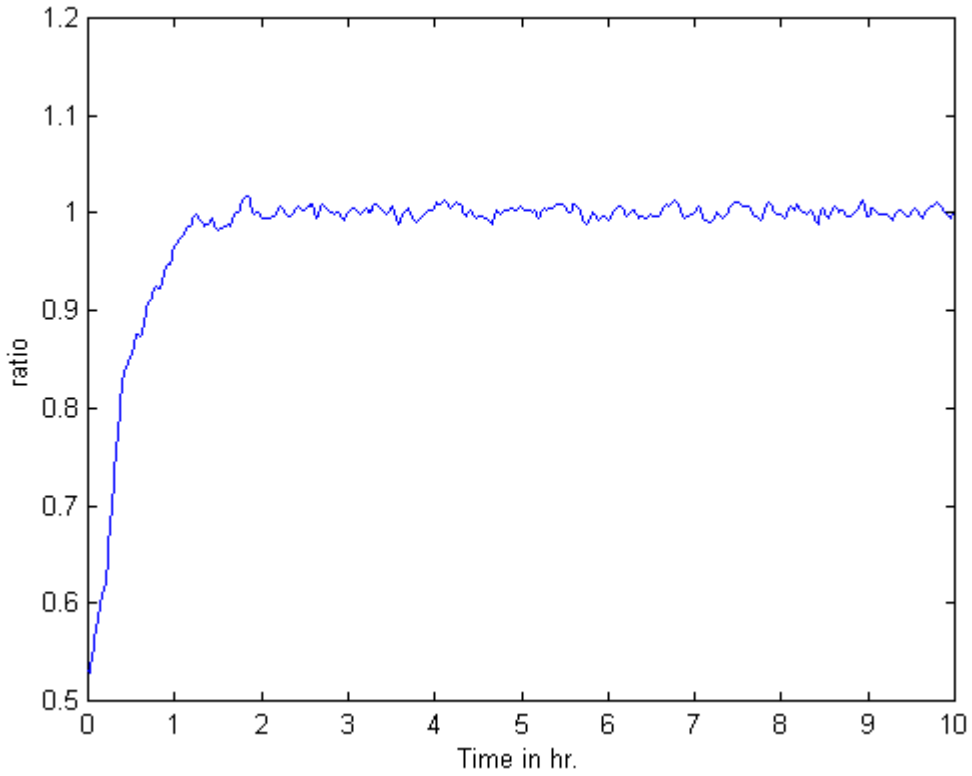

Fig. 8.3.3.4: Raglan to Strathcona ratio of existing Repulper tank process which is controlled with H_2 optimal control.

8.3.4 Conclusion of H_2 optimal control

Although it is too bad that "H_2 optimal control" cannot achieve our tracking objectives, it is found that at least it does not render the system unstable. The pump speed is also well controlled at about 962RPM. The problem of the incapability of minimizing the state errors is probably due to the fact that we do not have the right outputs so that state information can be deduced accurately.

8.4 Conclusion of Linear MIMO Control

We have gone through lots of efforts in trying to find the right design to control our linearized nonlinear Repulper tank system to its best. On one hand, it is exciting to see that simple linear MIMO state feedback pole placement works much better over all state feedback control design we used in this study. It also provides very good robustness performance. On the other hand, it is disappointing that H_2 optimal control cannot resolve our state unavailability problem. This means, as we stated earlier in chapter 7, we cannot control the system with only one tank. Hence, indeed, only the Three-Phase alternative control system can really control the system to achieve all tracking objectives while coping with the uncertainties.

Chapter 9

Conclusion

In conclusion, throughout this research, we have developed and tested new design schemes, the alternative process control system, and new nonlinear control methods, namely the general switching and robust switching control.

We have successfully designed and verified the Three Phase design, which can significantly reduce the effect of uncertainties, while performing satisfactorily and robustly. We have also concluded that based on the original one tank system, the Repulper tank, it is difficult to control the system since we do not have full state information due to the highly sensitivity of the states to errors in SG_S and SG_R.

In terms of controller design, we have compared different controllers, nonlinear and linear. Although the nonlinear controllers applying to the original plant does not work properly, the linear counter part with pole placement works satisfactorily. Meanwhile, the

three phase nonlinear design at the end however can provide very accurate control compared to the linear method of pole placement. We have found that simple state feedback pole placement method seems to be the best controller overall. It can attain tracking within an hour while being robust to input and parametric uncertainties, and its inputs do not chatter much. In the nonlinear controller design, we have verified that the Hurwitz diagonal A matrix, of input-output linearization, does stabilize the system asymptotically as it can correct any deviations from the setpoint. However, robustness is not guaranteed in input-output linearization. Further investigation of the robust input-output linearization shall be an interesting study.

Switching control can perform also but the g matrix of the system has to be non-singular. Moreover, if g matrix is in a diagonal or triangular format, robust switching control can be employed which guarantee robustness and stability. Although the pole placement control scheme in our study does have robustness capabilities, the state information cannot be obtained correctly due to the sensitivity of its values to the random fluctuations of the specific gravities of Strathcona and Raglan. However, all nonlinear controller inputs inevitably chatter to certain extent. Further studies could hence be on the improvement of the chattering behavior of the inputs by the nonlinear controllers. On the other hand, comparatively, linear controllers, for example the one designed with pole placement method, only fluctuate within a relatively small range. This is the advantage of linear controller.

Though unfortunate, it is perceivable that the H_2 optimal controller would fail. Again, this is due to the fact that the nonlinear Repulper system itself does not have enough appropriate measurable outputs which can make either state estimation and state derivation feasible.

Hence, from this study, it is found that to resolve a problem, the most important step is to fully understand the problem. Without a deep and thorough understanding of the basics of the problem, any extra efforts could be wasted. Also, in developing solutions to the method, it is important to have a creative and open mind so that no method is biased. All

nonlinear and linear controllers are just the tools for a control engineer to solve problems. There should not be any preference or prejudice against any one of them. But probably, the creative and workable solution could be a mix of different types of controller as we do in this study.

References

Bélanger, P. (1995). *Control Engineering, A Modern Approach*. Saunders College Publishing.

Boulet, B. (2001). *Robust Industrial Control. Part 2: Robust and Optimal Control.* Coronado Systems, Montreal, 2001.

Burns, R. (2001). *Advanced Control Engineering.* Butterworth-Heinemann, Oxford, England.

Dahleh, M. A. and Diaz-Bobillo, I. J. (1995). *Control of Uncertain Systems.* Prentice Hall, New Jersey.

Doyle, J. C., Glover, K. Khargonekar, P. P. and Francis, B. (1989). "State Space Solutions to Standard H_2 and H_∞ Control Problems". *IEEE Trans. Automatic Control*, vol. 34, pp. 831-847.

Francis, B. A & Khargonekar, P. P. (Eds.) (1995). *Robust Control Theory*. Springer-Verlag, New York.

Henson, M. A. & Seborg, D. E. (Eds.) (1997). *Nonlinear Process Control*. Prentice Hall, New Jersey.

Isidori, A. (1995). *Nonlinear Control Systems (3rd Edition.).* Springer-Verlag, London, England.

Levine, S. (Eds.) (1996). *The Control Handbook.* IEEE Press, Boca Raton, Fl..

Kolavennu, S. & Cockburn, J. C. (2001). "Synthesis of Robust Controllers for Nonsquare Multivariable Nonlinear Systems*".* *Proceed. of the American Control Conf.*, pp. 4032-4037.

Michalska, H. (2001). *Lecture Notes, Nonlinear Systems Course.* McGill University.

Oppenheim, A. V. & Willsky, A. S. (1997). *Signals and Systems.* Prentice Hall, New Jersey.

Sarachik, P. E. (1997). *Principles of Linear Systems.* Cambridge University Press, New York.

Sastry, S. S. (1999). *Nonlinear Systems: Analysis, Stability and Control*. Springer, New York.

Sastry, S. S. & Isidori, A. (1989). "Adaptive Control of Linearizable Systems". *IEEE Trans. Automatic Control*, vol. 34, pp. 1123-1131.

Stefani, R. T., Shahian, B. Savant Jr., C. J. & Hostetter, G. H. (2002). *Design of Feedback Control Systems (3rd Ed.).* Oxford University Press, New York.

Utkin, V. I. (1992). *Sliding Modes in Control Optimization.* Springer-Verlag, Berlin.

Zhou, K. and Doyle, J. C. (1998). *Essentials of Robust Control.* Prentice Hall, New Jersey, 1998.